COLLECTIVE DYNAMICS OF EVOLVING POPULATIONS AND THEIR STRATEGIES WITH APPLICATION TO MEDICINE

BY

ZHENYU WANG

DISSERTATION

Submitted in partial fulfillment of the requirements
for the degree of Doctor of Philosophy in Physics
in the Graduate College of the
University of Illinois at Urbana-Champaign, 2012

Urbana, Illinois

Doctoral Committee:

Professor Karin A. Dahmen, Chair
Professor Nigel Goldenfeld, Director of Research
Professor Yoshitsugu Oono
Assistant Professor Yann R. Chemla

Abstract

This dissertation focuses ultimately on the topic of evolution, which is the foundation of modern biology. I hope to understand, in a general sense, evolution on a population scale by investigating individual level interactions.

In this dissertation, I present four projects in biophysics performed under the supervision of Professor Nigel Goldenfeld: Population dynamics of viruses and their hosts, game theory and the social life of microorganisms, a novel mechanism enhancing cooperation in evolutionary game theory, and evolutionary robust strategies for delivery of antibiotics.

In the first project, starting with stochastic rate equations for the fundamental interactions between microbes and their viruses, we derive a mean-field theory for the population dynamics of microbe-virus systems, including the effects of lysogeny. In the absence of lysogeny, our model is a generalization of that proposed phenomenologically by Weitz and Dushoff. In the presence of lysogeny, we analyze the possible states of the system, identifying a novel limit cycle, which we interpret physically. To test the robustness of our mean field calculations to demographic fluctuations, we have compared our results with stochastic simulations using the Gillespie algorithm. Finally, we estimate the range of parameters that delineate the various steady states of our model.

In the second project, we present a mean field model for the phase diagram of a community of microorganisms, interacting through their metabolism so that they are, in effect, engaging in a cooperative social game. We show that as a function of the concentration of the nutrients glucose and histidine, the community undergoes a phase transition separating a state in which one strain is dominant to a state which is characterized by coexisting populations. Our results are in good agreement with recent experimental results, correctly reproducing quantitative trends and predicting the phase diagram.

In the third project, we propose a novel mechanism to enhance cooperation in evolutionary game theory. Explicitly incorporating stochasticity in the phenotypic decision making process, and the interaction between evolution and ecology in the dynamic landscape, we demonstrate that for a wide variety of cooperative games of the prisoner's dilemma type, cooperation eventually becomes the dominant strategy as long as the rules

are permitted to evolve in response to the changing environment. Therefore, the ubiquitously observed cooperation in nature may come from stochastic phenotype and evolutionary landscape rather than the detailed type of competition. Altruism becomes an advantageous strategy, because it avoids being exploited by selfish agents.

In the last project, we treat antibiotic resistance, which is a major concern in public health. Compared with conventional antibiotics, we show that the emergence of antibiotic resistance can be significantly delayed by using narrow and ultra-narrow spectrum antibiotics to target pathogens, rather than the entire microbiome. We also develop a new strategy that involves spoofing quorum sensing channels of communication, causing premature expression of virulence factors. When combined with ultra-narrow spectrum antibiotics, our strategy removes infections and most importantly does not lead to the emergence and spread of antibiotic resistance genes.

To my parents.

Acknowledgments

As an undergraduate, I was die-hard to become a physicist. I chose University of Illinois at Urbana-Champaign as my graduate school not because my advisor Nigel Goldenfeld is here, not because Carl Woese is here, but because Department of Physics here ranks the best in condensed matter physics. I still remember Robert B. Laughlin's laughing at the huge error bars in biology. "It is nasty," he commented. Well, laughing at biology might trace back to a century ago, when Lord Ernest Rutherford quipped, "All science is either physics or stamp collecting"[1]. However, now all my four projects are in biophysics. Is it nasty? Well, error bars may be large in some cases, but there is physics, absolutely.

I still remember Nigel's shining eyes when he introduced "Biology's next revolution" at our orientation. Wisdom and passion permeated in every one of his cells. I understood at once that the problems are in biology, but the approaches are in physics. All my prejudice evaporated, I knew I liked Nigel, his style, his thinking, and his research.

I entered the graduate school to learn how to do physics, or more precisely, to learn the Western intuition in doing physics. I knew Nigel had it. More luckily, he was willing to teach me. No word could describe my happiness when I was given the opportunity to join Nigel's group. Bravo!

My five years working with Nigel has proven that choosing him as my advisor is the wisest decision in my graduate school. It has been a time to reconfigure my brains.

Nigel is a true physicist, always thinking something big, something deep and something unique. He is a true advisor, patient to teach, willing to teach, and happy to teach, in physics, in career, in all aspects of life. He is a true friend, before, now and forever.

Students and postdocs in Nigel's group are my great treasures. Patrick Chan, Nicholas (Nich) Guttenberg, Patricio Jeraldo, Tom Butler, Maksim Sipos, Hong-Yan Shih, Farshid Jafarpour, Nicholas (Nick) Lee-Ping Chia, David Reynolds, Luiza Angheluta, Andreas Menzel, Lanying Zeng, Michael Assaf everyone is resourceful, colorful and helpful. I think every one is impressed by Nich's ability to show preliminary simulations at the end of a meeting. I thank him for crazy ideas. Patricio and Maksim are two geeks in our group, who I always admire. I would like to thank them for bailing me out once and again. Tom was

my officemate till he left. I thank him for helping me on my research and English, and sharing with me his music. I have much to thank Nick in research and in life.

I am lucky to work in the same theme at the Institute for Genomic Biology as Professor Carl Woese. I clearly remember one day he walked into my office to shake hands with me and told me that he liked the introduction of my prelim paper. His smiles and greetings are like sunshine in the afternoon.

I thank my collaborator Professor Douglas A. Mitchell for his contributions in the project on antibiotic resistance and for his help on my career.

I thank Professor Karin A. Dahmen, Yoshitsugu Oono, Yann R. Chemla and Ido Golding for being on my committee.

Of course I would like to thank all my friends here and far away. They are the third dimension in my life on this two-dimensional flatland.

Last but not least, I would like to thank my parents. Without them, all would have been different.

The work in this dissertation on fundamental aspects of evolution was partially supported by the National Science Foundation grant number NSF-EF-0526747.

Table of Contents

List of Tables

List of Figures

Chapter 1

Introduction

Approximately five centuries ago, Nicholas Copernicus (1473 - 1543) famously dragged the Earth away from its holy position as the center of the entire universe. Worshipping and pursuing elegance and brevity, he put the Earth revolving around the Sun together with other planets, discarding Claudius Ptolemaeus's exquisite and complex design of epicycles on epicycles. Although the heliocentric model was still a naive infant, a historic revolution was launched. When the Earth was no longer so special as humans had imagined, why should the Sun be that special or even the Milky Way galaxy? Today, the once sacred Earth ends up to be a most ordinary planet at a brim far, far away from the center of the universe.

Two hundred years ago, another revolution began, this time in biology. Charles R. Darwin (1809 - 1882) and Alfred R. Wallace (1823 - 1913) mercilessly dragged humans away from their holy position at the center of all life. Attached to a history of evolution longer than any human record, *Homo sapiens* too has evolved from other species while mountains elevate and flatten. Carl Woese completed the indignity visited upon humans when he unveiled the phylogeny of life, placing humans at the periphery of a huge three-domained tree, composed mostly of microbes. While admitting that humans were not that special, we again were astonished when the human genome was mapped out in 2001. Instead of a previous estimation of about 100,000 protein-coding genes, it turned out that the human genome encodes only about 20,000 - 25,000 genes [24, 25], about four times that of *Pseudomonas aeruginosa* (Gram-negative bacterium) [26] and *Saccharomyces cerevisiae* (budding yeast) [27, 28] (both about 6000), not much more than the simple *Caenorhabditis elegan* (nearly 20,000) [29], and only half as many as *Oryza sativa* (rice) [30, 31]. Intuitively perceiving the number of genes as a measure of organismal complexity, we were more or less disappointed and frustrated. Our euphoria of superiority continued to evaporate when the genome-wide nucleotide divergence between chimp (*Pan troglodyte*) and human was revealed to be only 1.23% and may be even smaller [32]. Creating unprecedented civilization, we humans, are apparently not that special or superior, or are we? As a book made up of only four letters and twenty words, genomes do not sound incomprehensible. It is simple in what is printed out, but what is encoded implicitly is beyond our wildest dreams.

This dissertation focuses ultimately on the topic of evolution, which is the foundation of modern biol-

ogy. We hope to understand, in a general sense, evolution on a population scale by investigating detailed and specific individual level interactions. That is to say, evolution is an emergent property of interacting populations. Always bearing in mind the big picture of evolution and ecology, we start our journey with stochastic rate equations and master equations in statistical physics, and apply them to compute the population dynamics of microbe-virus systems. Analyzing fixed points and limit cycles in the phase diagram describing the population dynamics, we reveal non-triviality in derivations from the microscopic level and further provide physical interpretations and estimations testable in experiments.

Next I became interested in cooperative phenomena, which are ubiquitous in biology. In particular, I focused on a recent experiment that quantifies the degree of cooperation in budding yeast as the environment changes. It is hard to use the same approach of population dynamics as in the first project here because of the high complexity in the metabolism and transportation mechanisms, which should require systems biology. As an alternative, we retreat to mean field level and employ game theory. We successfully formulated a model building up a direct link and showing consistent results between game theory and experimental measurable quantities.

In order to dig deep into the origin and maintenance of cooperation, in the third project, we put forward a novel mechanism encouraging cooperation in evolutionary game theory. Explicitly incorporating stochasticity in the phenotypic decision making process, and the interaction between evolution and ecology in the dynamic landscape, we demonstrate that for a wide variety of cooperative games of the prisoner's dilemma type, cooperation eventually becomes the dominant strategy as long as the rules are permitted to evolve in response to the changing environment.

Understanding nature brings pleasure, but the power of theory is to predict. During the last 70 years or so, the degree to which humans can influence the biosphere has become much more extensive, in particular with the widespread use of antibiotics throughout the world. My last project turns out to be a reverse-engineering problem: How to fight the emergence of antibiotic resistance? In other words, how to constrain the population of pathogens so that no matter how they evolve, they are always bounded inside some regions in the phase diagram safe to human? We design the next generation of antibiotics with presumably no antibiotic resistance, and suggest practical treatment methods.

1.1 Micro-organismal Wonder World

The term "microorganism" specifies a form of life by its scale in a rather loose fashion. It refers to an organism with a size typically around half to a few micrometers, but may range down to a hundredth of and

up to several hundred micrometers. It can be acelluar, unicelluar, multicellluar or a cell cluster, covering diverse species, including bacteria, archaea, eukarya, and even viruses. Microorganisms were discovered by Anton van Leeuwenhoek (1632 - 1723) in 1675, and were later studied in the field of microbiology.

In this dissertation, we treat several micro-organismal systems using population dynamics and game theory. We focus on some model species in eukaryotes, bacteria and their viruses, but the methods and discussions are not limited to the specified examples, and applicable to other systems.

Microbes and their viruses are the most genetically diverse, abundant and widely distributed organisms across the planet [33, 34, 35, 36]. Microbes are major contributors to the global biogeochemical cycles and catalyze the reactions that have over evolutionary time brought the Earth's surface to its present redox state [37]. Similarly, viruses, especially in the oceans, manipulate marine communities through predation and horizontal gene transfer [38, 39], recycle nutrients and thus drive the biological pump which leads *inter alia* to the sequestration of carbon in the deep ocean [40, 41, 42, 43, 44, 45, 46, 47, 48, 49].

Horizontal gene transfer (HGT) [50, 51] is a process in which an organism transfers genetic material to another cell that is not its offspring. It is very common in the micro-organismal world, and happens intra-, and inter-species, and even across domains such as between bacterial and animals [52, 53]. Recently, such evidence for horizontal transfer of genes and even transposons was found in mammals, fish, and tetrapods [54, 55, 56]. Through horizontal gene transfer, it is very convenient to shuffle genes in the micro-organismal world. In other words, micro-organisms are able to share, absorb and discard genes, especially under stressful conditions [57]. Horizontal gene transfer, to a great extent, is sometimes thought to disrupt the traditional perspective of species in the vertical gene transfer world, where genes are generally passed on from ancestors to offsprings [51] (Figure 1.1 and 1.2). The ribosomal tree of life tracks the evolutionary history of a lineage through highly conserved genes, and so this is unaffected by the presence of HGT. However, the idea of a species as having a fixed and narrowly-delimited genome appears not to be correct, with accumulating evidence in favor of the pan-genome concept in which there are wide variations in genome contents as organisms access pools of genes through the virosphere or from other microbes with which they are in contact through a shared ecological niche [58]. HGT significantly accelerates the spread of genes, which propagates antibiotic resistance, as we would like to discuss in more details later.

Furthermore, the special role of viruses in the micro-organismal world complicates gene transfer processes. The interaction between viruses and their hosts is far more intricate than the physical relation between classical predators and preys. Viruses act more like self-replicable gene-reservoirs. As an example, we are now ready to introduce here the specific microbe-virus system that we will discuss in more details in Chapter 3 of this dissertation. This system is composed of a set of viruses (λ phage), which can infect a bacterium

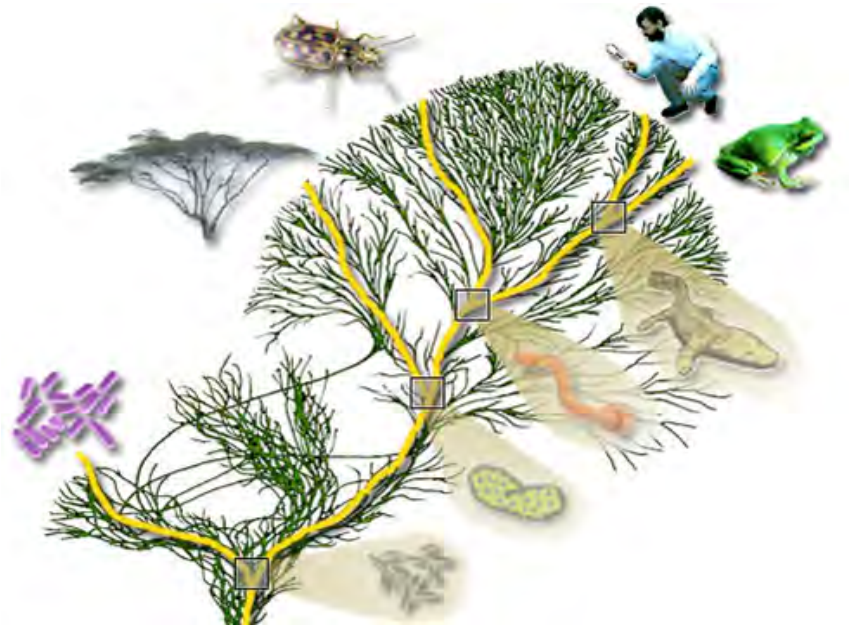

Figure 1.1: Vertical evolution and the "tree of life". After Ref. [6].

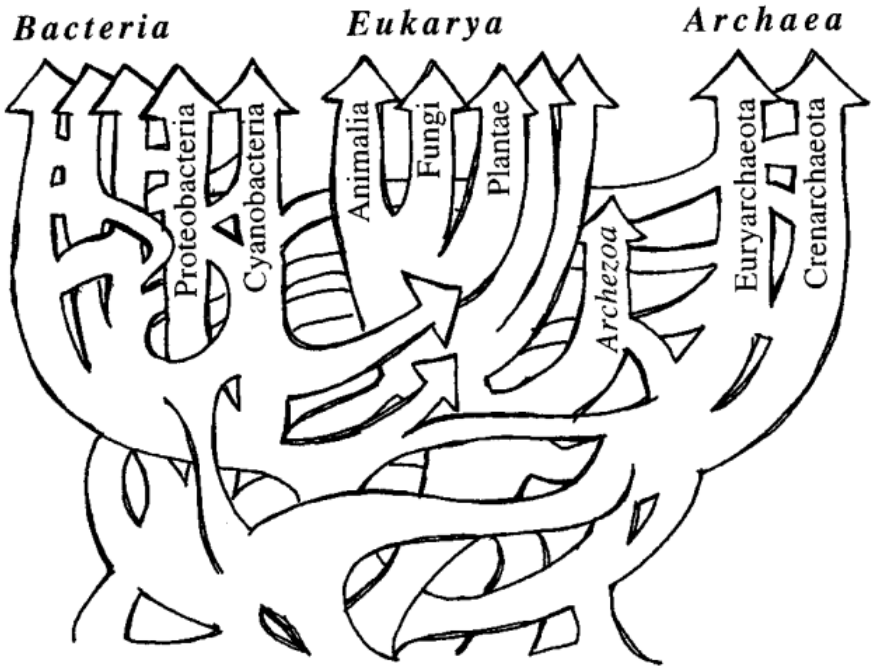

Figure 1.2: Horizontal evolution and the "tree of life". After Ref. [7].

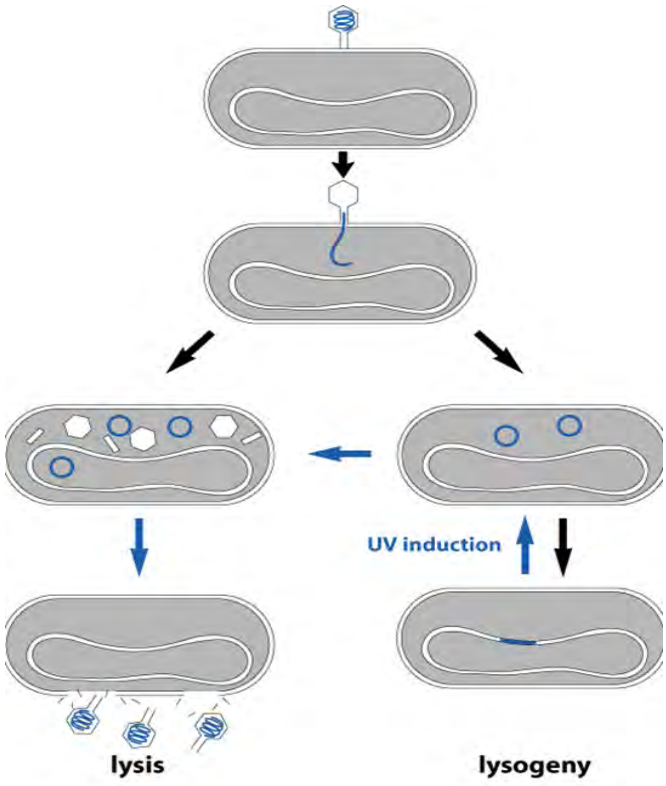

Figure 1.3: Two pathways in temperate phage infection: Lysis and lysogeny. In the lytic pathway, the host cell is killed. A large number of phages will assemble using the host's genetic material and molecular machinery, and be released into the environment. Another pathway—lysogeny—incorporates viral genetic material into the chromosome of the host. The prophage replicates with the host and its offsprings, and can be subsequently released, typically triggered by the stress response of the host to environmental changes. After Ref. [8].

(*Escherichia coli*). Upon temperate phage infection, there are two pathways awaiting the host bacterium [8] as sketched in Figure 1.3. In the first pathway—lysis—the bacteriophage produces a large number of copies of itself utilizing the bacterium's genetic material and molecular machinery. As a result, the bacterium ceases its metabolic function, and ruptures, releasing the newly assembled bacteriophage inside. The other pathway is lysogeny. In this process, the intruder integrates its own DNA into the genome of the bacterium, enters a dormant stage and becomes a prophage. The infected bacterium is known as a lysogen—a relatively stable state [59], immune to superinfection from the same or related strains, and proceeding under normal replication life-cycles. The DNA of the bacteriophage is duplicated, along with that of the host during cell replication. The lysogenic state can be terminated by environmental stress such as starvation, pollution or ultraviolet irradiation, resulting in the process known as prophage induction: the exit of the prophage from the host genome, and subsequent lysis of the original bacterium and its bacterial descendants. We would like to emphasize the miracle and duality of prophages here. For viral sake, prophages are sheltered inside their hosts. They are temporarily dormant but potentially massive in future phage production. For host's sake, prophages may economize hosts' metabolism [60]. Suppressing unnecessary metabolic activities by expressing repressors and transcriptional regulators, they downshift hosts' energy cost and help the survival of both in harsh environments.

Horizontal gene transfer and genetic switch in phage infection are illustrated as glimpses into the micro-organismal wonder world. The complicated interactions call for both universal and detailed analysis and modeling.

1.2 Coexistence and Cooperation

There are millions of species on the planet. About 1.3 million eukaryotes are recorded, named and cataloged, but more are reported each year. A recent taxonomic classification [61] under debate predicts 8.7 million globally. Even in the human gut, a metagenomic sequencing in 2010 [62] revealed on average at least 160 bacterial species for each individual. How can so many species coexist in a limited range of resources and spaces? The famous "paradox of the plankton" is a long-standing enigma [63, 64, 65] on the origin, maintenance and prosperity of biodiversity.

Coexistence of different species in the same niche may expose them to fierce survival competition for limited nutrition and space, and antagonism as predators and preys, but may also bring them to cooperation [66].

Cooperation is the behavior of an individual dedicating its own resource or effort to confer benefit on

others or the whole community. Cooperative behavior is widely observed at all levels of biology. J.B.S. Haldane's famous saying that "I will jump into the river to save two brothers or eight cousins" [67, 68] descriptively illustrates self-sacrifice in exchange for the benefit of others. Teamwork is another good example of cooperation, pervasive not only in human society [69], but also in other mammals [70], such as wolves [71] and bats [72, 73], and social insects, such as bees [74] and ants [75].

Down to the level of micro-organisms, horizontal gene transfer [76, 77, 78, 79] and quorum sensing [80, 81] are two examples of mechanisms manifesting cooperation. Horizontal gene transfer, contrary to vertical gene transfer from a parent to its offsprings, is a gene-sharing mechanism, operative inter- and intra-species, and even across different domains of life. Quorum sensing coordinates gene expression according to a local population density. To this repertoire of cooperation we add lysogen, a coexistent state of an initially antagonizing host and phage. They cooperate and exploit each other in energy expenditure [60] to survive through unfavored environments.

Furthermore, multicellular organisms are themselves a question for cooperation: Why and how can the majority of the cells of an individual take part in metabolism and daily functioning while a few are endowed with the privilege of passing genes to the next organismal generation [82]? Even on the cellular level, genes and proteins cooperate in gene expression [83] and other cellular processes [84].

In sum, coexistence of different species is observed in myriad habitats, and cooperation is a universal phenomenon at all levels of biology.

1.3 Evolution and Coevolution

Carl Woese once said that his key word is "evolution". It is the evolution of life over billions of years that brings us the colorful, beautiful and wonderful planet we stand on today. The special evolvability in life complicates biology, but also establishes and distinguishes it from physics and chemistry.

Evolution is generally recognized on a long timescale such as phylogeny and tree of life. Richard E. Lenski tracks the evolution of *Escherichia coli* over half million generations [85], and observed ever-increasing fitness [86]. It is also possible to notice evolution on a much shorter timescale as the evidence offered by A.P. Hendry et al. [87] for reproductive isolation in an introduced sockeye salmon after less than 13 generations.

Evolution is usually reckoned as the process of adaption for species to their environment via mutation and natural selection. Such a process actually should be bidirectional or reticulated instead of unidirectional because every individual or species serves as the evolutionary background for other individuals or species in the process of its own evolution. In predator-prey ecosystems, both types of agents are stressing and being

stressed by their counterparts, leading to a coevolutionary arms race [88]. Such a Red Queen effect is widely observed in nature. For example, the spirochete, a pathogen that causes Lyme disease, changes its surface protein frequently by insertion of new patches of DNA into its genome so that it can evade the searchlight of the immune system [89] of the host. The cost and payoff, and evolvability vary for different organisms.

It is being increasingly realized that the classical view of microbial viruses purely as predators is too limited. Many microbe-virus interactions are lysogenic. Viruses can transfer genes to and from bacteria, as well as being predators of them, so that the virosphere should properly be recognized as a massive gene reservoir [90, 91, 51, 49]. Thus there is a coevolution of both communities in a much deeper sense regarding gene shuffling, the effects of which are complex and far-reaching [92, 93, 94, 42, 91, 95, 51, 49], even including the manipulation of bacterial mutation rates [96]. This nontrivial interaction between microbes and viruses has not gone unnoticed, with wide interest among biologists, ecologists and geologists [97, 98, 99, 100, 34, 101, 102, 95, 60, 103, 104].

These findings highlight the importance of considering ecosystem dynamics within an evolutionary context. Conversely, evolution needs to be properly understood as arising from a spatially-resolved ecological context, as was first recognized by Wallace over 150 years ago [105]. That speciation, and adaptation in general, arises at a particular point in time and space has a number of deep consequences that have not yet been incorporated into current theory. First, it means that evolutionary dynamics proceeds by the propagation of fronts, resulting in a complex and dynamical pattern of speciation, adaptation and genome divergence that reflects its intrinsic dynamics and that of the heterogeneous and dynamical environment [106, 107, 108, 109]. Second, as fronts expand, there are only a few pioneer organisms at the leading edge, and so demographic fluctuations are much larger than in the bulk. Such fluctuations profoundly influence the spatial structure of the populations, and during the last few years have been recognized to play a major role in population cycles [110] and even spatial pattern formation [111]. Third, the existence of horizontal gene transfer and genome rearrangement processes is strongly coupled to spatial distribution. For example, it is known that the probability of conjugation events is dependent on the local density, being essentially one per generation in closely-packed biofilms, but an order of magnitude smaller in planktonic culture [112]. Moreover, the mechanism of horizontal gene transfer is also dependent on the density, with viral-mediated transduction being the most relevant mechanism at low density. How these patterns of evolutionary dynamics and species distribution play out is essentially unexplored. However, there have recently been the first reports of observations of the coupling between evolutionary and ecological timescales. In one such system (a predator-prey system realized in rotifer-algae interactions), it has been demonstrated that rapid evolutionary dynamics is responsible for the unusual phase-lag characteristics of the observed population oscillations [113]. Thus,

rapid evolution is not only a major force for adaptation, but can have marked ecological consequences too.

The complex interplay between evolution and the environment is nowhere more important than in early life, where the key questions concern how life emerged from abiotic geochemistry. Early life experienced demanding environments, whose closest modern day correspondence might be deep ocean hydrothermal vents or hot springs. It is known that there are high occurrence of lysogens in both environments [36, 114], suggesting that microbe-phage interactions might also be important in the early stages of life, with lysogens playing an important role as a reservoir of genes and perhaps even aiding in the stabilization of early life populations through the limit cycle mechanism discussed in this dissertation.

1.4 Arms Race: Human VS Pathogens

Bacteria are a major cause and spread of diseases. The fight of humans against pathogens dates back to early human history. As a milestone, in 1928, Sir Alexander Fleming (1881 - 1955) discovered penicillin. In the 1940th, clinical treatment was introduced. Saving millions of lives, the potential for antibiotics to improve human health cannot be exaggerated.

However, the fast evolution and adaptation of bacteria has shattered our long-term ideal dream to stop diseases with antibiotics once and for all [115, 116, 117]. Development of new antibiotics and the resulting development of antibiotic resistance seem to trap us in a never-ending arms race (Figure 1.4). Since the 1960s, discovering new classes of antibiotics has nearly bogged down while increased antibiotic resistance has been observed [4]. In United States alone, millions of kilograms of antibiotics are consumed by human and at least an order of magnitude higher in animal industry and agriculture. Antibiotics are more incautiously used in developing countries. The wide use and abuse of antibiotics worldwide expedite antibiotic resistance. The situation aggravates with multidrug resistance (MDR), whose frequency also increases significantly with time [118, 19, 9]. The threat of no effective antibiotics is on the horizon, and is already a reality for a number of infections, such as gonorrhea [119] and tuberculosis [120]. Actually many scientists have warned human of the return of the dark ages [121, 4].

In order to slow down the pace of emergence and spread of antibiotic resistance, we propose and analyze two general schemes. The first is to narrow down the spectrum of antibiotics focusing on pathogens and bailing out healthy microbiota from conventional antibiotics. In this way, the source of resistant genes shrinks for pathogens. We demonstrate delayed emergence of resistance in narrow and ultra-narrow spectrum antibiotics. The second scheme, named Quorum Sensing Spoofing (QSS), is to take advantage of the quorum sensing mechanism in expressing virulence. The highlight is no antibiotic resistance in QSS. We also design

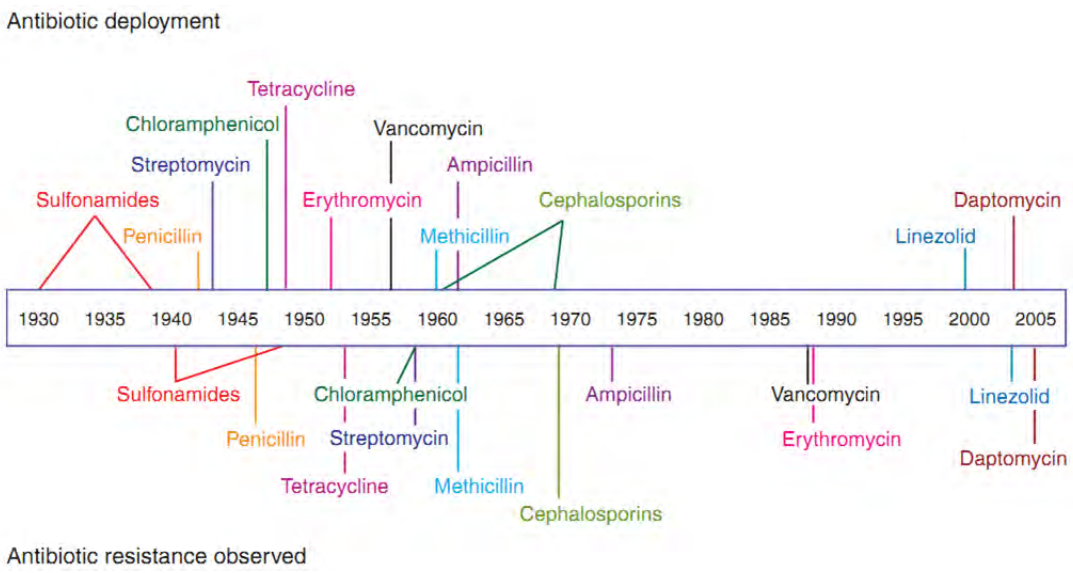

Figure 1.4: Timeline of antibiotic deployment and the evolution of antibiotic resistance. After Ref. [9].

dose cycles combining ultra-narrow spectrum antibiotics with Quorum Sensing Spoofing, and show efficiency in treatment with extremely low resistance against ultra-narrow spectrum antibiotics in drug alternations.

1.5 Dissertation Outline

This dissertation is structured as follows:

Chapter 2 and Chapter 3 are dedicated to the population dynamics of viruses and their hosts[122]. As a preliminary exercise, we treat a lysis-only model first in Chapter 2. We apply the same technique to lysogenic viruses and analyze fixed points and limit cycles of the full lysogeny-lysis model in Chapter 3.

Chapter 4 presents our theory of cooperation in a micro-organismal snowdrift game[123]. It directly links game theory with experimental measurable quantities.

Chapter 5 also focuses on game theory and cooperation, but from a totally different point of view. It introduces a novel mechanism enhancing cooperation in evolutionary game theory.

Chapter 6 presents our first attempt to apply population dynamics to medicine. It is dedicated to the design of next generation of antibiotics.

Chapter 7 is the conclusion with my thoughts and reflections on physics, biology and interdisciplinary research.

Chapter 2

Population Dynamics of Lytic Viruses and Their Hosts

2.1 Introduction

Numerically, viruses are the most abundant living entities on the planet with an estimated population of at least 10^{30} in the ocean alone [34, 41]. By "viruses", we refer to both bacterial and archaeal viruses. Bacterial viruses are also commonly known as "phages" or "bacteriophages".

The taxonomy of viruses is most probably still in its infant stage of "stamp collecting". (Lord Ernest Rutherford (1871 - 1937) once quipped that "All science is either physics or stamp collecting" [1].) The present virus classification is a derivation of D.E. Bradley's scheme [124] based on nucleic acid type, genome structure and morphology. In 2005 the International Committee on Taxonomy of Viruses (ICTV) approved 3 orders and 73 families [125]. Figure 2.1 illustrates common virus morphotypes. The majority of viruses have double-stranded DNA (dsDNA), some with single-stranded DNA (ssDNA), some with single-stranded RNA (ssRNA), and very rare with double-stranded RNA (dsRNA). Among the various types, some are virulent (lytic) viruses, which will lyse the host upon infection, and some are temperate (lysogenic) viruses, which are endowed with binary pathways of lysis and lysogeny as illustrated in Figure 1.3. Table 2.1 lists common lytic and lysogenic viruses infecting *Escherichia coli*.

Our goal in this chapter is to lay a theoretical foundation for describing the interplay between ecology and evolution in the context of microbe-virus systems, as these are arguably amongst the most important and probably the simplest of the complex systems in biology. The questions that will ultimately interest us are the evolutionary pressures that tune genetic switches governing the lysis-lysogeny decision, as well as the factors that shape prophage induction in response to environmental stress [126, 127, 128]. Such a foundation must begin with a proper account of the population dynamics itself, before coupling in detail to other levels of description involving genome dynamics, for example. Thus, we have chosen to focus in the present chapter and Chapter 3 on the dynamics of microbe-virus systems, taking full account of both of the major viral pathways. In these two chapters, we are not specific about whether we are dealing with bacterial or archaeal viruses, but because most of the experiments to date are carried out on bacteria, we

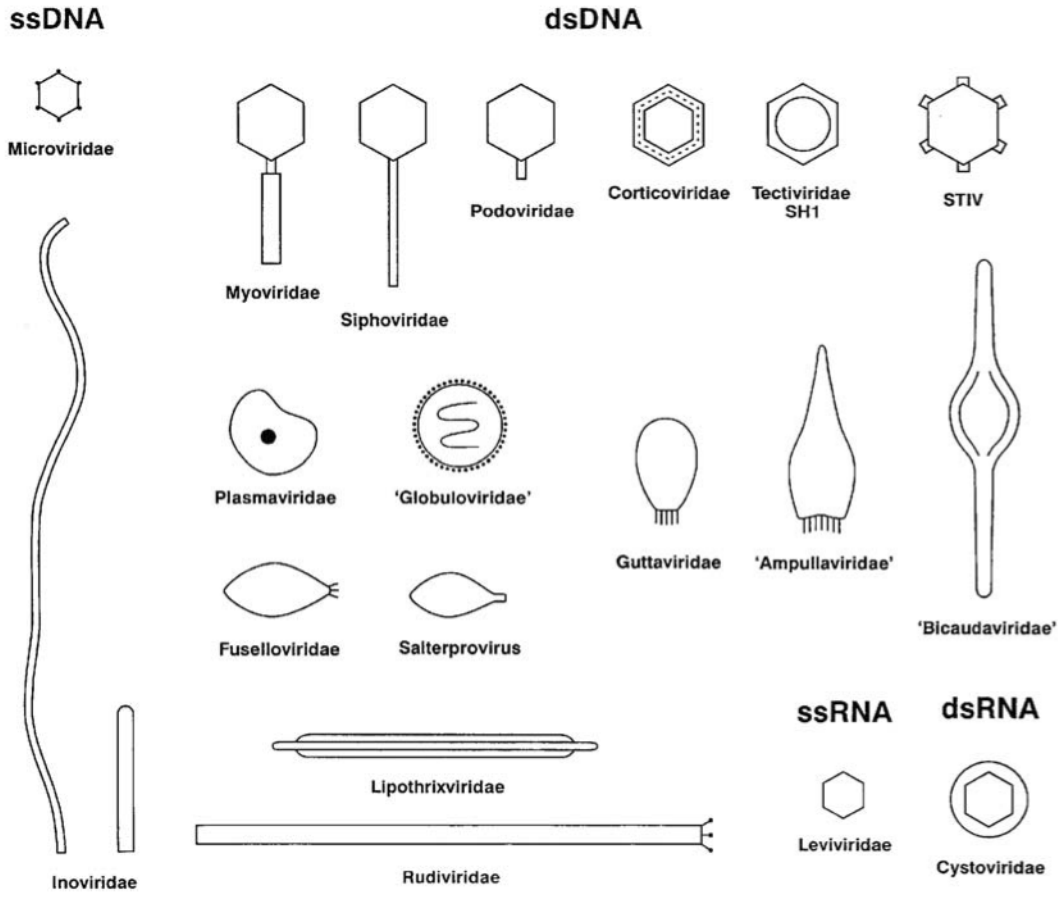

Figure 2.1: Typical virus morphotypes classified according to the nucleic acid type, genome structure and morphology. After Ref. [10].

Table 2.1: Common virulent and temperate viruses infecting *Escherichia coli*. T: Temperate phage; L: Virulent phage. After Ref. [2].

Name	Family	Life Cycle
λ	*Siphoviridae*	T
MS2	*Leviviridae*	L
Mu	*Myoviridae*	T
P1	*Myoviridae*	T
P2	*Myoviridae*	T
P4	*Myoviridae*	T
Φ80	*Siphoviridae*	T
ΦX174	*Myoviridae*	T
PRD1	*Tectiviridae*	L
T2	*Myoviridae*	L
T3	*Podoviridae*	L
T4	*Myoviridae*	L
T5	*Siphoviridae*	L
T7	*Podoviridae*	L
R17	*Leviviridae*	L

have tended to identify the microbes as bacteria and the viruses as phages, even though this is not required by the mathematics.

2.2 Population Dynamics: Ensemble VS Individual Level

We now discuss briefly existing treatments of population dynamics in the context of microbe-virus systems. In 1977, Levin et al. [129] extended the celebrated Lotka-Volterra equations to model the dynamics between virulent phages and their victims, where only virulent phages are considered. A number of extensions have been proposed, extending the level of biological realism to include such features as the time delay arising between infection and lysis as well as the evolution of kinetic parameters [130, 131, 132, 133, 88]. In 2007, Weitz and Dushoff [11] proposed another way to improve the classic predator-prey model. Their attempt was mainly based on the experimental observation that the ability of a bacteriophage to lyse hosts degrades when the bacteria approach their carrying capacity [134, 135, 136]. Adding a new term to account for the saturation of the infection of the bacteriophages, they obtained an interesting phase diagram in which the fate of the bacteria-phage community can depend on the initial conditions. However, the new term is put in by hand, based on intuition which needs detailed mathematical support. Furthermore, they focused on virulent phages and excluded the temperate ones that elicit lysogeny, now regarded as essential to the survival of microbial communities through fluctuating environments [99, 60, 103].

These works are based upon an ensemble-level description of the community, as in the classic work on predator-prey systems [137]. However, as is well-known [137], the simplest of these models fails to capture the intrinsic cyclical behavior of predator-prey populations despite apparently incorporating fully the basic interactions that should give rise to cycles. This paradox was resolved by the important work of McKane and Newman [110], who showed that cyclical effects could only be captured at the level of an individual-level model, and arose through the amplification of demographic noise. Their work showed how the conventional ensemble-level equations for predator-prey systems arose as the mean field limit of the appropriate statistical field theory, with the essential effects of demographic noise entering the analysis as one-loop corrections to mean field theory, in an inverse population size expansion. These effects can also be treated in a slightly more convenient formalism using path integrals [138]. The literature also does not have an explicit representation of lysogeny as it modifies the population dynamics of both host and phage.

The use of an individual-level model is important for a separate reason. By starting from microscopic rate processes, we can capture specific biological interactions and derive the corresponding mean-field population dynamics systematically. Such models are not always straightforward to write down phenomenologically, as

shown by the fact that the equations assumed by Weitz and Dushoff [11] are not, as we show below, the most general form that takes into account the effects of host fitness on lysis.

The purpose of this chapter and Chapter 3 is to provide a detailed theory of the population dynamics for host-phage communities. In contrast to earlier work, we pose the problem at the microscopic level, working with an individual-level model of bacteria and phage. From this fundamental description, we are able to derive the usual community level description analogous to Lotka-Volterra equations from a mean field theory. Our results encompass both virulent phages, such as those in Weitz and Dushoff's work [11], and lysogenic phages which have not been studied mathematically up to now.

In this chapter, as a preliminary exercise, to present the technique, we treat a lysis-only model applicable to lytic viruses, in which we derive a set of dynamical equations roughly in the same form as in Weitz and Dushoff's paper [11] except for an additional parameter, which generally results in a relatively unimportant shift in the phase diagram. We will extend the technique to treat the full lysogeny-lysis model applicable to lysogenic viruses in Chapter 3.

2.3 Derivation of Population Dynamics from an Individual-level Model

In this section, we adapt the classic predator-prey model to the host-phage communities from a microscopic or individual-level model. For simplicity, we first focus on two-component competition, where lysogens are excluded in spite of their biological importance. Hence, we are considering virulent phages and their hosts. Following the procedure given by McKane and Newman [110], we derive the population dynamics for the host-phage system, which Weitz and Dushoff [11] had written down phenomenologically. Here we work at the level of mean field theory, and we do not, in this chapter, include the extension necessary for representing spatial degrees of freedom. Our individual-level model formalism is still needed, however, to systematically derive the population dynamics from the microscopic interactions. In our model, the host-phage dynamics differentiates itself from the classic predator-prey model in two ways: (1) only the host population is restricted by carrying capacity due to resource limitation and (2) the lysis of one host releases a particular number of phages (for example, about 100 replicates for lambda phage [8]), instead of only one predator in the classic predator-prey model. The above two points need to be accounted for carefully in the set up of the model, especially in the introduction and application of the carrying capacity, which will be explained explicitly as follows.

In our host-phage community, we have only one species of host and one species of phage which preys upon

the former. Let us label the hosts by A and phages by B, whose populations are m and n, respectively. The hosts, either heterotrophic or autotrophic, need to consume environmental resources, which are renewable in every cycle, for survival and reproduction. All the environmental limitations on the hosts are abstracted into a maximal host population, which is denoted by the carrying capacity K. The phages, on the other hand, do not rely on the consumption of natural resources for maintenance once they are released into the environment. Thus, there is no such hard constraint on the phage population. Although phages are not restricted by K, we still introduce a virtual carrying capacity W for phages from dimensional considerations. It can be imagined that $W \to \infty$ so that no true carrying capacity is imposed on the phage population. The carrying capacities can be better visualized if we conceive space to be equally divided into K units for hosts and W units for phages. These units will be referred to as the host layer and phage layer, respectively. In the host layer, each unit is either occupied by one host or unoccupied, i.e. an empty site E. The total number of empty sites E is $K - m$. We construct the phage layer in a similar manner and denote the empty sites there by ϕ although the phage population is not confined actually.

The population dynamics of the system can thus be modeled as arising from the following six microscopic events (Table 2.2):

Table 2.2: Microscopic events in the lysis-only model.

description	symbols
birth of host	$AE \xrightarrow{b} AA$
death of host due to longevity	$A \xrightarrow{c} E$
death of host due to crowding effect	$AA \xrightarrow{d} AE$
host-phage interaction	
· under good metabolism	$AEB \xrightarrow{e} EE\alpha B$
· under poor metabolism	$AAB \xrightarrow{f} EA\beta B$
death of phage	$B \xrightarrow{g} \phi$

Here, b, c, d, e, f and g are all constant rates. All the events above are written with constraints, with a nonlinear relation being incorporated automatically by adding empty sites E to the left of the arrows to reflect the restriction of carrying capacity K. For example, the birth of the host is density dependent, which needs an empty site to accommodate the newly-born host. If no empty site is found, such an event can not happen. Since we consider only the mean field case, no spatial inhomogeneity is introduced. There is

no concept of locality here, either. As long as an empty site is found, the newly-born host is permitted. The crowding effect describes the competition in survival for limited natural resources among hosts. No such crowding effect exists for phages, which is in line with our assumption that there is no true carrying capacity confining the phage population. The two events in host-phage interaction are carefully chosen to give a minimal model while encompassing reduced lysis when the host population is approaching its carrying capacity. On the left hand side of the arrows, we use "AE" and "AA" to label the good and poor metabolic status of the host, respectively. In this way, the effect of phage infection is entangled with the metabolism of its host. On the right hand side of the arrows, α and β are the numbers of progeny for phage reproduction under good and poor metabolism, respectively. There are two primary reasons which may account for the reduced lysis effect. The first is the decrease in the phage reproduction number [134], i.e.

$$\alpha > \beta \,, \tag{2.1}$$

because phages need bacterial genetic materials, molecular machinery and energy in the synthesis of their replicates. When the normal function of the host is down-regulated, phage replication is correspondingly down-shifted. The second reason is reduced efficiency during phage infection, either in adsorption rates or viable infection, which leads to a diminishing of the infection cycle [134], i.e.

$$e > f. \tag{2.2}$$

It might seem as if the model is discrete in the representation of metabolism, since we put in good and poor metabolism by hand. However, note that the actual metabolism of the community may be somewhere between good and poor, i.e. a linear combination, depending on the probability or fraction to enter either event. Hence, the separation of good and poor metabolism is an essential part of our model, which yields the reduced lysis effect within the context of a minimal model. Finally, although phages do not age, their death can be induced by the rupture of capsids, and the corresponding rate is constant with time [2].

The time evolution of the whole community is accessed by random sampling. In each time step, we have a probability μ to draw units in the host layer and a probability ν to draw units in the phage layer. In the host layer, we may draw either one unit with probability ω or two units with probability $1-\omega$. In the phage layer, only one unit is drawn. If a combination not listed in Table 2.2 is drawn, such as EEB, nothing happens. Thus all we need to consider are the above events. Using simple combinatorics, it is straightforward to obtain the probability for the combinations as in Table 2.3), where the factor 2 accounts the equality in probability for events AE and EA, or AEB and EAB.

Table 2.3: Probabilities for the combinations in the lysis-only model.

combination	probability
A	$\mu(1-\nu)\omega\frac{m}{K}$
AA	$\mu(1-\nu)(1-\omega)\frac{m(m-1)}{K(K-1)}$
AE	$\mu(1-\nu)(1-\omega)\frac{2m(K-m)}{K(K-1)}$
AEB	$\mu\nu(1-\omega)\frac{2m(K-m)}{K(K-1)}\frac{n}{W}$
AAB	$\mu\nu(1-\omega)\frac{m(m-1)}{K(K-1)}\frac{n}{W}$
B	$(1-\mu)\nu\frac{n}{W}$

Thus we obtain the transition matrices for each kind of variation in the population during each time step, such as $\langle T(m+1,n|m,n)\rangle$, and further the evolution for the probability in the population with m hosts and n phages at time t $P(m,n,t)$. The reader is referred to Appendix A for calculational details.

The average of the population is given by summation

$$\langle m\rangle = \sum_{mn} mP(m,n,t), \tag{2.3a}$$

$$\langle n\rangle = \sum_{mn} nP(m,n,t). \tag{2.3b}$$

Thus, the time evolution for the population size is

$$\begin{aligned}\frac{d\langle m\rangle}{dt} &= \langle T(m+1,n|m,n)\rangle - \langle T(m-1,n|m,n)\rangle \\ &\quad - \langle T(m-1,n+\alpha-1|m,n)\rangle \\ &\quad - \langle T(m-1,n+\beta-1|m,n)\rangle, \end{aligned}\tag{2.4a}$$

$$\begin{aligned}\frac{d\langle n\rangle}{dt} &= (\alpha-1)\langle T(m-1,n+\alpha-1|m,n)\rangle \\ &\quad + (\beta-1)\langle T(m-1,n+\beta-1|m,n)\rangle \\ &\quad - \langle T(m,n-1|m,n)\rangle. \end{aligned}\tag{2.4b}$$

Here we have taken the mean field theory limit and neglected all the correlations and fluctuations. Omitting angle-brackets for simplicity, the equations for the evolution in population are

$$\frac{dm}{dt} = rm\left(1 - \frac{m}{K}\right) - d_m m - \phi mn\left(1 - a_m\frac{m}{K}\right), \tag{2.5a}$$

$$\frac{dn}{dt} = \gamma\phi mn\left(1 - a_n\frac{m}{K}\right) - d_n n, \tag{2.5b}$$

where

$$r = \frac{(2b+d)\mu\,(1-\nu)\,(1-\omega)}{K}, \tag{2.6a}$$

$$\phi = \frac{2e\mu\nu\,(1-\omega)}{KW}, \tag{2.6b}$$

$$\gamma = \alpha - 1, \tag{2.6c}$$

$$d_m = \frac{(c\omega + d(1-\omega))\mu\,(1-\nu)}{K}, \tag{2.6d}$$

$$d_n = \frac{(1-\mu)\,\nu}{W}, \tag{2.6e}$$

$$a_m = 1 - \frac{f}{2e}, \tag{2.6f}$$

$$a_n = 1 - \frac{\beta f}{2\alpha e}. \tag{2.6g}$$

Considering Eq. (2.1), we notice that Eq. (2.6f) (2.6g) yield the following relation

$$0 < a_m < a_n < 1. \tag{2.7}$$

Generally speaking, $a_m \neq a_n$ unless

$$\alpha = \beta, \tag{2.8}$$

which implies that the reproduction numbers under good and poor metabolism are the same as in Weitz and Dushoff's model. This concludes the derivation of the equations for population dynamics from the individual or microscopic level.

2.4 Results

In this section we explore the predictions of the lysis-only model given by Eq. (2.5).

Let

$$t' = \frac{rt}{a_m}, \tag{2.9a}$$
$$\phi' = \frac{\phi\gamma K}{r}, \tag{2.9b}$$
$$d_n' = \frac{a_m d_n}{r}, \tag{2.9c}$$
$$d_m' = \frac{a_m d_m}{r} + 1 - a_m, \tag{2.9d}$$
$$m' = a_m \frac{m}{K}, \tag{2.9e}$$
$$n' = \frac{a_m n}{\gamma K}, \tag{2.9f}$$
$$a_n' = \frac{a_n}{a_m}. \tag{2.9g}$$

We can non-dimensionalize the evolution equations (2.5). Omitting the primes we obtain

$$\frac{dm}{dt} = m\,(1-m) - \phi m n\,(1-m) - d_m m, \tag{2.10a}$$
$$\frac{dn}{dt} = \phi m n\,(1 - a_n m) - d_n n. \tag{2.10b}$$

Setting

$$\frac{dm}{dt} = 0, \tag{2.11a}$$
$$\frac{dn}{dt} = 0, \tag{2.11b}$$

we obtain three fixed points. The first is a trivial fixed point

$$m = 0, \tag{2.12a}$$
$$n = 0, \tag{2.12b}$$

which is stable when

$$d_m > 1. \tag{2.13}$$

The second corresponds to the phage extinction phase

$$m = 1 - d_m, \tag{2.14a}$$

$$n = 0, \tag{2.14b}$$

which is stable when

$$0 < d_m < 1 - \frac{1}{a_n} \tag{2.15}$$

or

$$1 - \frac{1}{a_n} < d_m < 1, \tag{2.16}$$

$$\frac{\phi}{d_n} < \frac{1}{(1 - d_m)\left[1 - a_n\left(1 - d_m\right)\right]}. \tag{2.17}$$

The last is the coexistence of hosts and phages

$$m = \rho, \tag{2.18a}$$

$$n = \frac{1}{\phi}\left(1 + \frac{d_m}{\rho - 1}\right), \tag{2.18b}$$

where ρ is a root of

$$a_n \phi \rho^2 - \phi\rho + d_n = 0. \tag{2.19}$$

The coexistence phase comes into existence and will be stable when

$$\frac{\phi}{d_n} \geq 4a_n, \tag{2.20}$$

$$d_m < 1 - \rho. \tag{2.21}$$

The stability of the fixed points are governed by the Jacobian

$$\begin{pmatrix} (1 - 2m)(1 - \phi n) - d_m & -\phi m (1 - m) \\ \phi n (1 - 2a_n m) & \phi m (1 - a_n m) - d_n \end{pmatrix} \tag{2.22}$$

to the equations

$$m\,(1-m) - \phi mn\,(1-m) - d_m m = 0, \tag{2.23a}$$

$$\phi mn\,(1-a_n m) - d_n n = 0. \tag{2.23b}$$

Thus we obtain the three-dimensional phase diagram plotted in Figure 2.2. The basin of attraction for the trivial case is not plotted. Region II is the basin of attraction for coexistence fixed point only while region III is that for the phage extinction. Region I will either go to coexistence or phage extinction, depending on the initial conditions.

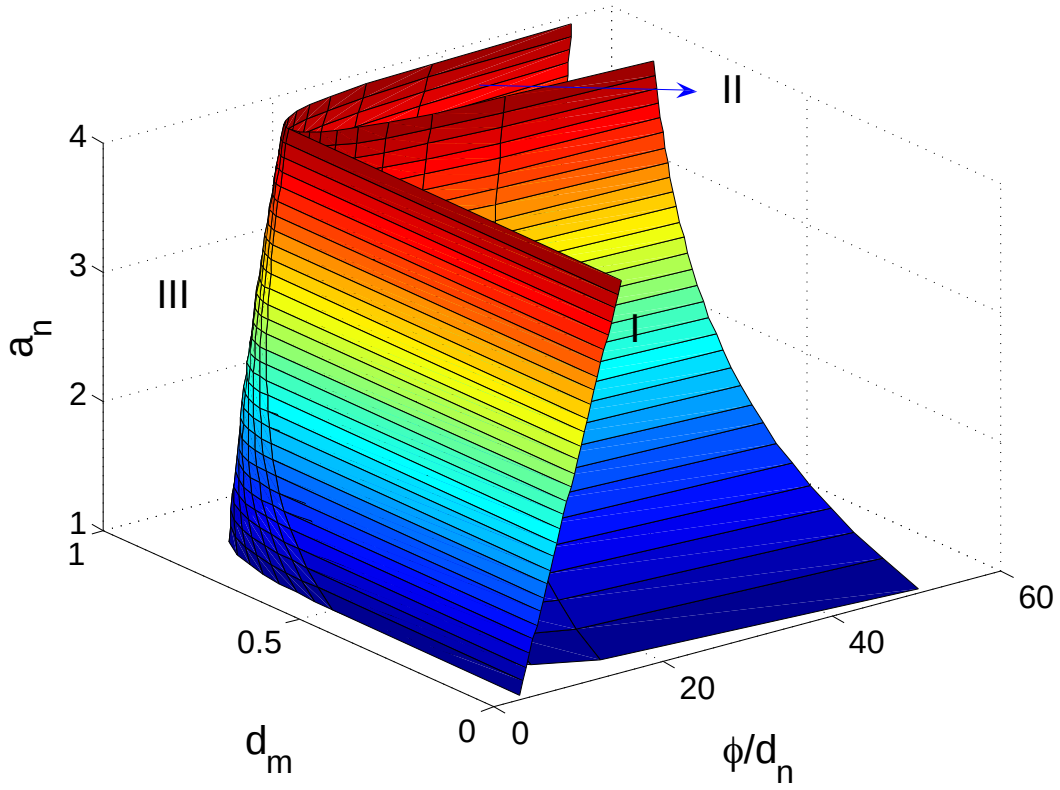

Figure 2.2: Three dimensional phase diagram for the lysis-only model. Region I depends on the initial conditions to flow to the phage extinction or coexistence fixed point. Region II and III are basins of attraction for coexistence and phage extinction fixed points, respectively.

2.5 Discussions and Conclusion

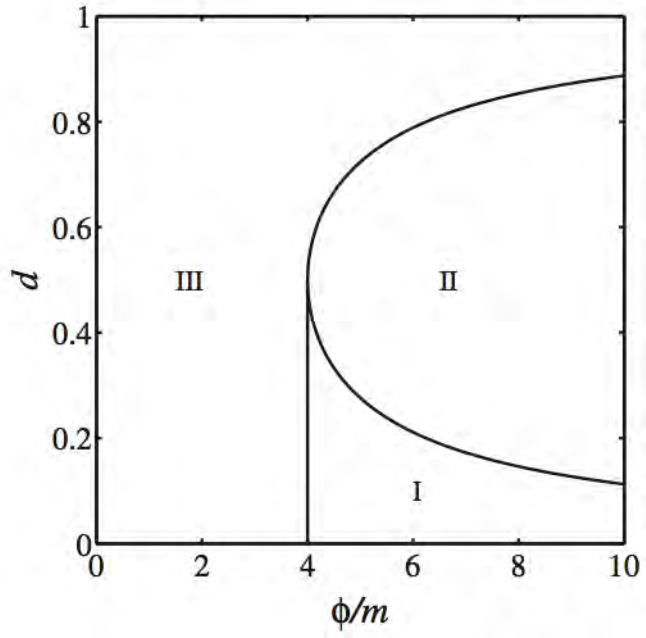

Figure 2.3: Phase diagram in Weitz and Dushoff's model. d, m and ϕ are dimensionless death rates for the host and phage, and their coupling coefficient, corresponding to d_m, d_n and ϕ in our model, respectively. Region I, II, and III have the same meanings as in Figure 2.2. After Ref. [11].

As we can see, the bottom plane in Figure 2.2 corresponds to the phase diagram in Weitz and Dushoff's model as shown in Figure 2.3, where $a_n = 1$. When

$$\alpha > \beta \tag{2.24}$$

leading to

$$a_n > 1, \tag{2.25}$$

there is a shift in the phase diagram with a rapid shrinkage of the basin of attraction for region II, where any initial condition flows to the coexistence phase. The boundary between region I and III also moves to larger $\frac{\phi}{d_n}$, which implies that the more the good and poor metabolisms differ from each other in the progeny number, the easier the phages are driven out of the system. In order to see the effect of the phase shift more clearly, let us tune $a_n = 1.3$ while keeping all the other parameters as those in Figure 2 (I) in Weitz and Dushoff's paper [11] (Figure 2.4). When $a_n = 1$, there is a neutral fixed point for coexistence. However, such a fixed point disappears (Figure 2.5) when $a_n = 1.3$. The flow diagrams are generated by 4^{th} order

Runge-Kutta method.

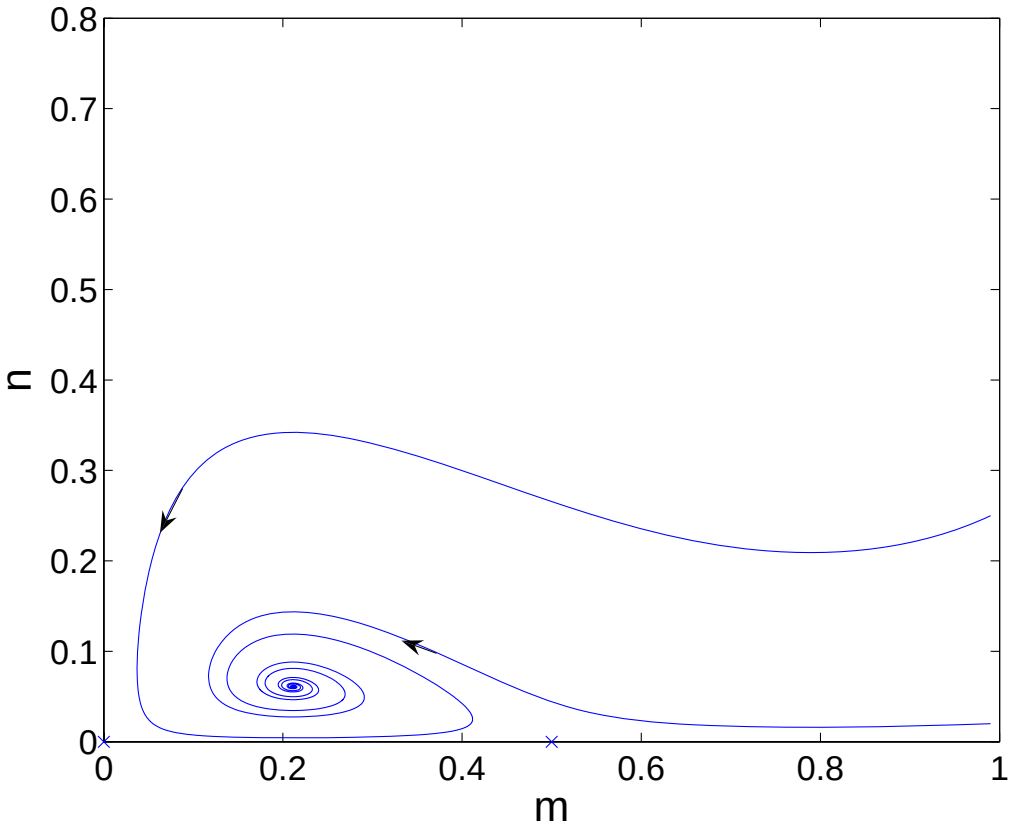

Figure 2.4: Flow diagram for $a_n = 1, \phi = 5, d_n = 1, d_m = 0.1$. "$\times$" denotes saddle points and "$\cdot$" is for stable fixed points.

In summary, we have obtained Weitz and Dushoff's model by detailed derivation from the individual or microscopic level and found a small shift in the phase diagram. Such a shift, as we see, can be observed experimentally by the onset of coexistence for the two species.

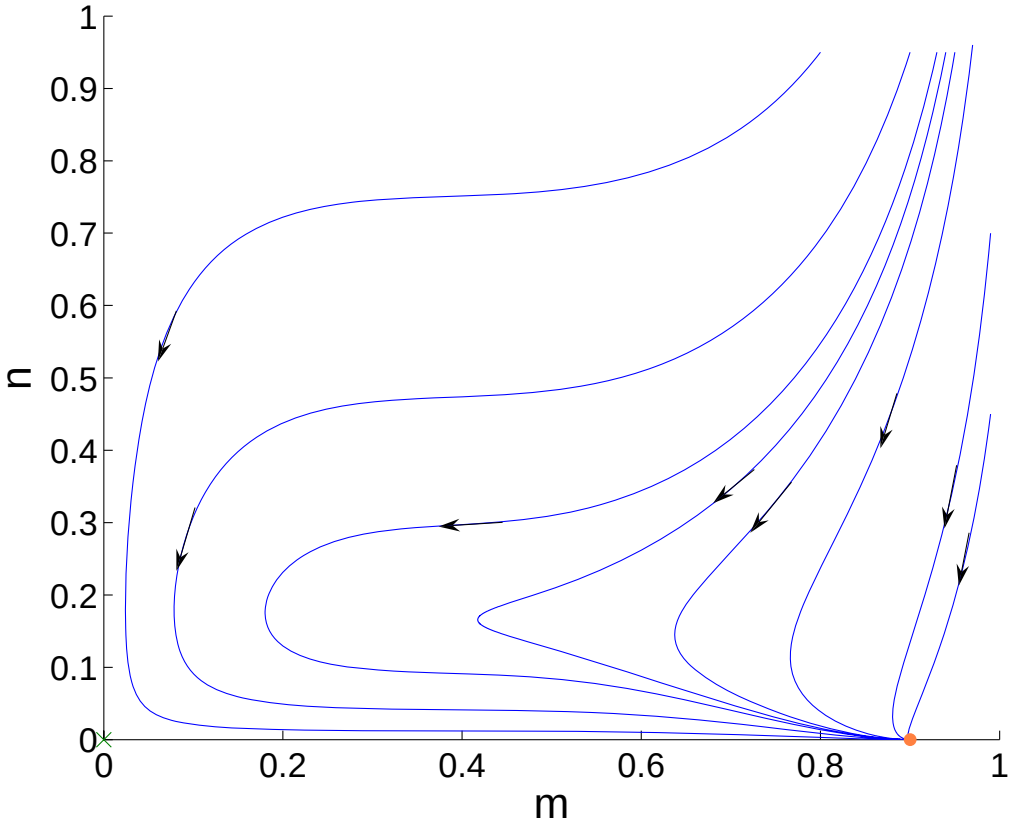

Figure 2.5: Flow diagram for $a_n = 1.3, \phi = 5, d_n = 1, d_m = 0.1$. "$\times$" denotes saddle points and "$\cdot$" is for stable fixed points.

Chapter 3

Population Dynamics of Lysogenic Viruses and Their Hosts

3.1 Introduction

In Chapter 2, we present the technique to systematically derive mean-field population dynamics for lytic viruses and their hosts using an individual-level model of microscopic rate processes. In this chapter, we continue to develop the formalism for the community of hosts and phages in the full lysogeny-lysis model. Interestingly, we find that for certain combination of parameters, the community exhibits a limit cycle for all the species in the phase space, even at the level of mean field theory. In order to interpret the corresponding range of parameters in a useful way for experimental observations, we map the parameters to rates in chemical reactions. In order to explore the robustness of our results, we demonstrate in Section 3.6 that the corresponding limit cycle arises also in stochastic simulations with the Gillespie algorithm. Finally, in Section 3.7 we estimate the feasibility of verifying our predictions in laboratory experiments.

3.2 Derivation of Population Dynamics from an Individual-level Model

In this section, we extend the lysis-only model in Chapter 2 to incorporate lysogeny and investigate the important role of lysogeny in host-phage dynamics. Now there are three types of organism in the community. There are "healthy" hosts, which have no integration of phage genes, lysogens, and free phages, which live outside bacteria membranes. We will label "healthy" hosts, lysogens and free phages by A, D, and B, respectively, with population sizes m, s and n. For the same reasons as in the lysis-only model, hosts and phages are thought of as being confined in different layers characterized by different carrying capacities. Hence both "healthy" hosts and lysogens are in the host layer with a total carrying capacity K. The empty sites in the host layer are denoted by E and their number is $K - m - s$. In the phage layer, the empty sites are labelled by ϕ as before.

The incorporation of lysogens brings us more microscopic events. There are two pathways after phage

infections: lysis and lysogeny. Immediate lysis for temperate phages is the same process as for virulent ones, which has been characterized by events in the previous section. Lysogeny is an option only for temperate phages, which will be investigated in detail here. First, there should be an event corresponding to lysogen formation, i.e. a phage integrates its DNA into the genome of the host and turns itself into a prophage. Second, lysogens will survive, replicate and die as "healthy" hosts. Last, environments might trigger prophage induction, which lyses the lysogen and releases the prophages inside. In all, there are eighteen microscopic events, which are listed in Table 3.1.

Table 3.1: Microscopic events in the lysogeny-lysis model.

description	symbols
birth of host	$AE \xrightarrow{b} AA$
	$DE \xrightarrow{b} DD$
death of host due to longevity	$A \xrightarrow{c} E$
	$D \xrightarrow{c} E$
death of host due to crowding	$AA \xrightarrow{d} AE$
	$DD \xrightarrow{d} DE$
	$AD \xrightarrow{\frac{1}{2}d} DE$
	$AD \xrightarrow{\frac{1}{2}d} AE$
host-phage interactions	
· lysis under good metabolism	$AEB \xrightarrow{e} EE\alpha B$
· lysis under poor metabolism	$AAB \xrightarrow{f} EA\beta B$
	$ADB \xrightarrow{f} ED\beta B$
· lysogeny under good metabolism	$AEB \xrightarrow{h} DE$
· lysogeny under poor metabolism	$AAB \xrightarrow{k} DA$
	$ADB \xrightarrow{k} DD$
prophage induction	
· under good metabolism	$DE \xrightarrow{p} EE\alpha B$
· under poor metabolism	$DD \xrightarrow{q} DE\beta B$
	$DA \xrightarrow{q} AE\beta B$
death of free phage	$B \xrightarrow{g} \phi$

Here b, c, d, e, f, g, h, k, p and q are constant reaction rates. α and β are phage reproduction numbers

under good and poor metabolisms, respectively. Although prophage induction enhances the survival ability for lysogens in several ways, such as suppressing the latter's metabolism [60] through down-regulation [139], for simplicity we have assumed the same birth and death rates for "healthy" hosts and lysogens. We have the condition

$$\alpha > \beta\,, \tag{3.1}$$

as before. Furthermore, there are the following advantages under better metabolism: more successful and effective infection (Eq. (3.2a)), greater possibility to lyse the host (Eq. (3.2b)), and faster prophage release (Eq. (3.2c)). Since the mechanism for the lysis-lysogeny decision making of initial infection is different from the genetic switch for prophage induction [8, 140] , we do not expect any special relationship between e and f, and p and q. These advantages can be expressed mathematically by the following inequalities:

$$e + h > f + k, \tag{3.2a}$$

$$\frac{e}{h} > \frac{f}{k}, \tag{3.2b}$$

$$p > q. \tag{3.2c}$$

We draw events from the two layers the same way as in the lysis-only model and this results in the probabilities shown in Table 3.2.

From these events, we obtain the following evolution equations for all the three species after the calculations provided in Appendix B:

$$\frac{dm}{dt} = rm\left(1 - \frac{m+s}{K}\right) - d_1 m - \phi_1 mn\left\{1 - \frac{1}{K}\left[(1-a_1)\,m + (1-2a_1)\,s\right]\right\}, \tag{3.3a}$$

$$\begin{aligned}\frac{ds}{dt} = {} & rs\left(1 - \frac{m+s}{K}\right) - d_1 s + \phi_2 mn\left\{1 - \frac{1}{K}\left[(1-a_{21})\,m + (1-2a_{21})\,s\right]\right\} \\ & - d_2 s\left\{1 - \frac{1}{K}[(1-2a_{22})\,m + (1-a_{22})\,s]\right\},\end{aligned} \tag{3.3b}$$

$$\begin{aligned}\frac{dn}{dt} = {} & [(\alpha-1)\,\phi_1 - \alpha\phi_2]\,mn\left\{1 - \frac{1}{K}\left[(1-a_{31})\,m + (1-2a_{31})\,s\right]\right\} \\ & + \alpha d_2 s\left\{1 - \frac{1}{K}\left[(1-2a_{32})\,m + (1-a_{32})\,s\right]\right\} - d_3 n,\end{aligned} \tag{3.3c}$$

where

$$r = \frac{(2b+d)\mu\,(1-\nu)\,(1-\omega)}{K}, \tag{3.4a}$$

Table 3.2: Probabilities for the combinations in the lysogeny-lysis model.

combination	probability
AE	$\mu\,(1-\nu)\,(1-\omega)\,\dfrac{2m\,(K-m-s)}{K\,(K-1)}$
DE	$\mu\,(1-\nu)\,(1-\omega)\,\dfrac{2s\,(K-m-s)}{K\,(K-1)}$
A	$\mu\,(1-\nu)\,\omega\dfrac{m}{K}$
D	$\mu\,(1-\nu)\,\omega\dfrac{s}{K}$
AA	$\mu\,(1-\nu)\,(1-\omega)\,\dfrac{m\,(m-1)}{K\,(K-1)}$
DD	$\mu\,(1-\nu)\,(1-\omega)\,\dfrac{s\,(s-1)}{K\,(K-1)}$
AD	$\mu\,(1-\nu)\,(1-\omega)\,\dfrac{2ms}{K\,(K-1)}$
AEB	$\mu\nu\,(1-\omega)\,\dfrac{2m\,(K-m-s)}{K\,(K-1)}\dfrac{n}{W}$
AAB	$\mu\nu\,(1-\omega)\,\dfrac{m\,(m-1)}{K\,(K-1)}\dfrac{n}{W}$
ADB	$\mu\nu\,(1-\omega)\,\dfrac{2ms}{K\,(K-1)}\dfrac{n}{W}$
B	$(1-\mu)\,\nu\dfrac{n}{W}$

$$d_1 = \frac{(c\omega + d(1-\omega))\mu\,(1-\nu)}{K}, \tag{3.4b}$$

$$d_2 = \frac{2p\mu\,(1-\nu)\,(1-\omega)}{K}, \tag{3.4c}$$

$$d_3 = \frac{(1-\mu)\,\nu}{W}, \tag{3.4d}$$

$$\phi_1 = \frac{2(e+h)\mu\nu\,(1-\omega)}{KW}, \tag{3.4e}$$

$$\phi_2 = \frac{2h\mu\nu\,(1-\omega)}{KW}, \tag{3.4f}$$

$$a_1 = \frac{f+k}{2(e+h)}, \tag{3.4g}$$

$$a_{21} = \frac{k}{2h}, \tag{3.4h}$$

$$a_{22} = \frac{q}{2p}, \tag{3.4i}$$

$$a_{31} = \frac{\beta f - k}{2(\alpha e - h)}, \tag{3.4j}$$

$$a_{32} = \frac{\beta q}{2\alpha p}. \tag{3.4k}$$

We note that

$$\phi_2 < \phi_1, \tag{3.5}$$

$$0 < a_1, a_{21}, a_{22}, a_{31}, a_{32} < 1, \tag{3.6}$$

$$a_{32} < a_{22}. \tag{3.7}$$

We also notice some kind of symmetry in the correction terms such as "$1 - a_1$" and "$1 - 2a_1$". a_1 originates from the poor metabolism of hosts A, which indirectly downshifts the efficiency of phage infection and synthesis. In equation (3.3a), "a_1" comes from the event $AAB \xrightarrow{f} EA\beta B$, while "$2a_1$" is from $ADB \xrightarrow{f} ED\beta B$. The factor "2" appears since "AD" is the same as "DA".

Considering

$$\alpha \gg 1, \tag{3.8}$$

for example,

$$\alpha \approx 100 \tag{3.9}$$

for lambda phage [8], we approximate

$$(\alpha - 1)\,\phi_1 - \alpha\phi_2 \approx \alpha\,(\phi_1 - \phi_2)\,. \tag{3.10}$$

Hence equation (3.3c) can be simplified as

$$\frac{dn}{dt} = \alpha\left(\phi_1 - \phi_2\right) mn\left\{1 - \frac{1}{K}\left[\left(1 - a_{31}\right) m + \left(1 - 2a_{31}\right) s\right]\right\}$$
$$+ \alpha d_2 s\left\{1 - \frac{1}{K}\left[\left(1 - 2a_{32}\right) m + \left(1 - a_{32}\right) s\right]\right\} - d_3 n. \tag{3.11}$$

3.3 Results

In this section, we explore the predictions of the lysogeny-lysis model given by equations (3.3a), (3.3b) and (3.11).

Let

$$t' = rt, \tag{3.12a}$$
$$\phi_1' = \frac{\alpha\phi_1 K}{r}, \tag{3.12b}$$
$$\phi_2' = \frac{\alpha\phi_2 K}{r}, \tag{3.12c}$$
$$d_1' = \frac{d_1}{r}, \tag{3.12d}$$
$$d_2' = \frac{d_2}{r}, \tag{3.12e}$$
$$d_3' = \frac{d_3}{r}, \tag{3.12f}$$
$$m' = \frac{m}{K}, \tag{3.12g}$$
$$s' = \frac{s}{K}, \tag{3.12h}$$
$$n' = \frac{n}{\alpha K}, \tag{3.12i}$$

and omitting the primes, the equations after non-dimensionalization become

$$\frac{dm}{dt} = m\left(1 - m - s\right) - d_1 m - \phi_1 mn\left[1 - \left(1 - a_1\right) m - \left(1 - 2a_1\right) s\right], \tag{3.13a}$$
$$\frac{ds}{dt} = s\left(1 - m - s\right) - d_1 s + \phi_2 mn\left[1 - \left(1 - a_{21}\right) m - \left(1 - 2a_{21}\right) s\right]$$
$$- d_2 s\left[1 - \left(1 - 2a_{22}\right) m - \left(1 - a_{22}\right) s\right], \tag{3.13b}$$
$$\frac{dn}{dt} = \left(\phi_1 - \phi_2\right) mn\left[1 - \left(1 - a_{31}\right) m - \left(1 - 2a_{31}\right) s\right]$$
$$+ d_2 s\left[1 - \left(1 - 2a_{32}\right) m - \left(1 - a_{32}\right) s\right] - d_3 n. \tag{3.13c}$$

Formally, the fixed points can be solved by requiring that

$$\frac{dm}{dt} = 0, \tag{3.14a}$$
$$\frac{ds}{dt} = 0, \tag{3.14b}$$
$$\frac{dn}{dt} = 0. \tag{3.14c}$$

However, we can only obtain four fixed points analytically. The first is the trivial case for the extinction of all the species

$$m = 0, \tag{3.15a}$$
$$s = 0, \tag{3.15b}$$
$$n = 0. \tag{3.15c}$$

The second is the "healthy" host extinction fixed point

$$m = 0, \tag{3.16a}$$
$$s = \frac{1 - d_1 - d_2}{1 - d_2\,(1 - a_{22})}, \tag{3.16b}$$
$$n = \frac{d_2}{d_3} s\,[1 - (1 - a_{32})\,s]\,. \tag{3.16c}$$

The third is the "healthy" host only fixed point

$$m = 1 - d_1, \tag{3.17a}$$
$$s = 0, \tag{3.17b}$$
$$n = 0. \tag{3.17c}$$

The last is the lysogen extinction

$$m = \frac{1}{1 - a_{21}}, \tag{3.18a}$$
$$s = 0, \tag{3.18b}$$
$$n = \frac{1 - m - d_1}{\phi_1\,[1 - (1 - a_1)\,m]}, \tag{3.18c}$$

whose existence requires that

$$(\phi_1 - \phi_2)(a_{31} - a_{21}) = d_3 (1 - a_{21})^2 . \tag{3.19}$$

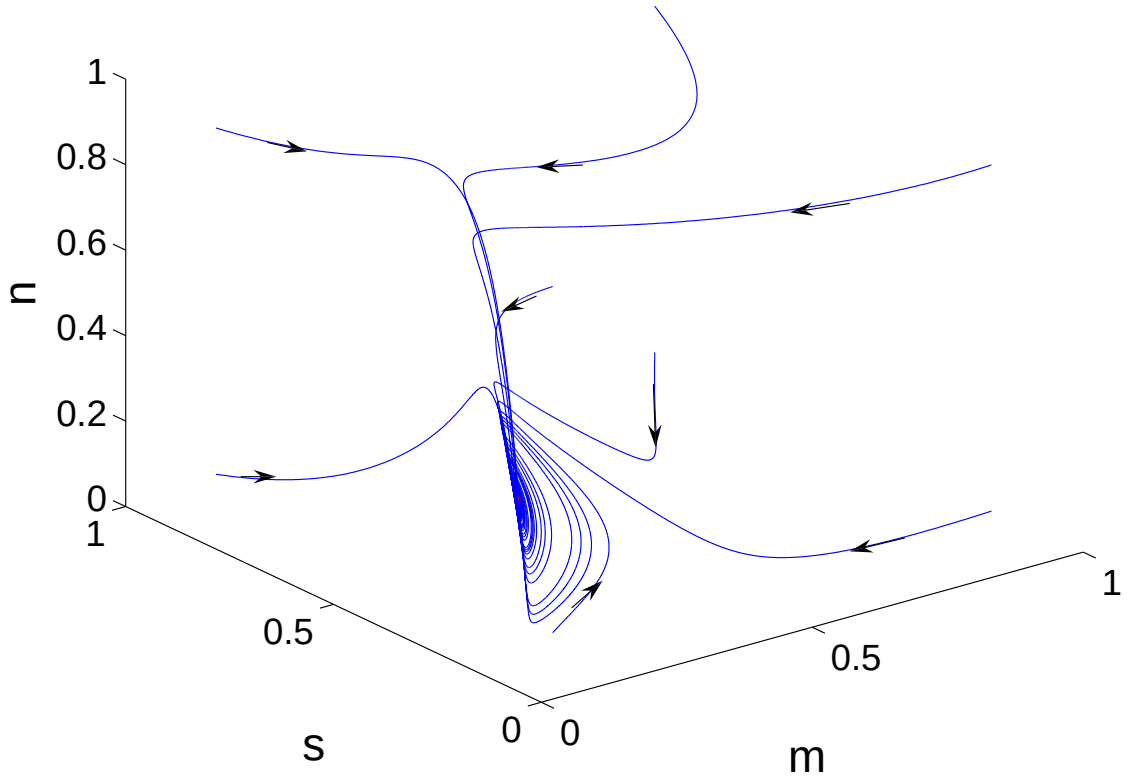

Figure 3.1: In the lysogeny-lysis model, a stable fixed point for the coexistence of all the three species. The parameters are $\phi_1 = 1, \phi_2 = 0.8, d_1 = 0.5, d_2 = 0.49, d_3 = 0.1, a_1 = a_{21} = a_{31} = 0.1, a_{22} = a_{32} = 0.5$.

The more interesting coexistence of all the three species is hard to solve analytically since the order of the equations

$$m(1 - m - s) - d_1 m - \phi_1 mn[1 - (1 - a_1) m - (1 - 2a_1) s] = 0, \tag{3.20a}$$

$$s(1 - m - s) - d_1 s + \phi_2 mn[1 - (1 - a_{21}) m - (1 - 2a_{21}) s]$$

$$- d_2 s[1 - (1 - 2a_{22}) m - (1 - a_{22}) s] = 0, \tag{3.20b}$$

$$(\phi_1 - \phi_2) mn[1 - (1 - a_{31}) m - (1 - 2a_{31}) s]$$

$$+ d_2 s[1 - (1 - 2a_{32}) m - (1 - a_{32}) s] - d_3 n = 0, \tag{3.20c}$$

is too high. Using a 4^{th} order Runge-Kutta method, we found numerically a stable fixed point, shown in Figure 3.1.

3.4 Discussion

As shown in Eq. (3.13), there are, in total, ten parameters so that the phase space is difficult to visualize. We have studied the general trend of the transition between phases, starting with the dependence on phage mortality rate d_3. In Figure 3.2, it is shown that when the phage mortality rate is low, the systems flows into a "healthy" host extinction phase. The phage population decreases with increase in the phage mortality rate, which is very reasonable physically. For intermediate values of d_3, there is coexistence for all the three species, while for large values of d_3, the only survival is "healthy" host, where all phages die out quickly out, leading to the extinction of lysogens.

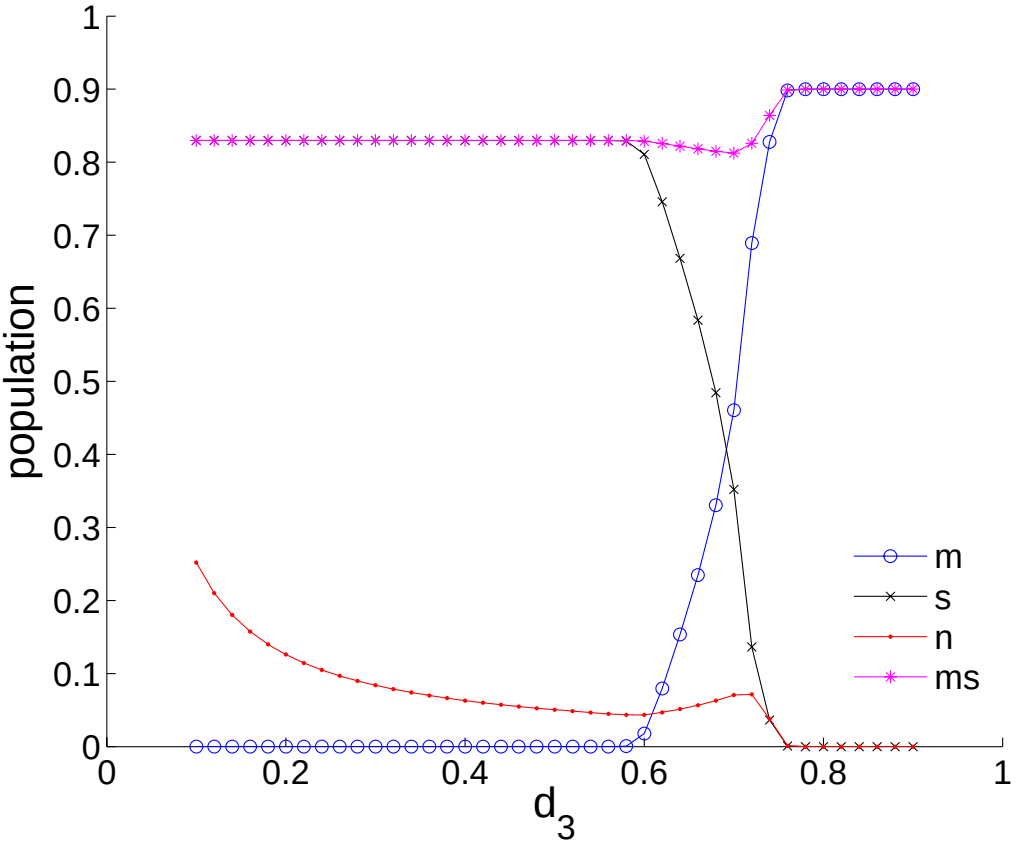

Figure 3.2: The population of the community with increasing phage mortality rate d_3. "ms" indicates the sum of m and s.

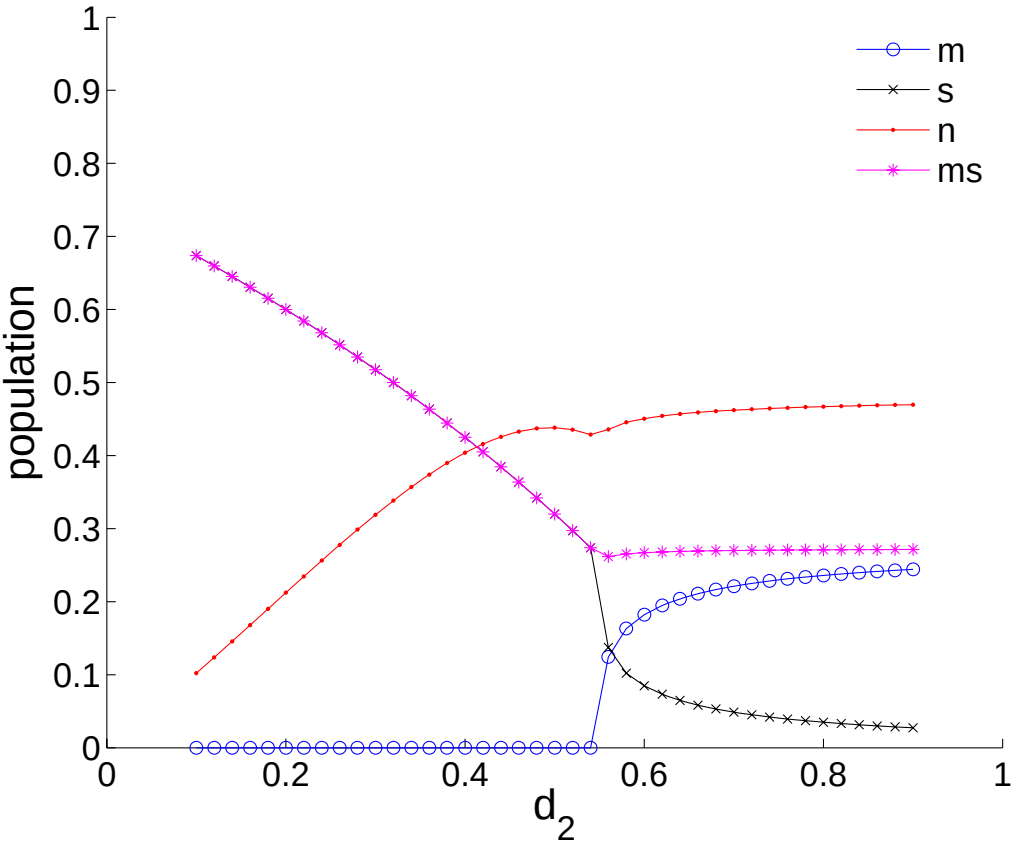

Figure 3.3: The population for the community with the increase in the lysis rate d_2.

We show the trend of the population with increasing lysis rate d_2 in Figure 3.3. The phage prospers with the increase in the lysis rate, while the lysogen diminishes. The peak in the phage population appears when there is a balance in the number of lysogens available to lyse and the lysis rate. When the lysis rate is beyond the threshold at 0.54, lysogen number falls dramatically and there is a proliferation of "healthy" hosts. The total host population is roughly the same afterwards while the phage population upshifts a little with the increase in the "healthy" host available to infect but does not change further when the ratio between "healthy" hosts and lysogens converges.

We have studied the effect of host mortality rate in Figure 3.4. Obviously the total host population will fall monotonically when the hosts are more likely to die. We draw attention to the interesting peak in the phage population. When the host mortality rate is low, the phage population is suppressed due to the overcrowding of the lysogens, which degrades the metabolism and hence the infection and synthesis of phages. When the host mortality rate is high, on the other hand, the phages have insufficient hosts to infect and their population also declines.

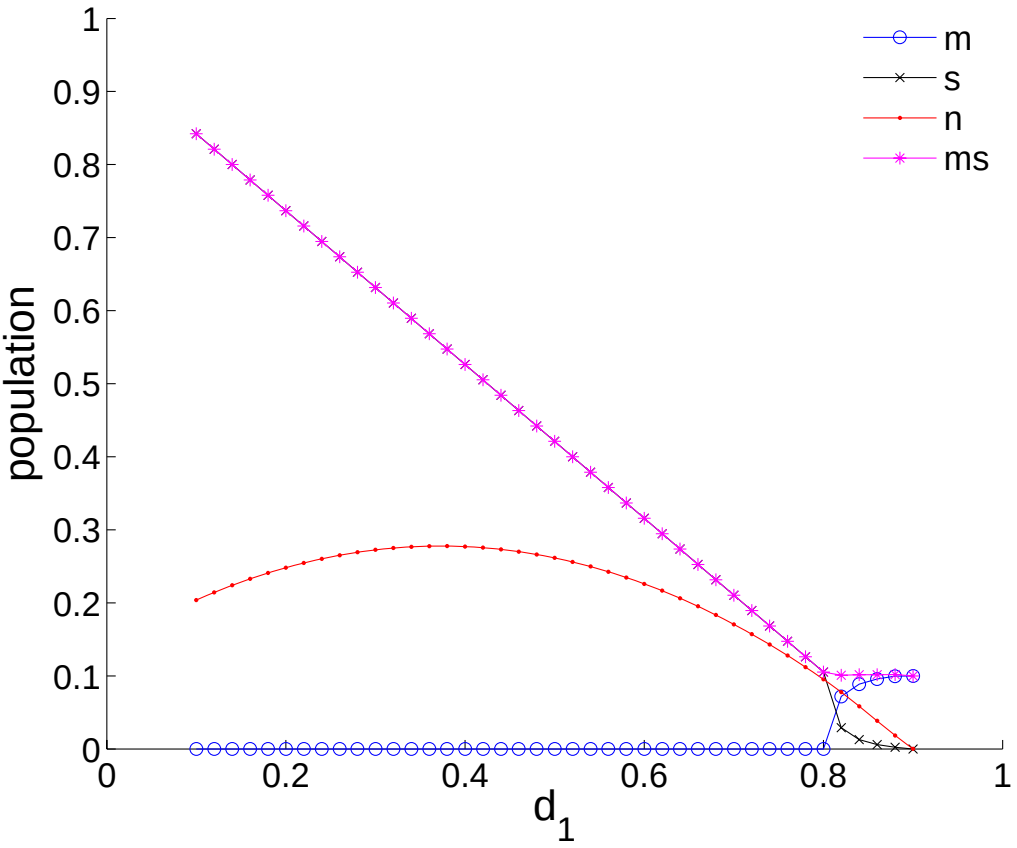

Figure 3.4: The population for the community with the increase in the host mortality rate d_1.

3.5 Existence of a limit cycle

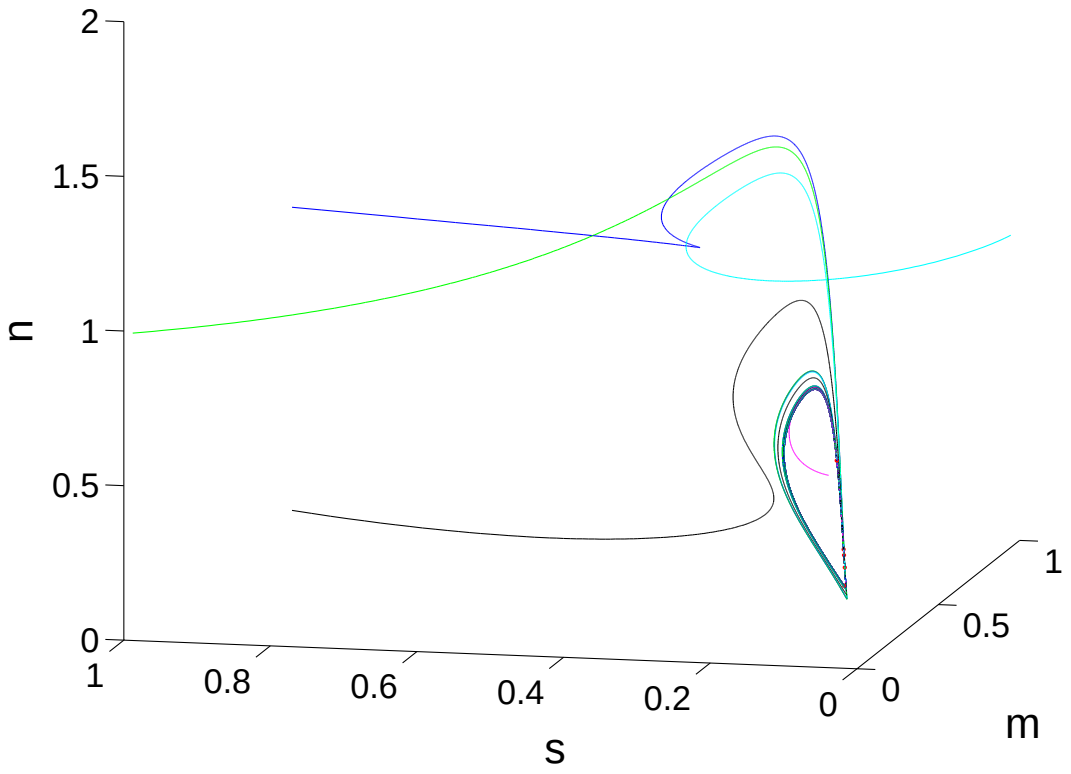

Figure 3.5: A limit cycle in the flow diagram for different initial conditions with parameters $\phi_1 = 1, \phi_2 = 0.8, d_1 = 0.5, d_2 = 0.49, d_3 = 0.03, a_1 = a_{21} = a_{31} = 0.1, a_{22} = a_{32} = 0.5$.

We have noticed that the dynamics exhibits a limit cycle [141, 142] for some combination of parameters (Figure 3.5). In this section, we describe our numerical evidence for this assertion and present a plausible physical interpretation of our finding. In order to verify that it is a limit cycle instead of some unexpected slowing down near a putative stable or neutral fixed point, we have chosen an initial condition located inside the conjectured limit cycle. If there is, in fact, no real limit cycle, the dynamics will flow inwards no matter how slow it will be. However, as we can see in Figure 3.6, the trajectory indicated by the red curve flows out. Hence we have observed in the flow diagram an oscillation in the population for all the three species. If we inspect neighboring time steps, it appears that the convergence is slow, since the deviation from step to step is very small. However, on longer time scales, we can see that the convergence is an

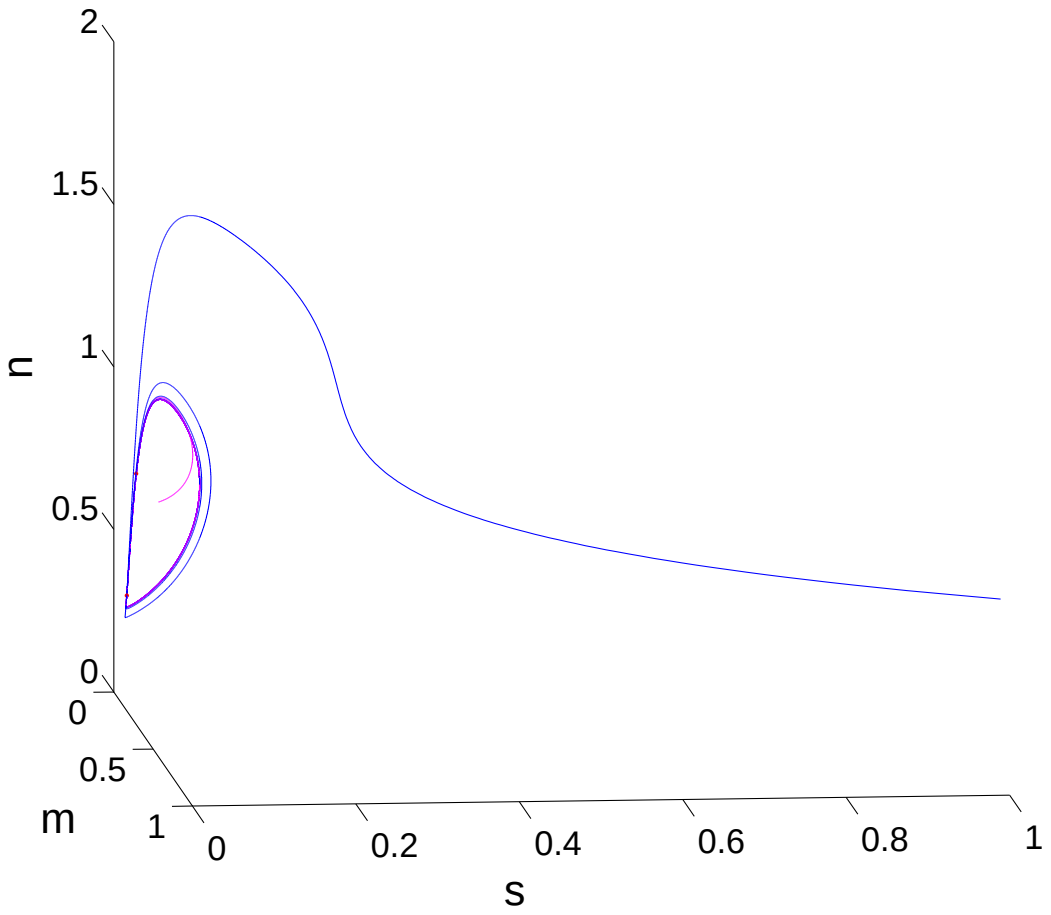

Figure 3.6: A limit cycle in the flow diagram with different initial conditions for parameters $\phi_1 = 1, \phi_2 = 0.8, d_1 = 0.5, d_2 = 0.49, d_3 = 0.03, a_1 = a_{21} = a_{31} = 0.1, a_{22} = a_{32} = 0.5$. The limit cycle is in a curved space. The blue curve initiated outside the cycle flows in while the red one from inside flows out.

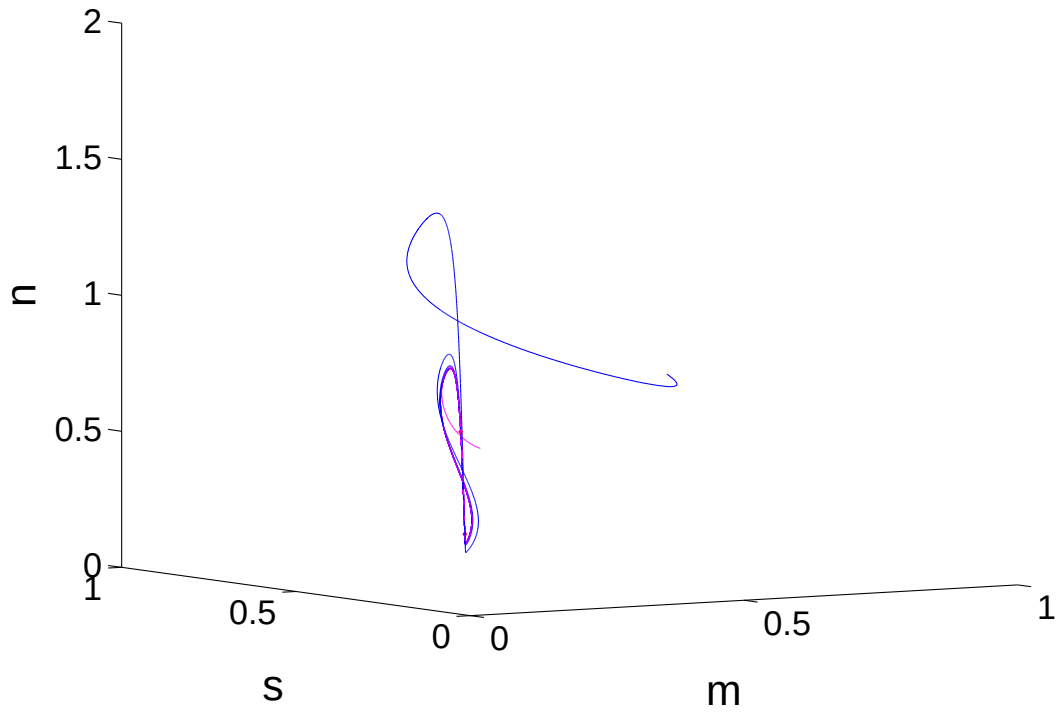

Figure 3.7: A limit cycle in the flow diagram with different initial conditions for parameters $\phi_1 = 1, \phi_2 = 0.8, d_1 = 0.5, d_2 = 0.49, d_3 = 0.03, a_1 = a_{21} = a_{31} = 0.1, a_{22} = a_{32} = 0.5$. The limit cycle is in a curved space.

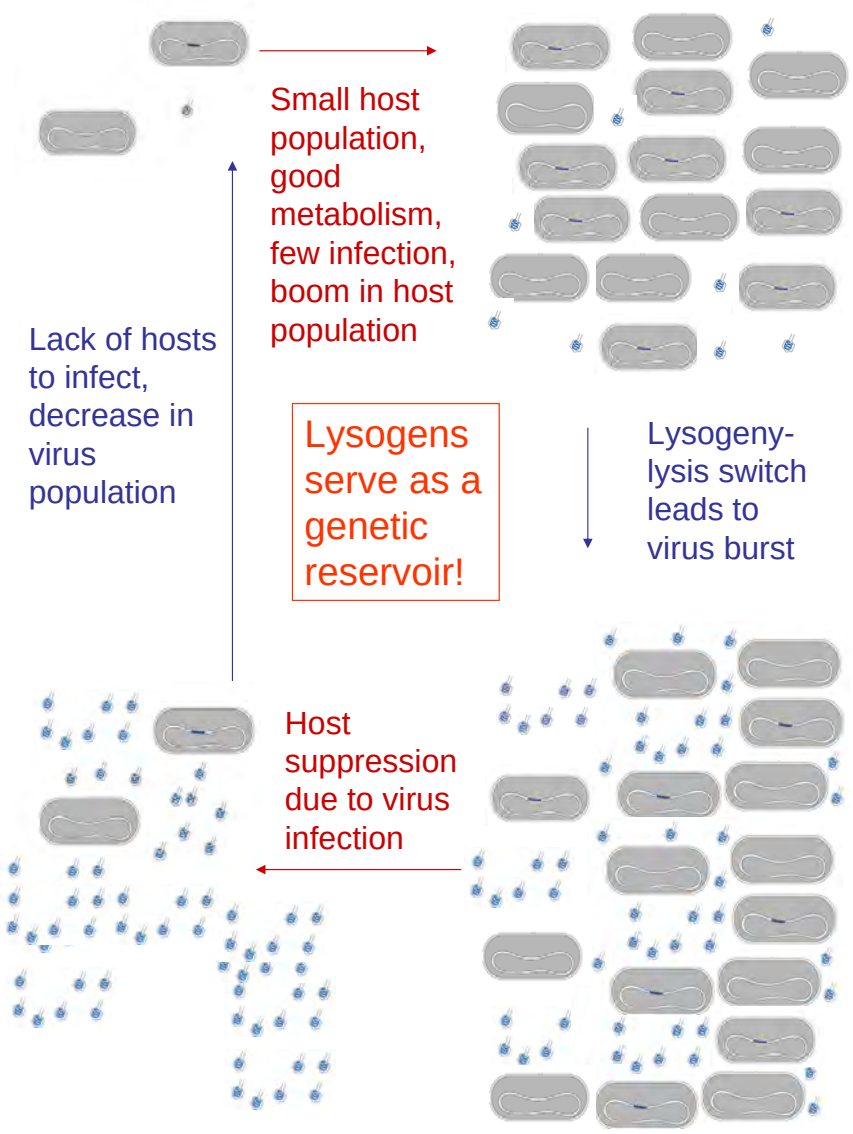

Figure 3.8: Cartoon explanation for the limit cycle. When the population for host and phages are both small, the host will enjoy a boom because of good metabolism and little phage infection. Meanwhile prophages replicate with the fast reproduction of lysogens. Once the lysogeny-lysis switch is triggered, the destruction of lysogens will yield a huge virus burst. Then "healthy" host will encounter intensive phage infection and hence be suppressed. When most of the host die out, phage population shrinks quickly due to lack of infection. In this way, a cycle forms.

illusion. Moreover, tilting the view angle, we see that the limit cycle is in some curved space instead of a single plane in Figure 3.7. In order to investigate the emergence of the limit cycle, we have scanned part of the parameter space. For example, there is a stable coexistence fixed point for $d_1 > 0.41$ while $\phi_1 = 1, \phi_2 = 0.8, d_2 = 0.9, d_3 = 0.048, a_1 = a_{21} = a_{31} = 0.1$, and $a_{22} = a_{32} = 0.5$. However, the above fixed point becomes unstable if $d_1 < 0.41$ leading to the limit cycle. As we see it, such an oscillation of the population in the community is a manifestation of the role of lysogens (Figure 3.8). When the population for host and phages are both small, the host will enjoy a boom because of good metabolism and little phage infection. Meanwhile prophages replicate with the fast reproduction of lysogens. Once the lysogeny-lysis switch is triggered, the destruction of lysogens will yield a huge virus burst. Then "healthy" host will encounter intensive phage infection and hence be suppressed. When most of the host die out, phage population shrinks quickly due to lack of infection. In this way, a cycle forms. Integrating its DNA into the genome of a lysogen, a prophage is sheltered although it is temporarily dormant in the sense of viral infection. Such a stage assists prophages to survive demanding environmental conditions and provides an opportunity to resurrect the population when there are abundant "healthy" hosts. Thus lysogens are perfect genetic reservoirs for phages for potential future burst [51, 60].

3.6 Stochastic simulation

Up to now, all the calculations above were carried out within the scope of mean field theory. As a next step, it is important to see to what extent such predictions are disturbed by demographic fluctuations, and especially whether the limit cycle in the lysogeny-lysis model is stable. A second goal of this section is to link the parameters the parameters in our model to those which could characterize real experiments. In this section, we perform stochastic simulations using the Gillespie's algorithm [143, 144], which is a very efficient strategy to simulate chemical reactions. The reaction rates (b, c, d,e, f and g in Table 2.2, and b, c, d, e, f, g, h, k, p and q in Table 3.1) are interpreted as average probability rates for the occurrence of the corresponding reactions in line with the Gillespie algorithm, where the effect of draw probability is incorporated automatically.

In the lysis-only model, the map between the two sets of parameters for reactions is

$$\widetilde{b} = bK, \tag{3.21a}$$

$$\widetilde{c} = c, \tag{3.21b}$$

$$\widetilde{d} = \frac{1}{2} dK, \tag{3.21c}$$

$$\widetilde{e} = eK, \tag{3.21d}$$

$$\widetilde{f} = \frac{1}{2} fK, \tag{3.21e}$$

$$\widetilde{g} = g, \tag{3.21f}$$

where tilde is used to indicate the probability rates in the Gillespie algorithm. Since there are more degrees of freedom in choosing microscopic event rates, different stochastic simulations may map into the same mean field phase diagram.

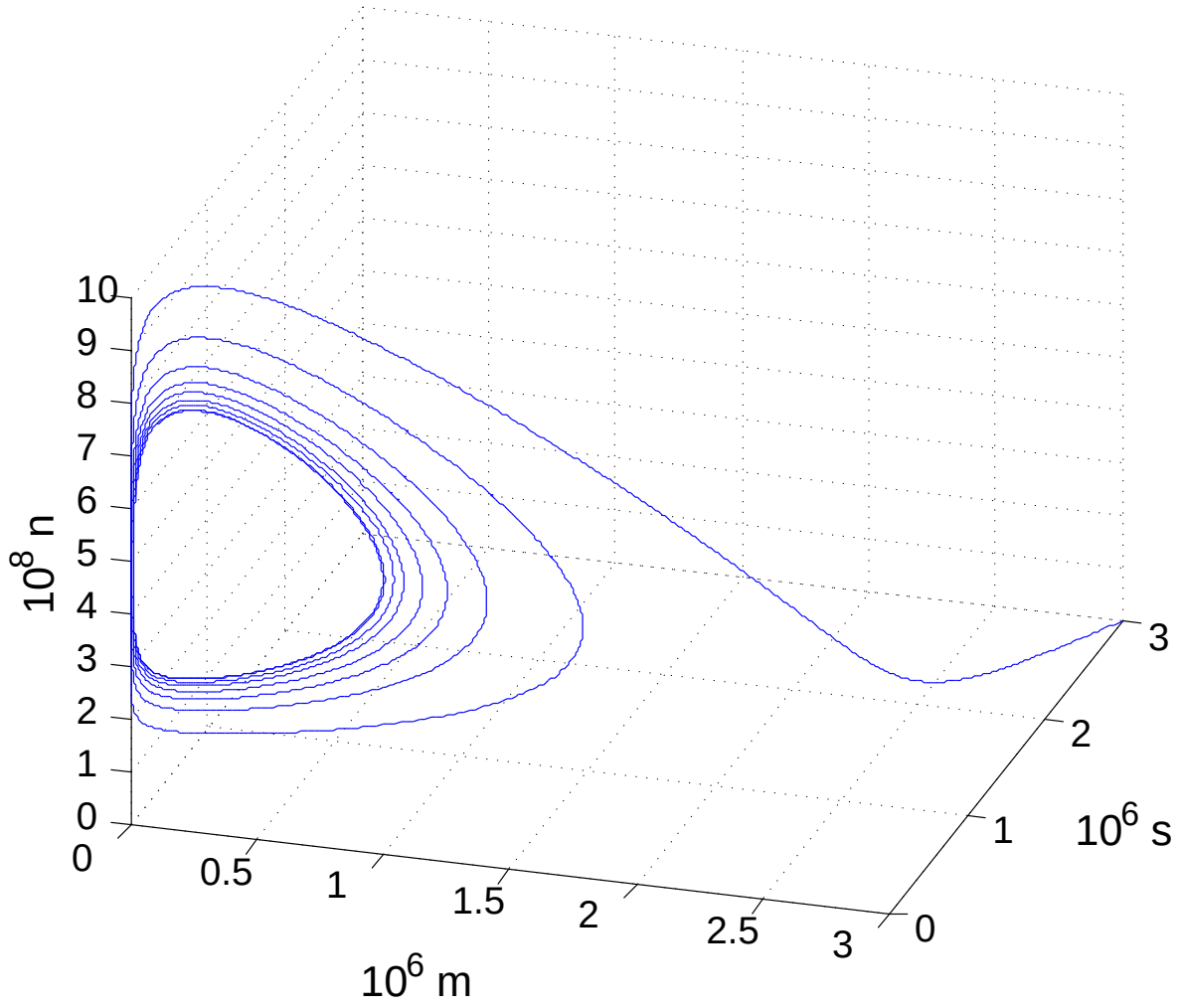

Figure 3.9: A limit cycle in the phase space with parameters in the Gillespie algorithm $\widetilde{b} = 0.4, \widetilde{c} = 0.1, \widetilde{d} = 0.2, \widetilde{e} = 1.2 \times 10^{-10}, \widetilde{f} = 1.2 \times 10^{-11}, \widetilde{g} = 0.018, \widetilde{h} = 4.8 \times 10^{-10}, \widetilde{k} = 4.8 \times 10^{-11}, \widetilde{p} = 0.54$, and $\widetilde{q} = 0.27$.

Our main interest is to explore the mean field limit cycle in the lysogeny-lysis model. We keep employing

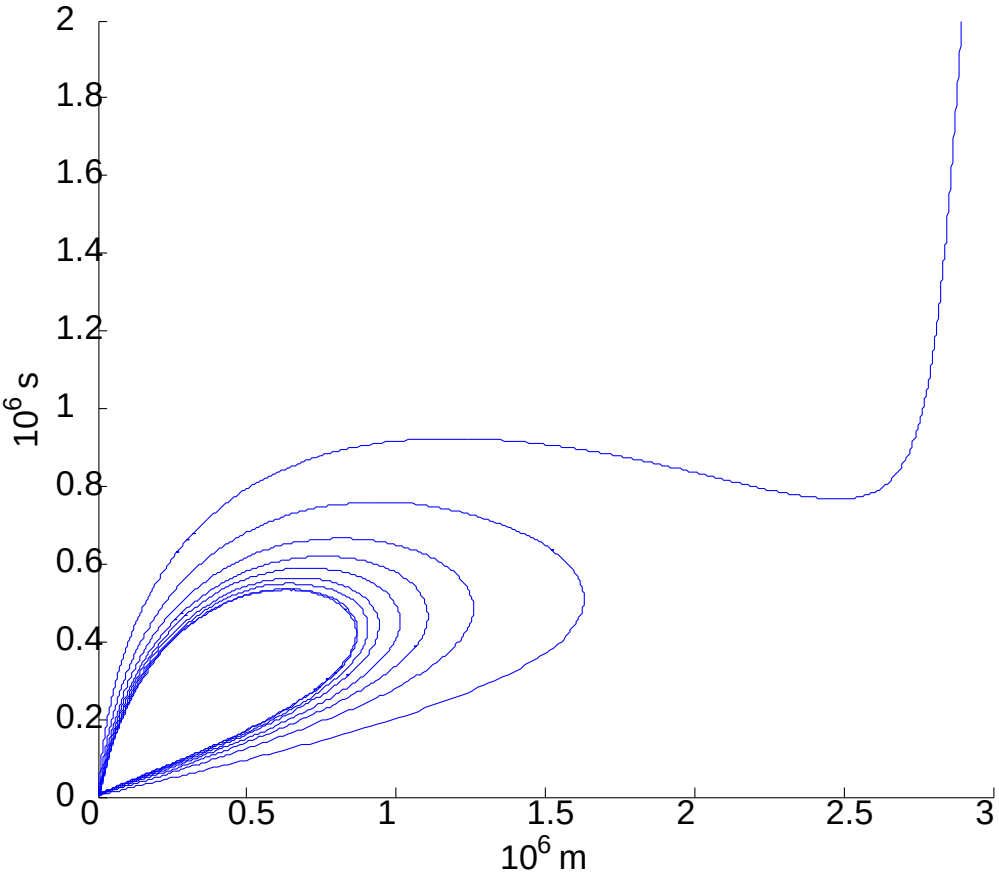

Figure 3.10: The projection of Figure 3.9 onto the m-s plane.

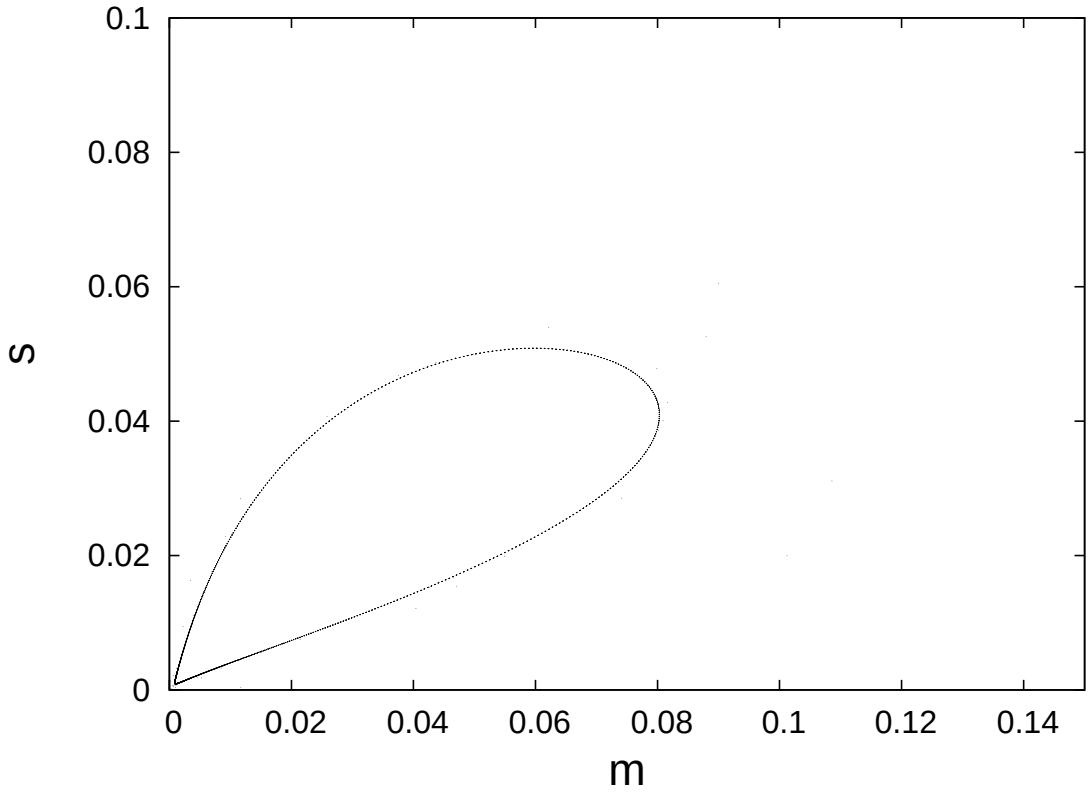

Figure 3.11: A limit cycle projected onto m-s plane in the mean field theory with parameters $\phi_1 = 1, \phi_2 = 0.8, d_1 = 0.5, d_2 = 0.9, d_3 = 0.03, a_1 = a_{21} = a_{31} = 0.1$, and $a_{22} = a_{32} = 0.5$.

the tilde symbol to label the probability rates in the Gillespie sense and the map is

$$\widetilde{b} = bK, \tag{3.22a}$$

$$\widetilde{c} = c, \tag{3.22b}$$

$$\widetilde{d} = \frac{1}{2}dK, \tag{3.22c}$$

$$\widetilde{e} = eK, \tag{3.22d}$$

$$\widetilde{f} = \frac{1}{2}fK, \tag{3.22e}$$

$$\widetilde{h} = hK, \tag{3.22f}$$

$$\widetilde{k} = \frac{1}{2}kK, \tag{3.22g}$$

$$\widetilde{p} = pK, \tag{3.22h}$$

$$\widetilde{q} = \frac{1}{2}qK, \tag{3.22i}$$

$$\widetilde{g} = g. \tag{3.22j}$$

In Figure 3.9, we show a limit cycle observed in our stochastic simulations. It is broadly consistent with the mean field predictions, as can be noted easily by the obvious similarities between Figure 3.10 and Figure 3.11, and Figure 3.12 and Figure 3.13 (when we project the three-dimensional phase space onto two dimensions), whose relationship is Eq. (3.12g), (3.12h) and (3.12i). As expected, we notice fluctuations in the stochastic simulation. For example, if Figure 3.9 were shown in better resolution, we can see that the curve fluctuates slightly around the limit cycle. Usually the fluctuation is two orders of magnitude smaller than the mean value. In order to explore the robustness of the limit cycle, we ran extensive tests to try and estimate their lifetime. For different parameter values that yield limit cycles in the mean field theory, we map them each to six sets of typical parameters in the Gillespie algorithm, varying $\widetilde{b}, \widetilde{c}, \widetilde{d}, \widetilde{e}, \widetilde{f}, \widetilde{g}, \widetilde{h}, \widetilde{k}, \widetilde{p}$ and $\widetilde{q}$ while obeying constraints. We run simulations for 10^{10} time steps each with five sets of different initial conditions. As long as the carrying capacity is large enough, we do not observe any disappearance of the limit cycle. Furthermore, they all run into the same limit cycle.

Hence we conclude that the limit cycle is inherent to the model and robust to stochastic fluctuations, which serves to confirm the essential role of lysogens in stabilizing the cycling in the populations.

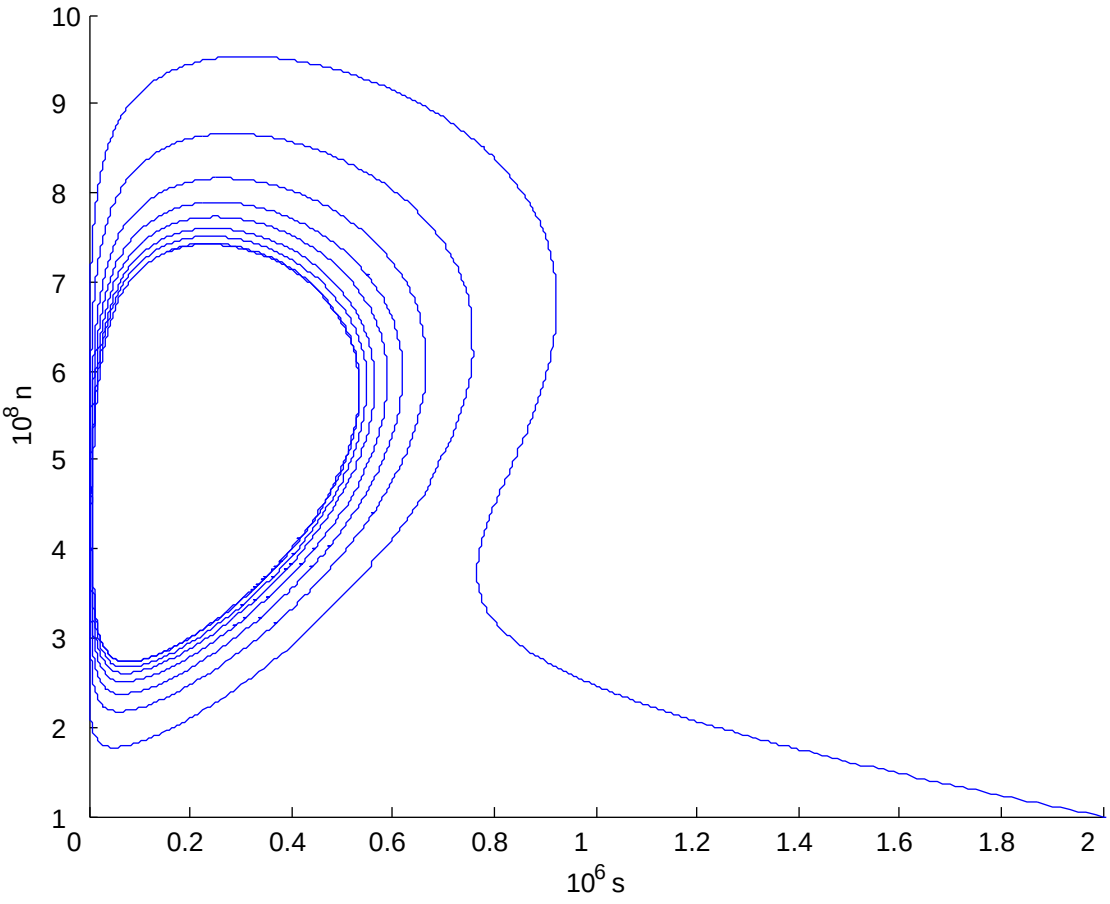

Figure 3.12: The projection of Figure 3.9 onto the s-n plane.

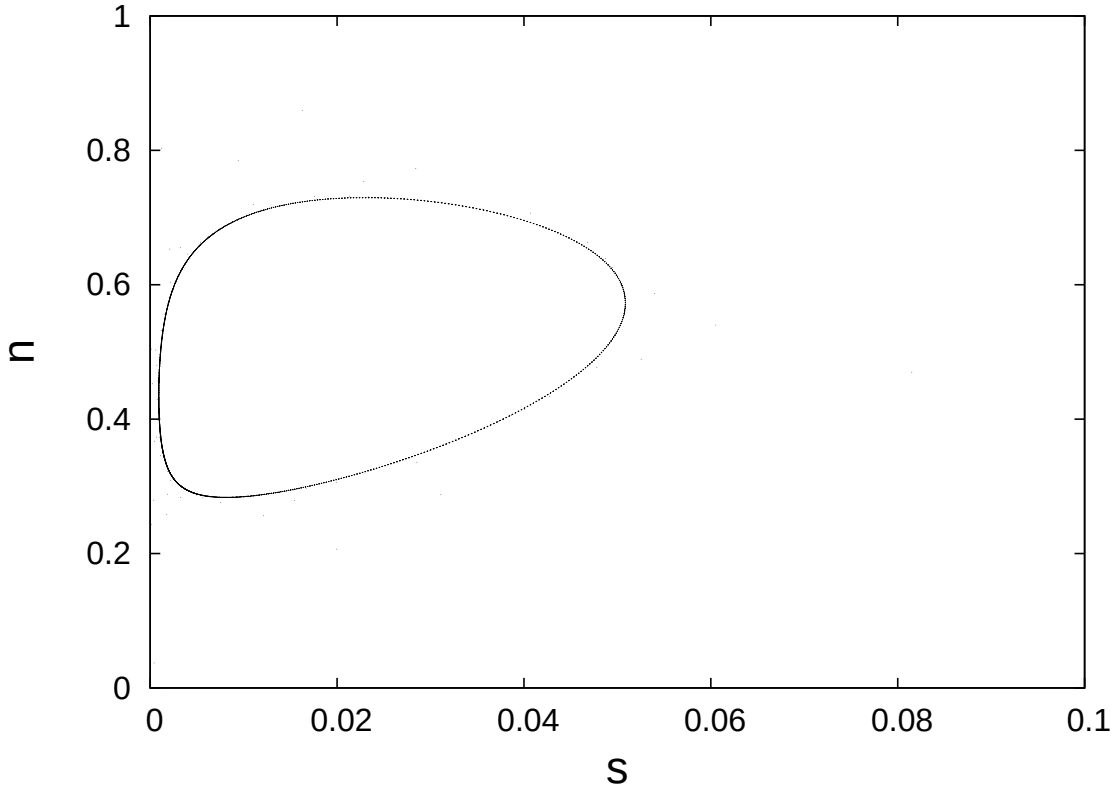

Figure 3.13: A limit cycle projected onto the s-n plane in the mean field theory with parameters $\phi_1 = 1, \phi_2 = 0.8, d_1 = 0.5, d_2 = 0.9, d_3 = 0.03, a_1 = a_{21} = a_{31} = 0.1$, and $a_{22} = a_{32} = 0.5$.

3.7 Parameters in the model

Up to this point, all the parameters above or their values we have explored are difficult to relate to experiment. The purpose of this section is to bridge the gap.

The birth rate of the host b is medium-dependent. Usually the expression of Lac proteins is highly suppressed by Lac repressors in a lacose-free medium to optimize energy investment and metabolism of the bacteria. In the above two models, we have categorized the death of the hosts to longevity and crowding. In fact, it is hard to mark a watershed clearly. Instead, what is observed is a population-dependent growth rate, which is a combined effect of b, c and d. Herein, the rate d for the death of the host due to crowding is introduced artificially to account for the actual population dependence. Thus, we are justified in assuming that the death rate of the host due to longevity c, which incorporates other physical and non-density-dependent factors, is fixed with the variation in host population. The growth rate for E. *coli* may drop to 0.2 h^{-1} at 37°C when glycolate serves as the carbon source but usually is in the range from 0.5 h^{-1} to 2.0 h^{-1} [145, 97]. The growth rate is species- and strain-specific, which for *Pseudoalteromonas* sp. strain SKA18 (accessible number AF188330 in GenBank) [134], for example, is an order of magnitude smaller. Similarly, lysis rate f, lysogeny rate k, prophage induction rate q, and replicate number per capita β, which are all under poor metabolism, are introduced manually to characterize the population-dependent feature of the interactions in order to leave their population-independent counterparts e, h, p and α fixed. In the case of virulent phages, such as one in the family Siphoviridae [146] attacking *Pseudoalteromonas* sp. strain SKA18 [134], corresponding to the lysis-only model, the reported lysis rate spans from 0.2 to 2.0 h^{-1} subject to the growth rate of the bacteria so that we can estimate e to be on the order of 1.0 h^{-1} and f to be an order of magnitude smaller than e.

For temperate phages in the lysogeny-lysis model, the spontaneous lysis rate is far smaller, being of the order of 10^{-9} to 10^{-7} per generation per cell [147]. The percentage of lysogens is assayed through prophage induction by the addition of mitomycin C, UV radiation or other environmental conditions that may inhibit lambda phage repressors. Under good metabolism the lysogeny rate h for λ phage infecting E. *coli* and prophage induction rate are on the order of 1 h^{-1} and 2 h^{-1}, respectively [148]. Their counterparts under poor metabolism are estimated to be one or two orders of magnitude smaller. For instance, the prophage induction rate for log-phase marine lysogens [149] is on the order of 0.03 h^{-1}. Replicate number per capita α is about 100 for phage λ [8], and may be up to 600 for phage W-14 [150], while β is about 20 or 30 for both. Although virions do not age [2], their mortality is caused by the destabilization of the capsid, which is dependent on physical conditions such as temperature, humidity and pH values. C. D. Jepson and J. B. March [151] reported that phage λ is highly stable, whose half life in suspension ranges from 2.3 days at

4.2°C to 36 days at 20°C. Even if we take the half life be one day, the corresponding death rate g is on the order of 10^{-6} per second and can be suppressed by cooling down. Actually, the loss of free phage in nature, to a great extent, is through diffusion since bacteria are more immobile due to their large particle size compared to that of phages. In laboratory, the death rate can be manipulated through continuous dilution and washing out, and a wide range of death rates can be realized.

When all the parameters are tuned properly, the limit cycle in the lysogeny-lysis model is observable in experiment. We estimate the period of the limit cycle to be on the order of days. Take Figure 3.10 as an example. A cycle there is composed of about $10,000$ computational steps, in other words $10,000$ events, which corresponds to about 120 [time unit] in the simulation. In Figure 3.10 the birth rate is 0.6 [time unit]$^{-1}$, while in the real world the life cycle of an E. *coli* in good laboratory conditions, for example, is about half an hour, which is 2 hour $^{-1}$. Hence the cycle is $120 \times 0.6/2 = 36$ hours, which is one day and a half. When we vary parameters in the Gillespie algorithm, as long as they map to the same limit cycle in the mean field theory, the period stays the same. The period will change only when it corresponds to different limit cycles in the mean field sense. When we increase d_1' in the mean field theory, the period may drop to 28 hours at the edge of the disappearance of the limit cycle.

3.8 Conclusion

We have derived the mean field population dynamics for host-phage communities both without (in Chapter 2) and with lysogens (this chapter). In the lysis-only model, we successfully obtained a description similar to the starting point assumed by Weitz and Dushoff [11], and we found that the phase diagram was modified only slightly to the difference in good and poor metabolism. In the lysogeny-lysis model, we identified the asymptotic states, which included not only coexistence and extinction fixed points, but population cycling of all microbes, lysogens and phages. Our findings support the notion that lysogens act as a reservoir and are in principle amenable to experimental verification. We simulated the stochastic process using the Gillespie algorithm and verified the robustness of our results to fluctuations, and especially demonstrated the stability of the limit cycle.

Although complicated, our model inevitably makes some drastic assumptions, among which the most severe is the omission of spatial structure. Discreteness in the occurrence of speciation and adaptation in time and space may have a complex interplay with spatial heterogeneity since it propagates with large fluctuations at fronts [106, 107, 108, 109]. Such demographic noise may also induce robust spatial patterns beyond mean field predictions [111]. Hence inclusion of spatial structure may yield interesting predictions about the spatial

structure of microbe-virus communities, with concommitant consequences for the evolutionary dynamics too. Another simplification is that we treat "healthy" hosts and lysogens in the same way regarding their natural birth, death and crowding effect. However, experimentally, the expression of prophage genes and the control of host gene expression by viral genes seem to impart to lysogens econominization in their metabolism [60]. When unnecessary metabolic activities are suppressed, lysogens optimize their energy expenses and therefore gain some survival advantage compared to "healthy" hosts in unfavorable conditions, which suggests that the natural birth, death and crowding effects of lysogens are distinct from those of "healthy" hosts. Hence our model is a reasonable minimal model that can capture the non-trivial role of lysogens in the population dynamics of microbe-phage communities, in addition to the usual predator-prey interactions, but more biological realism could be introduced.

This work can be extended in several ways, but perhaps the most interesting are those which relate to the evolution of the field of genes distributed amongst the microbes, viruses and lysogens. Lysogens are genome carriers of not only microbes but also prophages, capable of yielding virus bursts when triggered by environmental stress. In this way, the role of lysogens and viruses as a reservoir of genes is mediated through phage infection and the lysogeny-lysis switch by the metabolism of the host. The metabolism of the host is, in turn, to a great extent influenced by environmental conditions. Thus, this model is a starting point for ecology-mediated evolution. It is also useful to stress that each individual microbe or virus constitutes a part of another organism's environment. Thus, the effects which our work begins to treat, represent a microcosm of the intricate interplay between ecology and evolution in microbe-virus communities.

Chapter 4

Game Theory and the Social Life of Micro-organisms

4.1 Cooperation in Classic Game Theory

Cooperative phenomena in biology are difficult to treat because of the complexity and heterogeneity of the interactions, but a qualitatively successful approach is cooperative game theory—the effort to encapsulate the complex interactions into parameters describing the binary outcome of pairwise interactions between individuals [152, 153, 154, 155, 156, 157, 158]. The central element in game theory is the payoff matrix, which describes the score accruing to each member of an interacting pair depending upon their action in the game. As an example, we show a typical payoff matrix (4.1) for pairwise interactions in the classic prisoner's dilemma

$$\begin{array}{c} \\ C \\ D \end{array} \begin{array}{c} \begin{array}{cc} C & D \end{array} \\ \begin{pmatrix} R & S \\ T & P \end{pmatrix} \end{array}. \tag{4.1}$$

Two players can either "cooperate" (C) or "defect" (D). Mutual cooperation yields a reward R, whilst if both defect, they receive a punishment P. If one defects and the other cooperates, the defector receives a temptation T while the cooperator receives the sucker's payoff S. If $T > R > P > S$, then there is a dilemma: a rational player would defect to receive the highest payoff independent of the state of the other player, so that if both parties play rationally, each will end up with the punishment P. However, if they had both cooperated, they would have received the reward R.

Two-body interactions are paradoxical in cooperative games, a forceful indicator of how collective effects can override selfish one-body behavior. If the payoff matrix instead obeyed the inequalities $T > R > S > P$, then the rational strategy is to do the opposite of the other player. This condition leads to the so-called snowdrift game, which gives rise to the coexistence of both strategies

Classic game theory offers an approach to explain the ubiquitous cooperative phenomena in nature: Measure the payoff matrixes in various scenarios and justify that they fall in the regimes for cooperation.

4.2 Cooperation in Laboratories

4.2.1 An RNA Virus

The approach in game theory is easier said than done because the elements in the payoff matrixes, interpreted as fitness or growth rates, are usually very hard to measure in the well-established cooperative animal world such as monkeys, bats or fish [159]. However, empirical data come at last with technological advances in microbiology. Such seemingly abstract games have biological realizations in the dynamics of microbes and viruses.

In a pioneering study, Turner and Chao [160, 159] demonstrated that an RNA virus $\phi 6$ is engaging in the prisoner's dilemma by measuring the payoff matrix as shown in Matrix (4.2)

$$\begin{array}{c} \\ \phi 6 \\ \phi H2 \end{array} \begin{array}{c} \begin{array}{cc} \phi 6 & \phi H2 \end{array} \\ \begin{pmatrix} 1 & 0.65 \\ 1.99 & 0.83 \end{pmatrix} \end{array}. \tag{4.2}$$

In their experiment, $\phi 6$ is a wild-type complete strain, capable of producing all the necessary intracellular products for infection, and acts as a cooperator. ϕH2 is a mutant strain, which evolves a defector strategy when cultured at high multiplicities-of-infection. During the co-infection of a microbial host by these two strains, the fitness of the whole community increases initially, but drops eventually. The final drop is unexpected because in evolution fitness usually increases. The dilemma can be explained using game theory. By constructing the payoff matrix according to the measured mean fitness at different initial ratios of the two strains, the authors showed that the virus was effectively trapped in the prisoner's dilemma, which engendered the final drop.

To escape the dilemma of the phages, several years later, the same authors [161] cultured another strain ϕL1 to compete with ϕH2. This time the payoff matrix (4.3)

$$\begin{array}{c} \\ \phi L1 \\ \phi H2 \end{array} \begin{array}{c} \begin{array}{cc} \phi L1 & \phi H2 \end{array} \\ \begin{pmatrix} 2.24 & 1.25 \\ 3.47 & 0.83 \end{pmatrix} \end{array} \tag{4.3}$$

obeyed the inequalities $T > R > S > P$ and so conformed to the condition for the so-called snowdrift game, in which coexistence of the two strains were observed.

4.2.2 Budding Yeast

In the above two experiments, the payoff matrices are measured, but not controlled. In a recent experiment, a game theory payoff matrix was manipulated by genetically engineering *Saccharomyces cerevisiae* (budding yeast) [13].

Budding yeast's primary carbon intake is a monosaccharide, such as glucose and fructose. In a monosaccharide-absent environment, dormant genes are derepressed to digest alternative nutrients, such as disaccharide maltose and sucrose [162]. In the experiment, wild-type cooperator strains have an intact *SUC2* gene, which codes enzyme invertase to hydrolyze sucrose into glucose and fructose (Figure 4.1). However, 99% of the product is released back into the media, giving rise to the possibility that mutant defectors with the *SUC2* gene knocked out could make use of the metabolite without having to pay the price of manufacturing glucose. In order to tune the cost of cooperation and hence the payoff matrix, the authors engineered cooperators to be histidine auxotrophs, relying on histidine importation from the media. Having an intact histidine gene, defectors are not affected. Thus limitation of histidine concentration in the media coerces the metabolism of cooperators, increases the cost of cooperation, and thus affects the payoff matrix. By changing the glucose and histidine concentration provided with a fixed portion of sucrose, the authors empirically obtained a transition from the dominance of defectors, which corresponds to the prisoner's dilemma, to the coexistence of both strains, which is a snowdrift game (Figure 4.2).

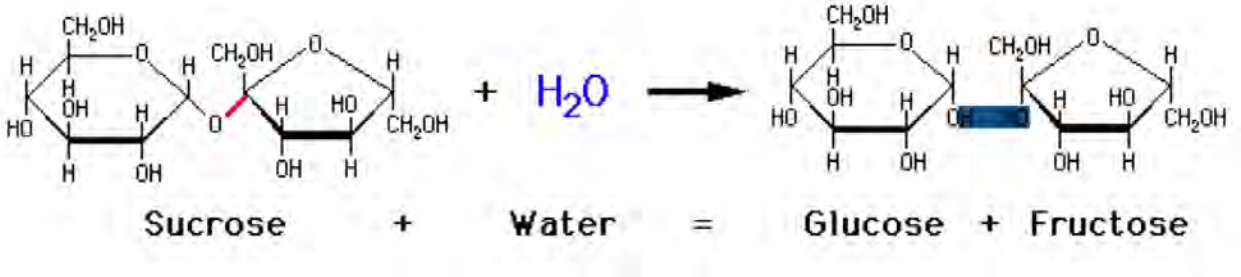

Figure 4.1: Enzyme invertase catalyzes sucrose hydrolysis into glucose and fructose. After Ref. [12].

The ability to manipulate collective properties of the microbial world by genetic engineering is impressive, but what is lacking is a predictive understanding of the direct dependence of cooperator fraction on nutrition concentrations.

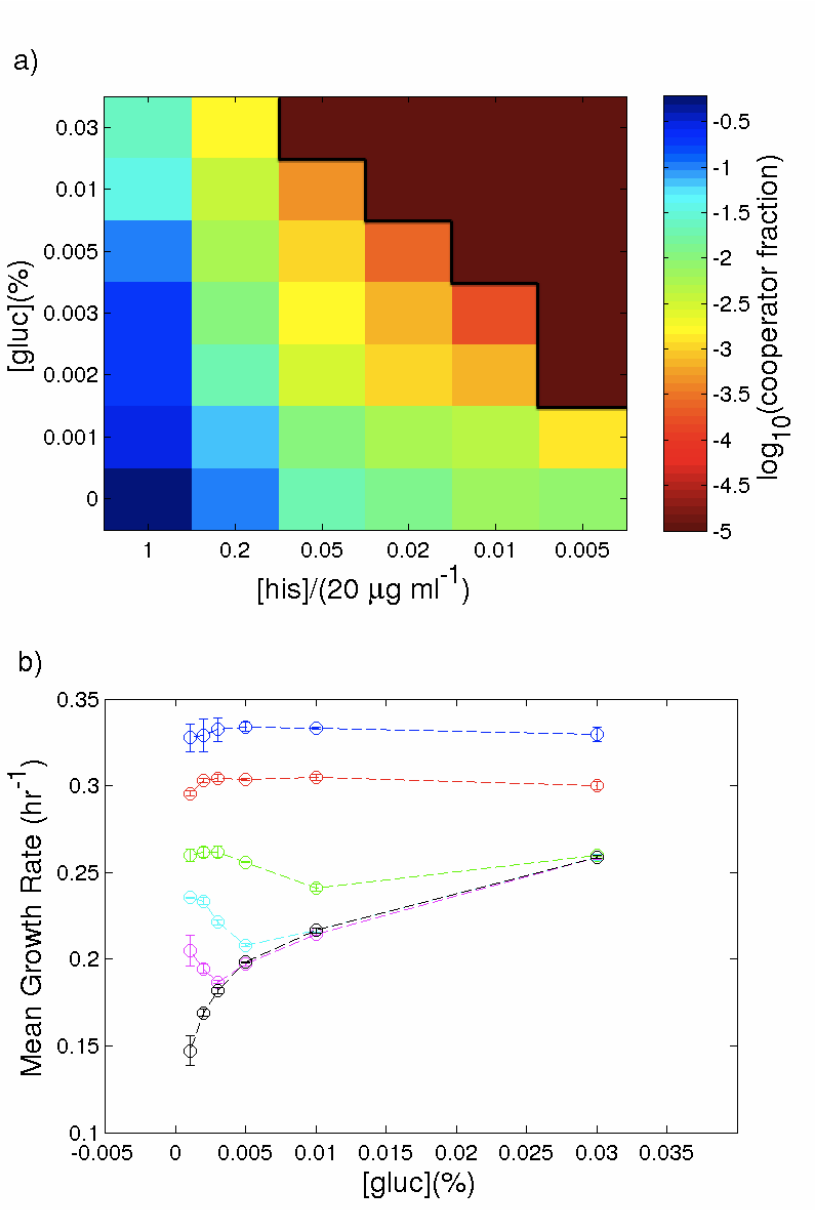

Figure 4.2: Coexistence of the two strains with variations in glucose and histidine concentration. After Ref. [13]. (a) Cooperator fraction scaled in the color bar with variations in glucose and histidine concentration at equilibrium. The black line is the boundary separating regimes for the prisoner's dilemma (above the line) and the snowdrift game (below the line). (b) Mean growth rate of the coculture with different glucose and histidine concentration at equilibrium. The lines from top to bottom corresponds to histidine concentration 1, 0.2, 0.05, 0.02, 0.01, and 0.005 ($\times$ 20 μg ml^{-1}), respectively.

4.3 Theory of Cooperation in a Micro-organismal Snowdrift Game

4.3.1 Goal

The purpose of this chapter is to build up a phenomenological model linking game theory and experimental measurable quantities. We would like to calculate the population structure, i.e. the fraction for cooperators and defectors, at different glucose and histidine concentrations, and reproduce the phase diagram for the transition from dominance of a single strain to coexistence of both as shown in Figure 4.2(a). We use phenomenological game theory because the collective effects here are highly nonlinear due to complex metabolism. Our model implies a consistent nonlinearity responsible for both yeast growth and glucose production.

4.3.2 Model

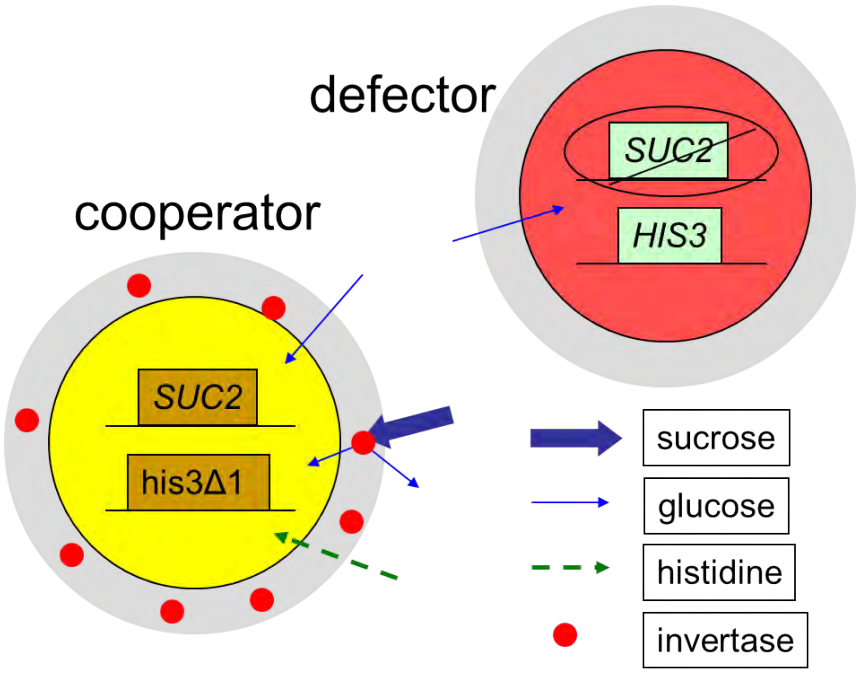

Figure 4.3: Schematic of nutrient flows in the experiment of Ref. [13]. Sucrose is hydrolyzed in the periplasmatic space (grey) of cooperators. The majority of the glucose produced diffuses back to the media, from which both strains import glucose. After Ref. [13].

The interactions between cooperator and defector strains are complicated for the following two reasons. First, there are two kinds of nutritional molecules: sucrose and glucose as sketched in Figure 4.3. Sucrose is

easy to handle because it has a single source and single mode of consumption, originating from the media and being consumed only by cooperators. However, glucose has two sources: the initial amount added into the media, and the local increment from sucrose decomposition by cooperators. The actual glucose concentration surrounding yeast cells depends on the cooperators' metabolism and concentration, whose relation is unknown. Second, in sucrose hydrolysis, cooperators experience a cost to synthesize invertase, but at the same time gain in generating glucose for themselves. The balance between the cost and benefit is subtle and hard to handle. In order to circumvent these two obstacles, we model a simple situation where the two strains are at the same nutrition level. This should be applicable to the experimental situation because cooperator strains ultimately live on the monosaccharide glucose no matter if it is absorbed from the surrounding media or decomposed from sucrose. In this way, our system can be simplified as a coexistence problem of two strains living on the same nutrition glucose.

Next we use game theory to identify the conditions for coexistence. The key is to construct a payoff matrix with experimental data. Here, the two strains are engaging in a cooperative game: if the payoff for defectors exceeds that of cooperators, defectors will dominate; if the payoff for cooperators exceeds that of defectors, cooperators will dominate. Therefore only when the payoffs for both parties are equal, will coexistence be achieved. The payoff for players is the mean fitness for strains, which is measured as the growth rate. Thus, our next task is to construct the dependency of growth rates on experimental observable quantities. We do this below using a mean field theory, modeled after the way in which cooperative interactions leading to ferromagnetism are described by an effective local field that adds to the externally applied magnetic field (see, e.g. Ref. [163]).

The first input is the nonlinear dependency of growth rate b (hr^{-1}) on glucose concentration g (%) according to the experiment (Figure 4.4):

$$b = \gamma_1 g^{\alpha}, \tag{4.4}$$

where $\gamma_1 = 0.44$, $\alpha = 0.15$ and g is $0.001 \sim 0.03\%$. In Eq. (4.4), the growth rate b varies nonlinearly with glucose concentration g. The nonlinear power α is unusual, and reflects cellular constraints, such as the nonlinear performance of hexose transporters and catabolic pathway enzymes. We cannot use first principles system biology to justify the nonlinear α, because the basic metabolic networks etc. are not well enough understood. Instead, we make a very simplified assumption: we interpret the nonlinearity as primarily reflecting aspects of the efficiency of hexose transporters across the cell membrane. Hence Eq. (4.4) implies that translocation flux rate through the membrane is proportional to the concentration raised to a nonlinear power α. Note that in principle, such translocation processes are influenced by the metabolism of the cells, but for now we regard that as negligible.

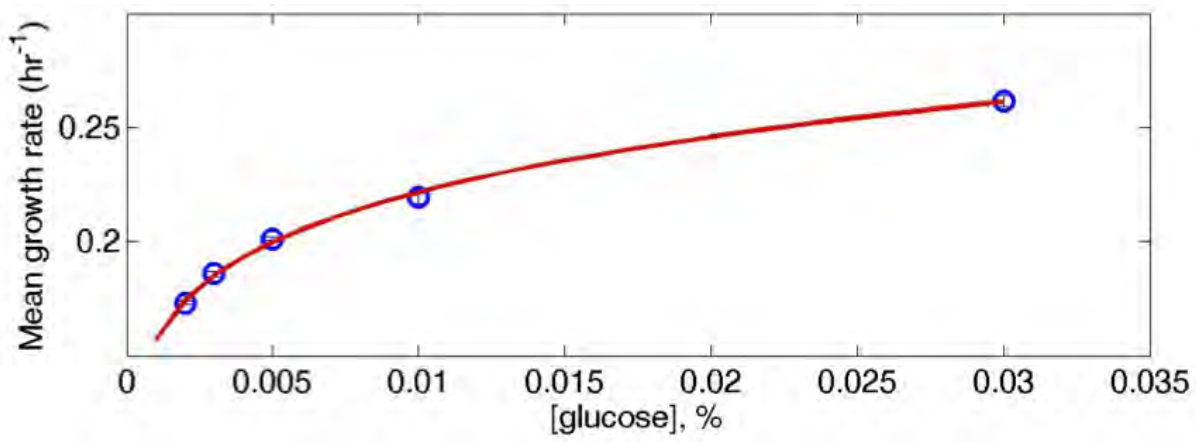

Figure 4.4: Growth rate b (hr^{-1}) varies nonlinearly with glucose concentration g (%) when there are only defectors. After Ref. [13].

Second, we include the presence of cooperators. Now, there are two sources of glucose. Besides the initial glucose added into the media, cooperators also produce glucose from sucrose decomposition. At the mean field level, every cooperator manufactures glucose at about the same rate. We assume that this rate does not have a significant dependence on the metabolism of cells; because the amount of invertase in each cell is not influenced by the metabolism, we assume that the performance of invertase is also not significantly influenced by the metabolism. Since the sucrose concentration is kept the same throughout the experiment, there is no need for us to explore the detailed form of such a production rate. The total glucose produced inside all the cooperator cells is thus proportional to the cooperator fraction f. Eq. (4.4) implies that the glucose imported into the cell scales as g^α due to the cellular constraints on the molecular translocation process. The same translocation passage limits the glucose output from cooperators, as evidenced by the report that the diffusion coefficient through the cell wall is anomalously small, estimated to be 1/20 of that in water [13]. Hence the flux of glucose released is proportional to the glucose produced inside the cells raised to the power α. Since the glucose manufactured inside the cells is proportional to the cooperator fraction f, the glucose contribution from cooperators is proportional to f^α with some coefficient of proportionality. We denote the coefficient as γ. As we note in the discussion about Eq. (4.4), the translocation process is affected by the metabolism of the cells. The coefficient γ, in this way, represents a general discount factor due to metabolism, which is a combined effect of the artificial discount in histidine limitation and the natural cost in cooperation. Including the contribution from cooperators as shown in Figure 4.5, we obtain the growth rate for defectors

$$b_d = \gamma_1 (g + \gamma f^\alpha)^\alpha, \tag{4.5}$$

where γ is a general discount factor that varies with histidine concentration, reflecting the artificial discount in histidine limitation and the natural cost of cooperation.

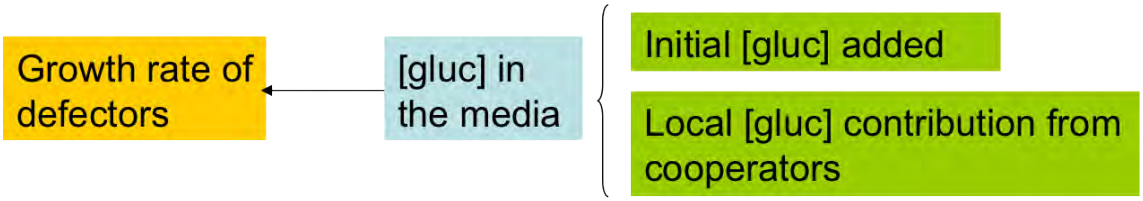

Figure 4.5: Sketch of sources of glucose for defectors.

We would like to emphasize that we are proposing that the glucose increment is related to the cooperator fraction instead of the absolute number of cooperators. There is a subtle difference here, because the defectors and the cooperators are competing for glucose. To see this, suppose that there are twice as many defectors as cooperators: then, each defector can, in mean field theory, capture 0.5 of the production of each cooperator. On the other hand, if there are equal numbers of defectors and cooperators, each defector captures approximately the entire production of a cooperator.

Third, we analyze the situation for cooperators. Compared with defectors, when they import glucose from the media, the translocation process is influenced by the metabolism as we learn from Eq. (4.4). Such a discount, representing a combined effect of the artificial discount in histidine limitation and the natural cost in cooperation, is represented by the same γ as in Eq. (2), because the same cellular processes are involved. Thus we obtain

$$b_c = \gamma\gamma_1(g + \gamma f^\alpha)^\alpha, \tag{4.6}$$

where b_c is the growth rate for cooperators. Last, we recall that there is a small amount of glucose that cooperators reserve for themselves. This amount is determined by the sucrose concentration and the cell's metabolism and transport processes, which are mediated by the histidine concentration. Since the sucrose concentration is always 5% during the experiment, we denote the benefit for a single cooperator cell by ζ, a single-variable function of histidine concentration only. Including this benefit for cooperation (Figure 4.6), we finally obtain

$$b_c = \gamma\gamma_1(g + \gamma f^\alpha)^\alpha + \zeta. \tag{4.7}$$

Eqs. (4.5) and (4.7) compose the central part of our model, including the contribution of cooperators to the increase in glucose concentration by the term γf^α. This model balances the cost γ for cooperators with the benefit ζ, both depending only on histidine concentrations. Note that as the cooperator fraction f increases, more glucose is trapped in cooperators, but the amount per cooperator does not change. The

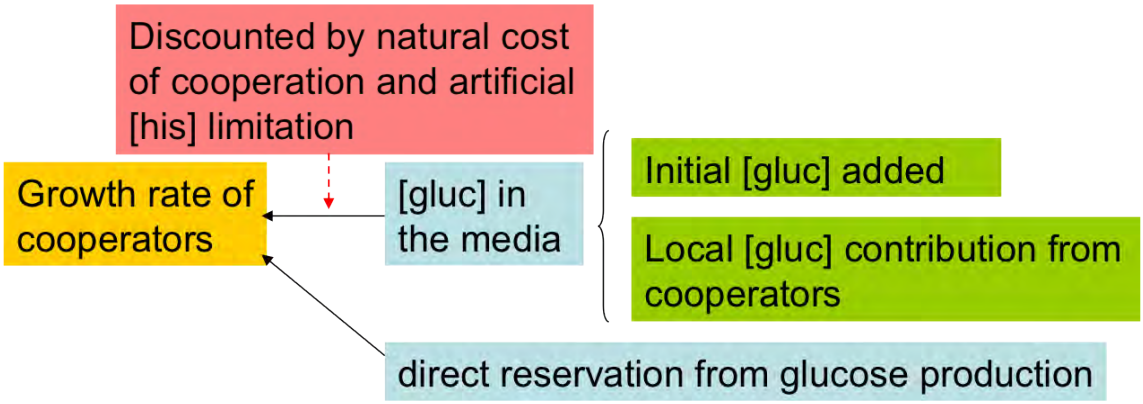

Figure 4.6: Sketch of sources of glucose for cooperators.

positivity of ζ is essential for the survival of cooperators, which makes it possible for the two engineered strains to engage in a snowdrift game.

4.3.3 Assumptions and Tests

In our model of cooperation, we have input three non-trivial arguments: (i) The two α's in Eqs. (4.5) and (4.7) are the same, representing the same translocation passage limitation on the glucose flux both into and out of yeast cells; (ii) The two γ's in Eq. (4.7) are the same, implying the same discount in yeasts' growth and sucrose decomposition by cost of cooperation mediated by histidine limitation; (iii) ζ is a single-variable function of histidine concentration, representing that cooperators are compensated for production of glucose.

Our arguments above motivated points (i)-(iii) assuming that it is primarily the phenomenology of transport of glucose through the cell membrane which is the growth-rate determining factor. However, in principle, other metabolic effects can be present. To test whether or not our assumptions are self-consistent and represent a good representation of the data, we compare the predictions of our equations with the data.

Ideally, we would like to be able to calculate the cooperator fraction as a function of glucose and histidine concentrations in Figure 4.2(a) from theory, but this would require a detailed description of the metabolism and growth dynamics of the organisms to obtain the parameters. As an alternative approach, we input experimental data to our equations and verify the consistency of our modeling by checking the standard deviations for different sets of data. Based on our reasoning from game theory that the growth rates for cooperators and defectors are the same at equilibrium, the measured growth rates of cocultures as a function of glucose and histidine concentrations shown in Figure 4.2(b) should be valid for either strain. Interpreting them as the growth rates for defectors, we can import the data in Figure 4.2 for various glucose and histidine concentrations into Eq. (4.5) and calculate the discount γ. According to our argument (i), we predict that γ

Table 4.1: Cost γ for cooperators at various histidine concentrations.

[his]/(20 μg ml^{-1})	1	0.2	0.05	0.02
γ	0.19	0.14	0.061	0.027
standard deviation σ_γ	0.02	0.02	0.006	0.006

should be the same at the same histidine concentration but different glucose concentrations; this is supported by the standard deviations shown in Table 4.1. We neglect the data for very small cooperator fractions, especially for the extinction of cooperators, such as those when histidine concentration is as low as 0.005, since they will either generate large deviation with very small bias in measurement or cause the cooperation term γf^α to vanish. Averaging among different glucose concentrations, we can see that the discount γ gets smaller when histidine is more dilute. The first two σ_γ are calculated with six data points where glucose concentration (%) ranges from 0.001 to 0.03. The latter two are smaller than the first two since fewer data are averaged. The smallness of the standard deviations has not been hard-wired into our model, and substantiates our assumption (i) because otherwise they might be orders of magnitude larger, as we will illustrate as follows. We show in Table 4.2 the average of γ and its corresponding standard deviation σ_γ if the increment of glucose concentration varied not with the same power α as we have assumed in our model, but linearly with cooperator fraction, as we might have initially guessed,

$$b_d = \gamma_1(g + \gamma f)^\alpha, \tag{4.8}$$

or even quadratically

$$b_d = \gamma_1(g + \gamma f^2)^\alpha. \tag{4.9}$$

The standard deviations σ_γ in Table 4.2 are at least two orders of magnitude larger than those in Table 4.1, and are even higher for the fit to Eq. (4.9) as shown in Table 4.3. The comparison among these tables demonstrates that the standard deviation is a good test of our assumption, and hence justifies the self-consistency of our theory.

Next, we interpret the data in Figure 4.2(b) as growth rates for cooperators and plug in the values of γ shown in Table 4.1 into Eq. (4.7). Our arguments (ii) and (iii) predict that ζ depends only on histidine concentration, which is consistent with the standard deviation for ζ in Table 4.4. The benefit for cooperators diminishes with the limitation in histidine. The latter two σ_ζ are bigger than the previous two since we extend the data for those not incorporated in the calculation of γ in Table 4.1. Overall, however, these

Table 4.2: Large standard deviation σ_γ to fit Eq. (4.8) in violation of assumption (i).

[his]/(20 μg ml^{-1})	1	0.2	0.05	0.02
γ	1.8	12	12	8
standard deviation σ_γ	1.5	9	7	4

Table 4.3: Large standard deviation σ_γ to fit Eq. (4.9) in violation of assumption (i).

[his]/(20 μg ml^{-1})	1	0.2	0.05	0.02
γ	5×10	4×10^3	8×10^3	9×10^3
standard deviation σ_γ	6×10	7×10^3	8×10^3	6×10^3

consistency checks are successful, a result that we emphasize is not "built-in" to our theory.

Table 4.4: Benefit ζ for cooperators at various histidine concentrations.

[his]/(20 μg ml^{-1})	1	0.2	0.05	0.02
ζ	0.269	0.260	0.241	0.222
standard deviation σ_ζ	0.003	0.004	0.007	0.02

4.3.4 Results

With the cost γ and gain ζ in hand, we can now predict the cooperator fraction at equilibrium. Setting $b_d = b_c$ in Eq. (4.5) and (4.7), we plot the predicted cooperator fraction in Figure 4.7(a). As a comparison, we replot the corresponding data from experiment [13] in Figure 4.7(b). Considering that the cooperator fraction varies nearly 4 orders of magnitude, the similarity between the theoretical calculation and experimental measurement is striking and supports our model.

4.4 Conclusion

In this chapter, we have proposed a phenomenological model for wild-type cooperator and mutant defector strains in a mixed media of glucose and sucrose. We circumvented the obstacle of modeling sucrose decomposition, which increases glucose concentration, incurs a cost as invertase syntheses for cooperators, and

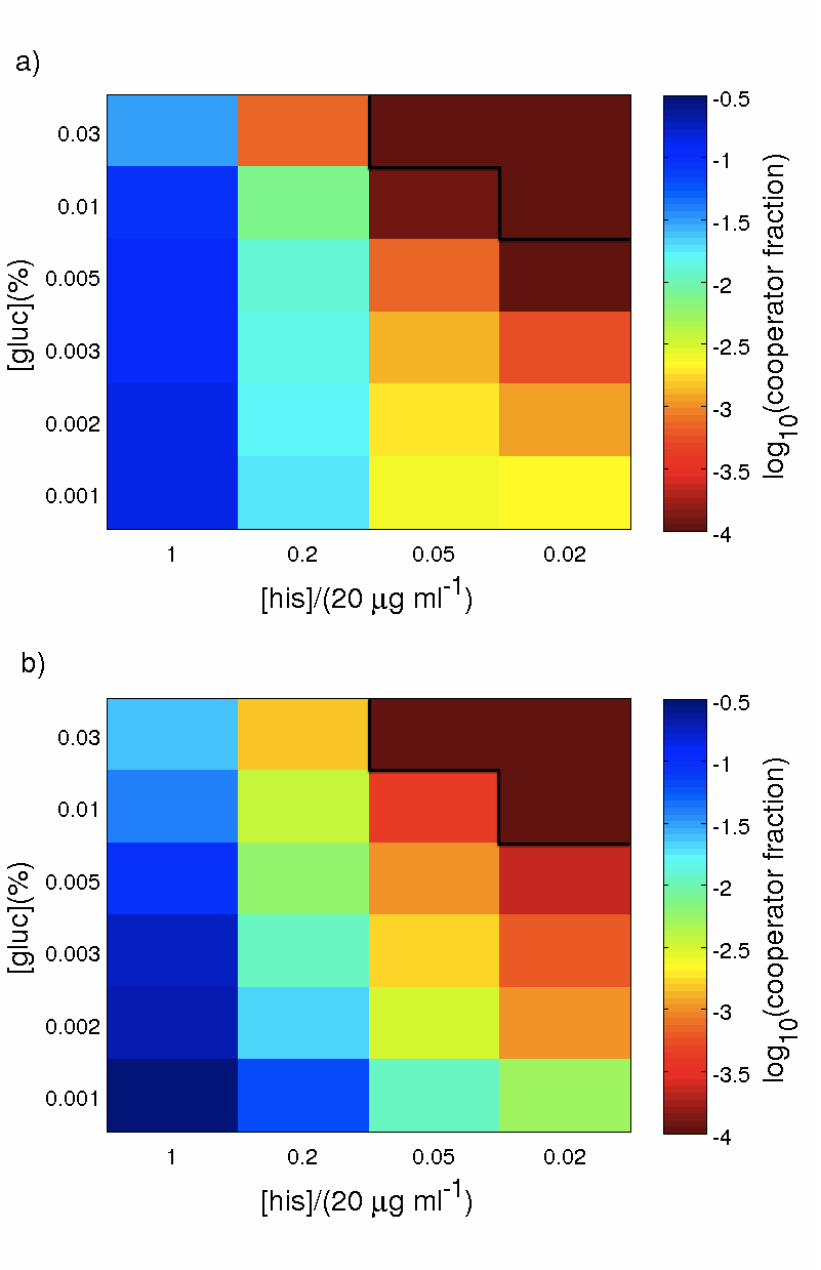

Figure 4.7: (a) Theoretical result for cooperator fraction at various glucose and histidine concentrations. (b) Corresponding experimental result for cooperator fraction at various glucose and histidine concentrations. In both panels, the black line is the boundary separating regimes for the prisoner's dilemma (above the line) and the snowdrift game (below the line).

rewards them with a small fraction of the glucose produced, by attributing cost and benefit for cooperation to growth rates. Then we determined the dependency of growth rates for defectors and cooperators on experimental quantities such as glucose and histidine concentrations. Despite our approximations, such as averaging over different glucose concentrations, the resulting calculation of cooperator fraction at equilibrium is consistent with experimental observations. So what did we actually predict? By requiring that $b_d = b_c$, we thus found, *in a non-circular way*, the condition for the phase boundary separating the prisoner's dilemma phase from the snowdrift phase of the system. Our mean field arguments also predict the trend, i.e. the sign of $\partial f/\partial g$ for fixed histidine concentration. These methods could be useful in the design of future experiments to manipulate collective properties of micro-organism communities.

Chapter 5

Novel Mechanism Enhancing Cooperation in Evolutionary Game Theory

5.1 Game Theory

As mentioned in Section 1.2, cooperation is widely observed at all levels of biology from human society to other animals from organisms to cellular processes. Cooperation in biology is difficult to treat and often resort to game theory, which abstracts complicated interactions into gain and loss in decision-making processes. Interpreting economic concepts of gain and loss as evolutionary fitness after J.M. Smith and G.R. Price [164] in 1973, evolutionary game theory has widely been used to explain cooperation in biology [165].

To give a brief introduction in game theory, let us start with a typical payoff matrix for two players

$$\begin{array}{c} \\ C \\ D \end{array} \begin{array}{c} \begin{array}{cc} C & D \end{array} \\ \begin{pmatrix} R & S \\ T & P \end{pmatrix} \end{array}. \tag{5.1}$$

Each player can choose either to "cooperate" (C) or "defect" (D). The payoffs correspond to the row player. If both players cooperate, each receives a reward R. If both defect, each receives a punishment P. If one cooperates and the other defects, the cooperator will get sucker's payoff S while the defector will get the temptation for defection T.

Prisoner's dilemma requires that

$$T > R > P > S. \tag{5.2}$$

In this scenario, a rational player would choose to defect if his opponent cooperates since $T > R$. He would again choose to defect if his opponent defects since $P > S$. That being said, a rational player would always defect irrespective of the strategy of his opponent. Since two rational players will follow the same logic, the result is mutual defection. Now here is the dilemma: If both parties were to cooperate, both would be rewarded rather than punished since $R > P$.

How to achieve cooperation in prisoner's dilemma? The first mechanism is reciprocal altruism proposed

by R.L. Trivers [166] and developed by R. Axelrod and W.D. Hamilton [167]. The basic idea is to play the prisoner's dilemma for repeated times, which is called iterated prisoner's dilemma (IPD) [168]. In IPD, each player must take into account the potential impact of his current strategy on the strategies of his opponent in the future. In the computer tournament of IPD in 1984 [168], the best strategy was "Tit-for-Tat"(TFT), which cooperates in the first round and copies the opponent's strategy in the previous round afterwards. TFT has three feature: 1) It will not defect first. 2) It retaliates if the opponent defects. 3) It forgives if the opponent started to cooperate again. In a world of TFTs, mutual cooperation is always achieved. Furthermore, TFT tends to train the opponent to cooperate. The success of TFT represents the achievement of cooperation. However, TFT does not score high facing totally random strategies [168]. What is more, as R. Boyd and J.P. Lorberbaum showed [169], no deterministic strategy, including TFT, is evolutionary stable in IPD. Other strategies such as generous TFT [170], which lowers the probability to retaliate, and Pavlov, the win-stay and lose-shift strategy [171], have been designed, but more or less relies on TFT.

Nowak proposed the following five key rules for cooperation [155]: 1) Kin selection encourages cooperation among relatives. 2) Direct reciprocity extends cooperation to unrelated individuals through expected repeated interactions, which is also characterized as "I help you, you help me." 3) Indirect reciprocity builds up cooperation on the basis of reputation in human society so that "I help you, somebody else helps me." 4) Network reciprocity provides more frequent interactions among network clusters considering spatial inhomogeneity. 5) Group selection imposes multi-level selections favoring groups with more cooperators. All the above five mechanisms can be established in a coherent mathematical framework by the inclusion of potential benefit for an individual.

In 1992, M.A. Nowak and R.M. May [172] proposed spatial prisoner's dilemma, which enables cooperators to cluster and hence persist. The spatial structure promotes cooperation in prisoner's dilemma [173], but fails in the snowdrift game [174].

Various other attempts have been made to promote cooperation such as continuous prisoner's dilemma [175, 176], players with different ability to spread their strategies [177, 178], and complex networks [179, 180]. F.C. Santos and J.M. Pacheco [181] shows in scale-free networks that strong correlation between individuals enhances cooperation. A. Melbinger [182] couples evolution in population structure with growth dynamics.

In all versions of model seeking cooperation in prisoner's dilemma, the key point is to increase the frequency of contact among cooperators beyond the population average.

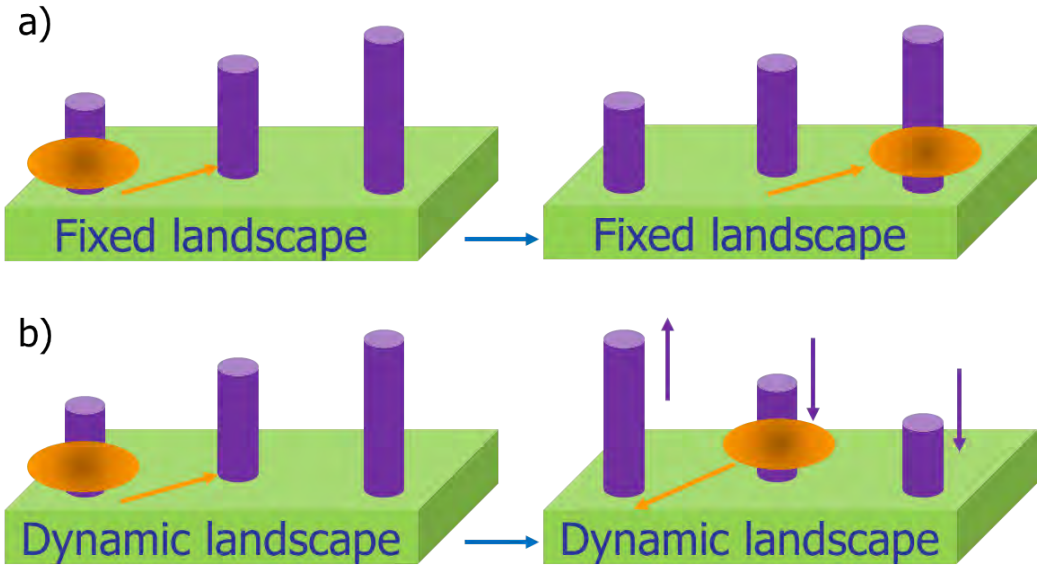

Figure 5.1: Difference between a fixed landscape and a dynamic landscape. The orange oval indicates the population. Purple cylinders of different hights indicate different fitness on the landscape. a) Evolution of the population adapting to a fixed landscape. The population moves to the cylinder with the highest fitness. b) Evolution of the population adapting to a dynamic landscape. The adaptation of the population changes the landscape. The population moves to the cylinder with the highest fitness, but not necessarily the previous one.

5.2 Dynamic Landscape

However, such mechanisms either work in a fixed landscape or do not put enough emphasis on the importance of a dynamic landscape, while in reality, the evolution of organisms is tightly coupled with the evolution of their environment (Figure 5.1). On one hand, organisms compete with each other for survival and reproduction. Mutation and selection are two mechanisms that enable and push organisms to adapt to their environment. These are driving forces for evolution of organisms in a fixed landscape, where a population moves toward a fitness maximum as shown in Figure 5.1(a).

On the other hand, each individual or species serves as an evolutionary background for other individuals and species. The simplest scenario here is the coevolution of two organisms such as the arms race between bacterium *Pseudomonas fluorescens* SBW25 and its DNA phage SBW25Φ2 as investigated by A. Buckling et al. [183]. Figure 5.2 demonstrates the general trend as ascending both in bacterial resistance and phage infectivity in approximately 400 generations during 50 transfers. Viewing bacterium *Pseudomonas fluorescens* SBW25 as the target organism and the phage SBW25Φ2 as its evolutionary background, we can see that during the improvement of bacterial resistance, phage infectivity, which is the landscape, also evolves with time, and vice versa. This is an example of coevolution of two, which can be extended to three and much

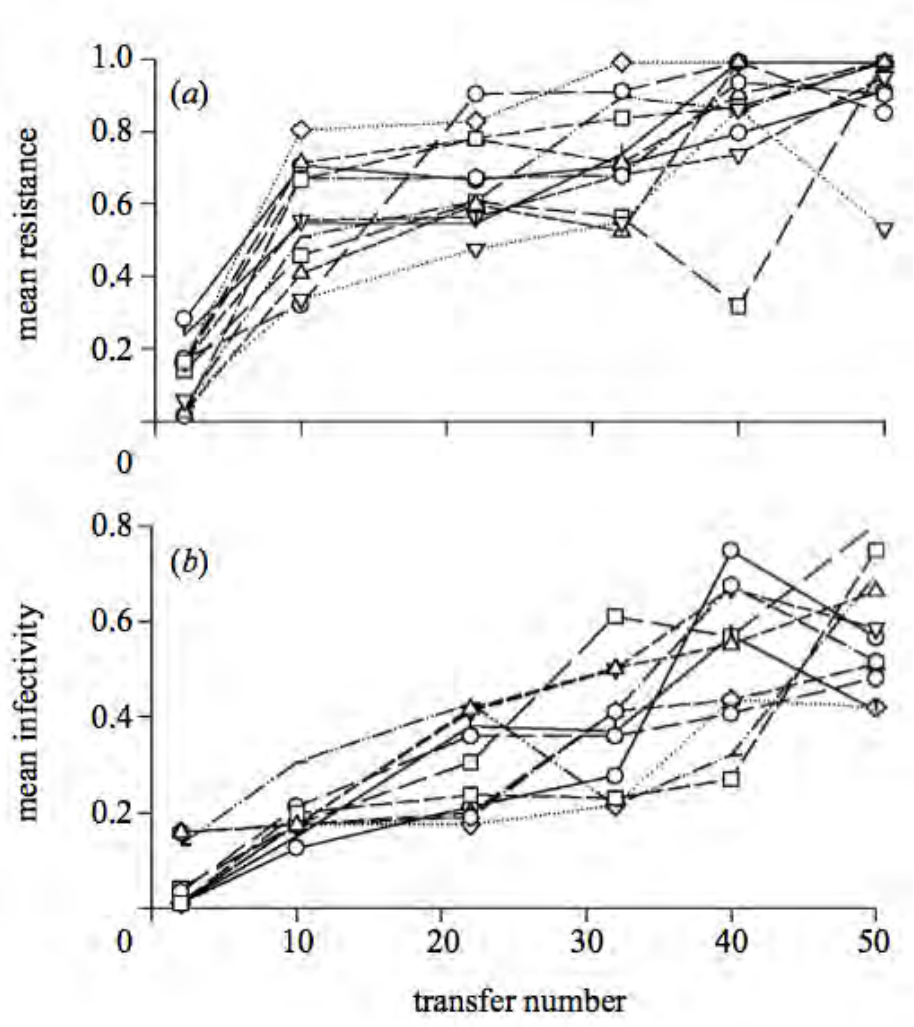

Figure 5.2: Coevolution between bacteria *Pseudomonas fluorescens* SBW2 and its phage SBW2Φ2. After Ref. [14]. (a) Increased bacterial resistance with time (transfer number) to sympatric phage populations. Different lines indicate different phage transfers. (b) Increased phage infectivity with time (transfer number) to sympatric bacteria populations. Different lines indicate different bacteria transfers.

more. Hence, the adaptive procedures of organisms react back onto the environment so that the environment is shaped by adaptations of organisms. For example, microbiota, which is beneficial to human health [184], coexist and compete with pathogens in the same niche. Taking antibiotics kills pathogens as well as the beneficial microbiota. The emergence of certain antibiotic resistance in the beneficial microbiota may seed the fast spread of resistance genes by horizontal gene transfer, so that it is not long before pathogens in the same niche acquire that kind of antibiotic resistance. Out of control by antibiotics, the burst in pathogen population will aggravate the living pressure of the microbiota in their competition for limited resources and space. Hence evolution should be tackled in a dynamic landscape, in which the fitness maximum in phase space may change with time as illustrated in Figure 5.1(b).

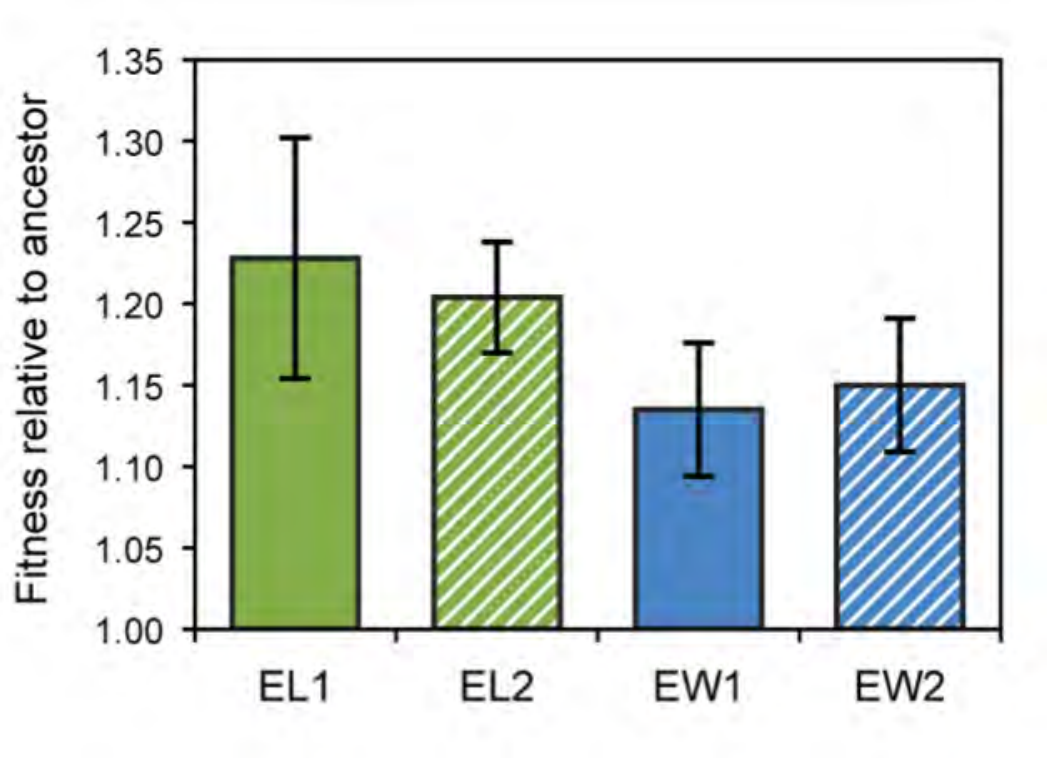

Figure 5.3: Comparison of fitness between two eventual winner (EW) and two eventual loser (EL) clones relative to the ancestor of the *E. coli* EW1 and EW2 take over the population despite their initial lower fitness compared to EL1 and EL2. After Ref. [15].

In this way, as we see it, evolutionary game theory might shed light on the long-time conundrum of the maintenance of cooperation because 1) the fitness maximum may change with time and 2) some transient states rather than the fitness maximum may be favored during evolution. These transient states are not any state, but some special ones promising to reach some fitness maximum in the long term with the evolution of the dynamic landscape. In other words, the ability to evolve, i.e. evolvability, is another criterion in evolution besides fitness. For example, R.J. Woods et al. [15] demonstrated in a population of *Escherichia coli* that two

clones with greater potential for future adaptation, despite their lower initial fitness, eventually outcompete another two after 1000 generations (Figure 5.3). In protein dynamics [185], conformational diversity such as fluctuations of side chains and exchange of second structures, providing new folds and functions, may be favored instead of a single but fixed structure. D.J. Earl and M.W. Deem [186] also showed theoretically that evolvability is a selectable trait during evolution. Therefore selection for fitness and evolvability in a dynamics landscape may enrich the context of evolutionary game theory.

5.3 Stochastic Decision Making

Furthermore, stochasticity is ubiquitous in nature and has attracted much attention. In most of the previous models, stochastic characteristics are, generally speaking, introduced through two schemes. The first is mutation at reproduction, which introduces random drift in offsprings' behaviors. The second is stochastic update rules [187] in contrast to the deterministic substitution by the best performer among all candidate strategies. Commonly used stochastic update rules include imitation of the better, where a player adopts a strategy with a probability proportional to the difference between its own score and better performers, and proportional update, which compares its own score with all candidates so that a downgrade to an inferior strategy is possible. These stochastic update rules at some level keep the diversity of strategies.

However, we would like to emphasize here another level of stochasticity: stochastic decision making. Such a decision making process is well-studied in the design of strategies in computer tournaments. A famous tournament is the iterated prisoner's dilemma (IPD) [167, 168], where two players will play the prisoner's dilemma for repeated times so that each player must take into account the potential impact of his current strategy on the strategies his opponent might choose in the future. Among various strategies in the tournament, one design is totally random irrespective of previous rounds. Although the random design does not win the tournament, the best deterministic strategy "Tit-for-Tat", where a player cooperates in the first round and copies the previous strategy of his opponent afterwards, could not score high against it. Stochastic decision making, favoring the maintenance of diversity in strategies, should be included in the seek for cooperation in game theory.

In biology, the map from genotype to phenotype is not one-to-one rigidly and rigorously [188]. Instead, there are high levels of stochasticity in the gene expression processes, such as transcription and translation. Genomes have neither the unique nor final words. Their expression is influenced by the environment. What is more, such influence may be so large as to alter the phenotypes [189, 16]. Therefore, we think it is important to endow both genotype and phenotype to each player in the game, the same way as nature does.

5.4 Stochastic Decision Making Strategy Evolving in a Dynamic Landscape

Now in the framework of evolutionary game theory, we propose a novel stochastic decision making mechanism encouraging cooperation beyond Nowak's five rules [155].

5.4.1 Dynamic Landscape in Game Theory

As we see in Section 5.1, if the payoff matrix satisfies Relation (5.2), it is a prisoner's dilemma. If the condition changes to the following one

$$T > R > S > P, \tag{5.3}$$

it is called a snowdrift game. This time a rational player would still defect if his opponent cooperates, but he would switch to cooperate if his opponent defects since $S > P$. In this case, the optimal strategy is the opposite of the opponent. Hence the outcome is the coexistence of both strategies. So there is diversity.

As illustrated by prisoner's dilemma and the snowdrift game, the payoff matrix defines the landscape of organisms because it is the rule for the game. The status of payoff matrix in game theory is similar to that of the Hamiltonian in physics systems, which determines the kinetics. A time-independent Hamiltonian provides a fixed landscape while a time-dependent one provides a dynamic landscape. If the problem were to be solved using a Hamiltonian, we would need to figure out how the Hamiltonian would evolve. Similarly, a constant payoff matrix corresponds to a fixed landscape while a varying one provides a dynamics landscape, which is exactly what we are looking for. So here is our first question: How should the payoff matrix vary?

5.4.2 Stochastic Phenotype in Game Theory

The second issue we need to address is the stochastic behaviors of players. The choice of strategies for each player is not necessarily determined at birth, and subject to environmental conditions and even the stochasticity in the environmental conditions. P.J. Choi et al.'s work in 2008 [16] is a good example illustrating both scenarios.

In their experiment, *Escherichia coli* cells are genetically engineered with two phenotypes as shown in Figure 5.4: 1) Uninduced cells with none or limited number of spotted fluorescence and 2) induced cells with highly fluorescent membranes. The production of permease, which is labeled with a yellow fluorescent protein (YFP), controls phenotype switching and lactose metabolism as well [190, 191]. At low inducer concentrations (Figure 5.5), partial dissociation of the tetrameric lactose repressor is followed by a fast rebinding, generating

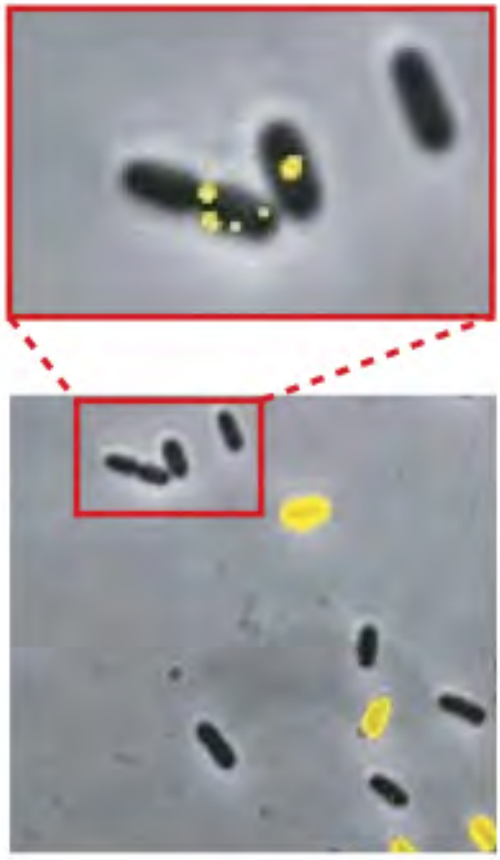

Figure 5.4: Two phenotypes in genetically engineered *Escherichia coli* cells in the presence of 30μM lactose analog methyl-b-D-thiogalactoside (TMG) inducer. Uninduced cells: none or limited number of spotted fluorescence. Induced cells: highly yellow fluorescent membranes. Upper panel dimensions 8μm $\times$13μm. Lower panel dimensions 31μm $\times$31μm. After Ref. [16].

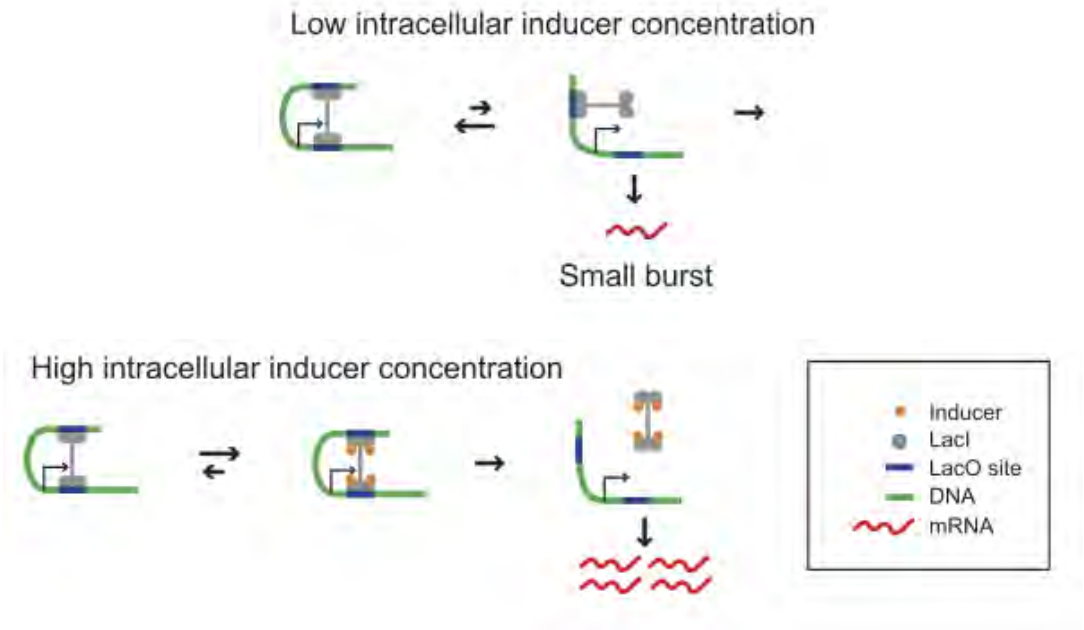

Figure 5.5: Dissociation of the lacose repressor at low and high inducer concentrations. Upper panel: At low inducer concentrations, partial dissociation is followed by a fast rebinding, yielding a small number of transcription. The *lac* operon is not induced. Lower panel: At high inducer concentrations, complete dissociation leads to a burst in transcription. The *lac* operon is induced. After Ref. [16].

Figure 5.6: A time-lapse sequence demonstrating phenotype switching in *Escherichia coli*. At an intermediate concentration of intracellular inducer (50μM TMG), the majority of the cells keep uninduced over the period, but one cell triggers induction of its *lac* operon by expressing many permease so that its phenotype changes from uninduced, which is dark, to highly fluorescence of yellow at time 30 minutes. After Ref. [16].

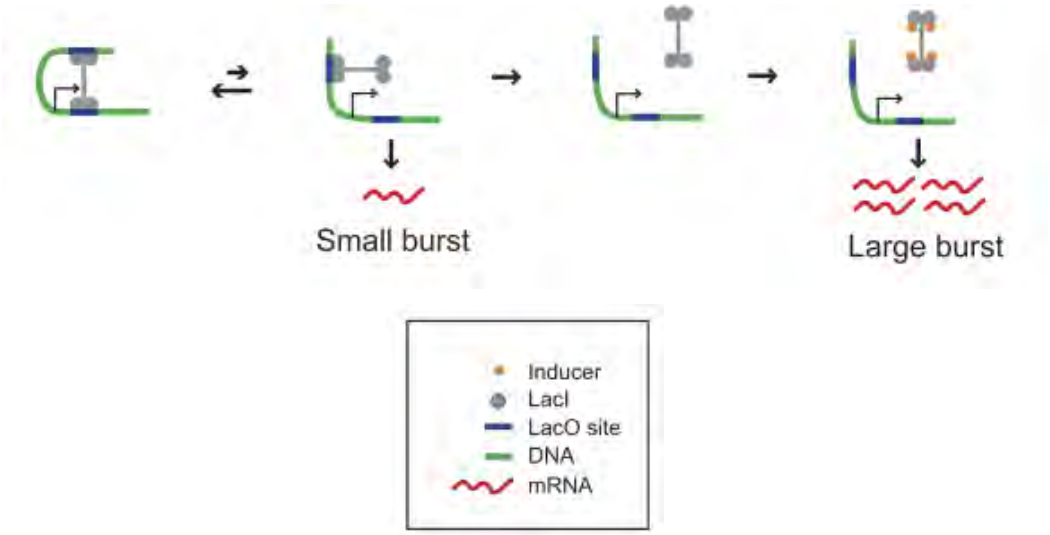

Figure 5.7: Dissociation of the lacose repressor at intermediate inducer concentrations. Partial dissociation is usually followed by a fast rebinding, yielding a small number of transcription, where the *lac* operon is not induced. Sometimes stochastic complete dissociation leads to a burst in transcription and the *lac* operon is induced. After Ref. [16].

no more than one transcript. The *lac* operon not induced, these cells are incapable of lactose metabolism. A small number of permease is synthesized, yielding limited number of spotted fluorescence. On the contrary, at high inducer concentrations, complete dissociation of the lactose repressor triggers positive feedback in permease expression. Induction of the *lac* operon enables lactose metabolism. Large burst of permease results in highly fluorescent membranes. Hence the all-or-none fluorescence phenotype is more than a toy switch in the micro-organismal wonderland. It visualizes the intrinsic state of the *lac* operon and the capability of the cell to metabolize lactose. The all-or-none fluorescence of the same cell at high and low inducer concentrations demonstrates environmentally determined phenotypes.

The more intriguing case is at intermediate concentrations. Figure 5.4 shows the coexistence of both phenotypes in a genetically identical population at 30μM lactose analog methyl-b-D-thiogalactoside (TMG), which indicates stochasticity in environmental conditions. Furthermore, Figure 5.6 records a time-lapse sequence of phenotype switching of an *Escherichia coli* cell at 50μM TMG. As Figure 5.7 illustrates, at intermediate concentrations, usually partial dissociation of the repressor is followed by a quick rebinding, but stochastic complete dissociation is able to induce the *lac* operon and lead to a large burst of permease production, yielding high fluorescence. Hence phenotype switching of the same cell as time goes on in the same media suggests stochasticity in environmentally determined phenotypes.

In order to account for the stochastic phenotypes in biology, we need another degree of freedom in our model of game theory. Whether a player is to cooperate or defect, in our eyes, is a phenotype, similar to the

all-or-none fluorescence. In order to separate genotype from phenotype, we need another level of description. So the second question is how to properly incorporate genotype?

5.4.3 Scheme

Figure 5.8 sketches a scheme of our answer to the above two combined questions: Stochastic phenotype in an evolutionary landscape. The top row emphasizes that evolution and ecology interact with each other. In the left branch, evolution imprints in the genome. Genotype, to a large extent, determines phenotype, still subject to external conditions. At the genotype level, each player has a gene p_c, which stands for the probability to cooperate. At the phenotype level, each player chooses its strategy based on the comparison of its gene p_c with a random variable each time drawn independently from an identical uniform distribution. The player will defect only when the latter exceeds the former; otherwise it will cooperate. In this way, we have distinguished genotype from phenotype explicitly. As in biology, reproduction passes on genotypes to descendants. We would like to emphasize the stochasticity embedded in our model here, which is significantly different from most of the previous models: Even coded by the same genotype, different players may have different choices of strategies, i.e. different phenotypes. Up to now, we have obtained a genuine stochastic model and answered the second question of the proper separation of genotype and phenotype. In the right branch, ecology is the fitness landscape for organisms. Using the language in game theory, it is the rule for the game, i.e. the payoff matrix. As we mentioned earlier, ecology is shaped by the adaption of organisms. Such an adaptation should be an emergent phenomenon, or in other words, a collective characteristic of the phenotypes for the whole community. Since the phenotypes are either to cooperate or defect, as a collective quantity, the cooperator fraction, in our view, serves as a good candidate to drive the dynamics of the landscape, i.e. the evolutionary ecology. Hence we require that the payoff matrix evolve with the cooperator fraction, which is our answer to the first question for the variation of the rule.

5.5 Evolving Prisoner's Dilemma

5.5.1 Model

Next, we would like to present our evolving prisoner's dilemma with the following payoff matrix

$$\begin{array}{c} \\ C \\ D \end{array} \begin{array}{c} \begin{array}{cc} C & D \end{array} \\ \begin{pmatrix} fc & f\eta \\ f[(1-\eta)c+d] & fd \end{pmatrix}, \end{array} \qquad c \tag{5.4}$$

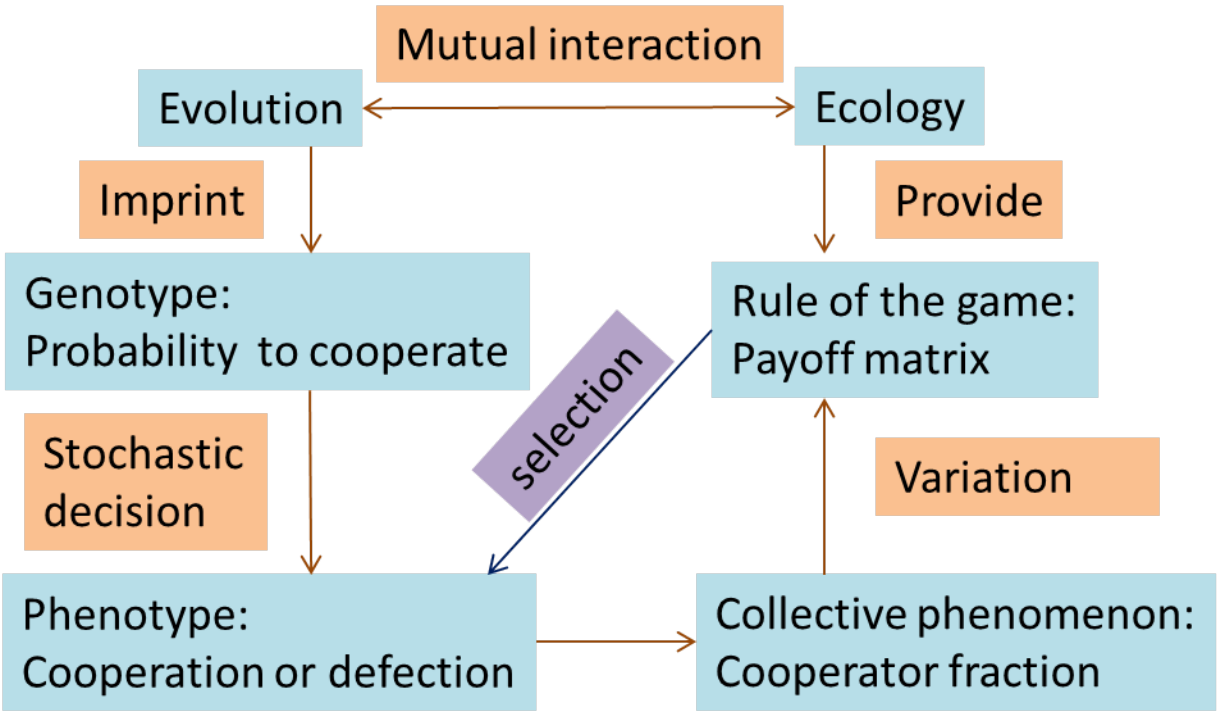

Figure 5.8: Scheme of the stochastic phenotype in evolutionary landscape.

where f is the cooperator fraction, c and d are the contribution from a cooperator and a defector, respectively, and η is the portion a cooperator reserves for itself. Without cooperator fraction f, it would be a usual payoff matrix where a defector simply grabs $(1-\eta)c$ from the cooperator and keeps its own d when encountering a cooperator. When f is multiplied, every element in the payoff matrix evolves, which provides a dynamic landscape. Does such a discount f make sense? According to J. Gore et al.'s experiment [17] (Figure 5.9) , cooperative yeasts grow much faster at high density than at low density in a sucrose culture. Since sucrose hydrolysis demands a cost from cooperators, the faster growth rate indicates higher contribution from cooperators at a higher cooperator fraction. It is a positive effect encouraging cooperation. Although the relation in experiment might not be linear, as a simplification, we multiply the contribution by f, and extend the multiplication factor to the whole payoff matrix to guarantee that the game remains in the regime of prisoner's dilemma no matter what cooperator fraction f is.

In our simulation, we choose

$$c = 11, \tag{5.5a}$$

$$d = 2, \tag{5.5b}$$

$$\eta = 0.1. \tag{5.5c}$$

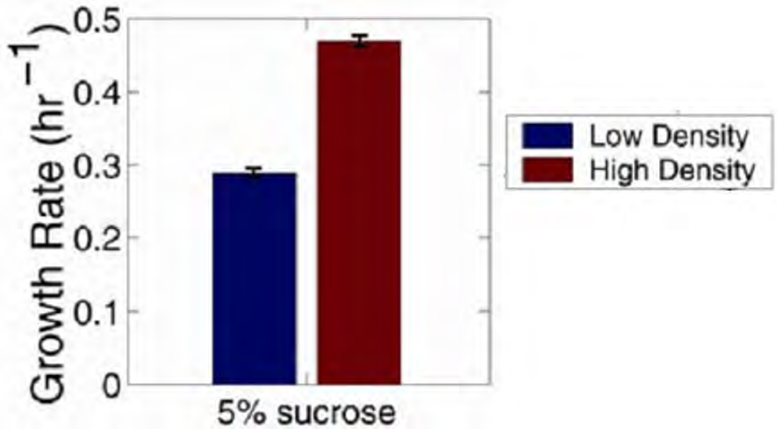

Figure 5.9: Wildtype budding yeasts grow much faster at high cell density than at low density in a 5% sucrose culture. After Ref. [17].

It satisfies the criterion for prisoner's dilemma (relation (5.2)) irrespective of the specific value of f except when cooperators extinct $f = 0$.

We perform simulations on a 513×513 lattice. The initial condition is a uniform distribution from 0 to 1 for all the genotypes, which interprets as a uniform range for the probability to cooperate from unconditional defectors to unconditional cooperators. At each round, a random number is generated to decide every player's phenotype, either to cooperate or defect, according to its genotype, which is the probability for cooperation. With all the phenotypic strategies determined, we update the payoff matrix with the current cooperator fraction. Next every player will play the game according to the current payoff matrix with its eight nearest neighbors on the lattice, and accumulate its score. Our lattice update is a Moran process [192, 193] with a constant update rate. Moran processes are commonly used in the dynamics of competing individuals while keeping the total population as a finite constant. As illustrated in Figure 5.10, each player is randomly chosen to be substituted by an offspring according to the update rate, which implies a fixed death rate for each player. When a player dies, its new-born descendant will compare the progenitor's accumulated score with the eight nearest neighbors, and inherit the genotype of the best performer. Then the round restarts. We would like to emphasize two points here, which is absent in previous models. (i) Even with the same set of neighbors' strategies, the same player's payoff is not unique, still depending on its own stochastic phenotype. (ii) A descendant inherits the genotype of the best performer, but not the best strategy, nor the best strategy combination, which is a sequence of cooperation and defection, because the phenotypic behavior is a sequence of stochastic decision making process. In this way, by explicitly separating genotype from phenotype, we have built up a simple stochastic evolutionary game theory model, where phenotype is selected by the fitness landscape, i.e. the rules, and at the same time, shapes the landscape through

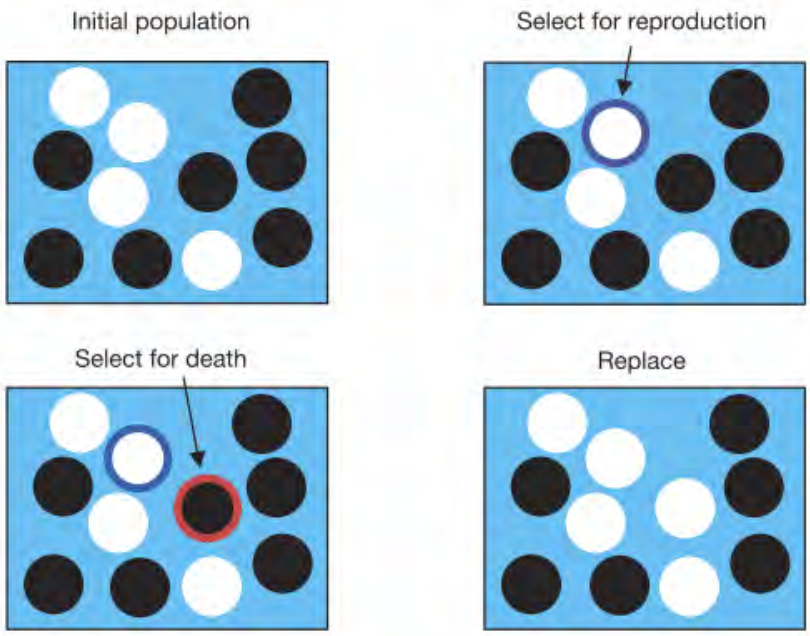

Figure 5.10: Sketch of the Moran process for stochastic evolution in a finite population of constant size. At each time step, an individual is randomly chosen to reproduce with a probability proportional to its score or fitness. Another individual is chosen to die. The offspring of the first replaces the second. Black and white dots indicate different species. After Ref. [18].

a collective power of the community, while genotype sits back of the phenotype and passes on through inheritance. Such a stochastic evolutionary mechanism is a minimal miniature of the nature.

5.5.2 Results

Figure 5.11 shows two snapshots for a simulation on evolving prisoner's dilemma at different time steps where cooperator fraction is 87.3% and 87.4%, respectively. Yellow dots represent cooperators and blue ones are defectors. Although the cooperator fraction is close to each other, the two snapshots significantly deviate in the scattering pattern of defectors and cooperators. These two snapshots are taken at approximately 20,000 time steps. It has long past the transition period, which is the first 30 time steps. The cooperator fraction has approached a semi-fixed point, but still keeps changing slightly. The pattern continuously evolves as the two snapshots contrast. Hence it displays a highly dynamic and forever-evolving system.

In Figure 5.11, the lattice update rate is 100% and the system reaches a coexistence of cooperators and defectors. We would like to compare it to Figure 5.12, where we decrease the lattice update rate to 1% and 50%, respectively, in order to demonstrate the selection advantage. The overwhelming dominance of cooperators in a prisoner's dilemma game is out of expectation. In a classic spatial game theory model,

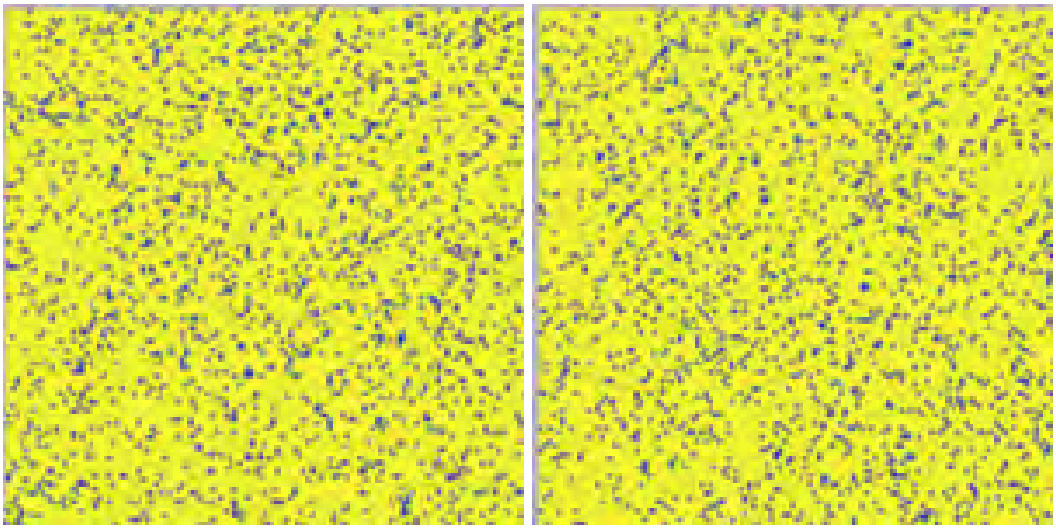

Figure 5.11: Simulation on evolving prisoner's dilemma for lattice update rate 100%. Yellow dots are cooperators and blue ones are defectors. The left and right panels are at different time steps with cooperator fraction 87.3% and 87.4%, respectively. The simulation runs on a 513×513 lattice while the two snapshots contrast the same top-left corner to demonstrate the forever-evolving feature of the patterns.

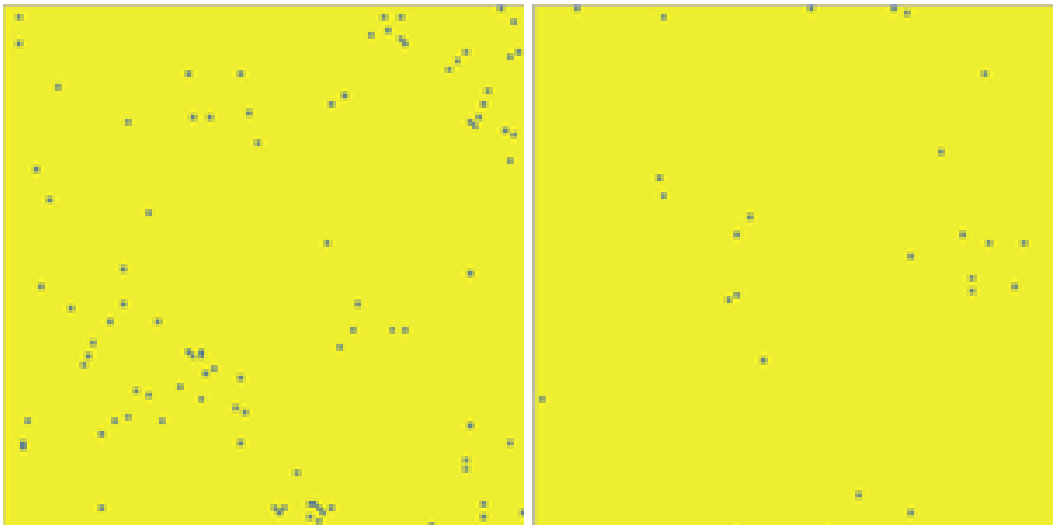

Figure 5.12: Simulation on evolving prisoner's dilemma for lattice update rates 1% (left panel) and 50% (right panel), respectively. Yellow dots are cooperators and blue ones are defectors. The cooperator fractions are both 99.9%. The simulation runs on a 513×513 lattice while the two snapshots contrast the same top-left corner to demonstrate the influence of details in evolutionary game theory on patterns.

little difference is observed in the phase diagram for cooperation fraction between the synchronized and asynchronized lattice updates [187]. Here the huge difference between Figure 5.11 and Figure 5.12 illustrates the subtlety in evolutionary game, where details of the game such as the update rate here are important [194].

5.5.3 Discussion: Timescale

Generally speaking, evolution is recognized on a long timescale. Adaption to the environment, emergence and fixation of new genotypes, and speciation of different lineages are achieved through many generations. This classic scenario corresponds to a slow lattice update rate, where advantageous strains are endowed with enough opportunities to take over the whole community.

Comparison	F_{ST}	F_{ST} (no Ssa85)	D	GD (P value)
River residents versus beach immigrants	0.008 (0.002–0.013)	0.008	0.010	0.365
River residents versus beach residents	0.025 (0.008–0.042)	0.017	0.054	0.002
Beach residents versus beach immigrants	0.015 (0.001–0.033)	0.012	0.026	0.030

Table 5.1: Genetic differentiation at six microsatellite loci between beach residents, river residents, and beach immigrants. D: Nei's unbiased genetic distance. F_{ST}: fixation index. GD: genotypic differentiation. Ssa85: locus that best differentiated river residents from beach residents with $F_{ST} = 0.054$. Huge difference in genetic differentiation identifies beach residents and river residents as two ecotypes. After Ref. [3].

However, fast selection, where selection is quicker than interactions among individuals, or with their environment [194], is also reasonable and supported by recent experimental discoveries [195, 196, 197, 198]. For example, A.P. Hendry et al. [87] offered evidence for reproductive isolation in an introduced sockeye salmon descending from a common ancestry after within only 13 generations. Two distinct ecotypes are identified in salmon inhabiting Cedar River and a Lake Washington beach with a geographical separation of 7 km. Table 5.1 compares genetic differentiation at six microsatellite loci between 3 salmon populations as beach residents, river residents, and beach immigrants. Figure 5.13 compares their male body depth, which is sexually selected, and female body length, which is important to protect eggs in flooding. The huge genotypic and phenotypic difference between beach and river residents in Table 5.1 and Figure 5.13, respectively, establishes their reproductive isolation.

Micro-organisms also exhibit rapid evolution in predator-prey systems. M.A. Duffy and L. Sivars-Becker

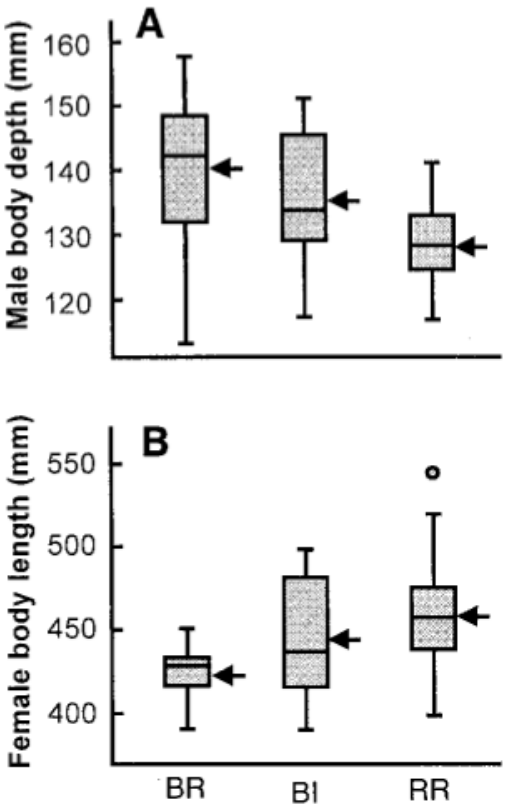

Figure 5.13: Comparison of (A) standardized male body depth and (B) female body length between beach residents (BR), beach immigrants (BI), and river residents (RR). Boxes contain 50% of the data and bars for the remainder. Horizontal lines, arrows and the circle indicate medians, means, and an outlier, respectively. Huge difference in both male body depth and female body length for BR and RR identifies them as two ecotypes. After Ref. [3].

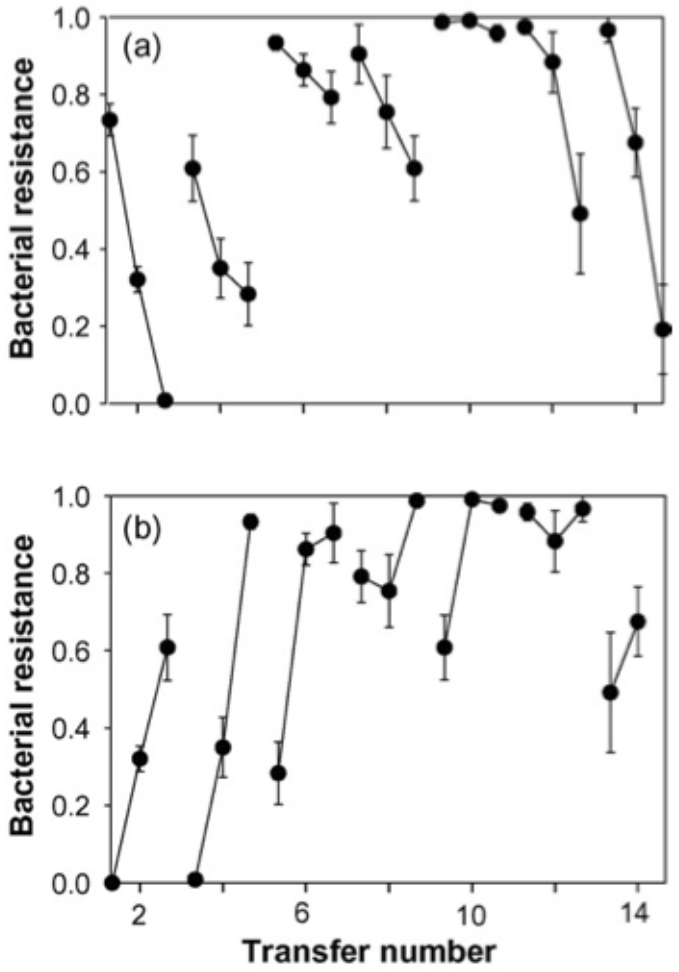

Figure 5.14: Coevolution between bacteria *Pseudomonas fluorescens* and its phage Φ2. After Ref. [14]. (a) Each line represents bacterial resistance to past, contemporary and future sympatric phage populations. The negative slope shows increased phage infectivity. (b) Each lines represents resistance of past, contemporary and future bacterial to a given sympatric phage population. The positive slope shows increased bacterial resistance.

[3] reported that *Daphnia dentifera* from lakes with recent epidemics were more resistant to infection by its parasite *Metschnikowia bicuspidata*. M.A. Brockhurst et al. [199] systematically investigated coevolution between bacteria *Pseudomonas fluorescens* and its lytic phage Φ2 for 120 generations during 16 transfers. Figure 5.14 shows coevolution of phage infectivity and bacteria resistance in the predator-prey systems. The decreased bacterial resistance to past, contemporary and future phage (Figure 5.14 (a)) demonstrates improved phage infectivity while the increased bacteria resistance of past, contemporary and future transfers to a given sympatric phage population (Figure 5.14 (b)) manifests improved bacteria resistance. Hence rapid evolution is visible between different transfers, each containing 7.5 generations on average.

Besides, in social and cultural evolution, the timescales of selection and interaction are comparable to each other [194].

Therefore, different lattice update rates map to different reasonable scenarios. Our results show that slow and intermediate (Figure 5.12) selection are more promising to encourage cooperation compared to fast selection (Figure 5.11). In other words, the keynote in nature encourages cooperation!

5.5.4 Discussion: Origin of Cooperation

According to the classic game theory, defection is both a Nash equilibrium and an evolutionary stable strategy in the regime of prisoner's dilemma. Large efforts have been devoted to promote cooperation [175, 200, 174, 201]. Unexpectedly, our model presents something more startling. It might yield the dominance of cooperation subject to the update rate of the lattice. However, defectors in our model will never have a chance to dominate the whole community. The striking difference between our model and classic prisoner's dilemma models raises two questions. First, what is the key mechanism that supports coexistence? Second, what is the origin of the dominance of cooperators? These two questions, in fact, both root in the origin of cooperation.

As a comparison, we perform a simulation with the stochastic behaviors of players but without the feedback of the community onto ecology, which is the fixed landscape. We see that coexistence is still achieved but the cooperator fraction drops to $20 \sim 40\%$. Therefore, the coexistence of the cooperators and defectors attributes to the separation of genotype and phenotype as sketched in Figure 5.8, while the dominance of cooperators results from the evolving rules.

In order to further illustrate the origin of cooperation in more details, we track the evolution for the distribution of cooperator fractions as shown in Figure 5.15. We can see that initially cooperator fraction drops as more unconditional or nearly unconditional defectors, with low cooperation probability, mushroom, which is consistent with the classic selection advantage of defectors. The rapid diminishing of unconditional

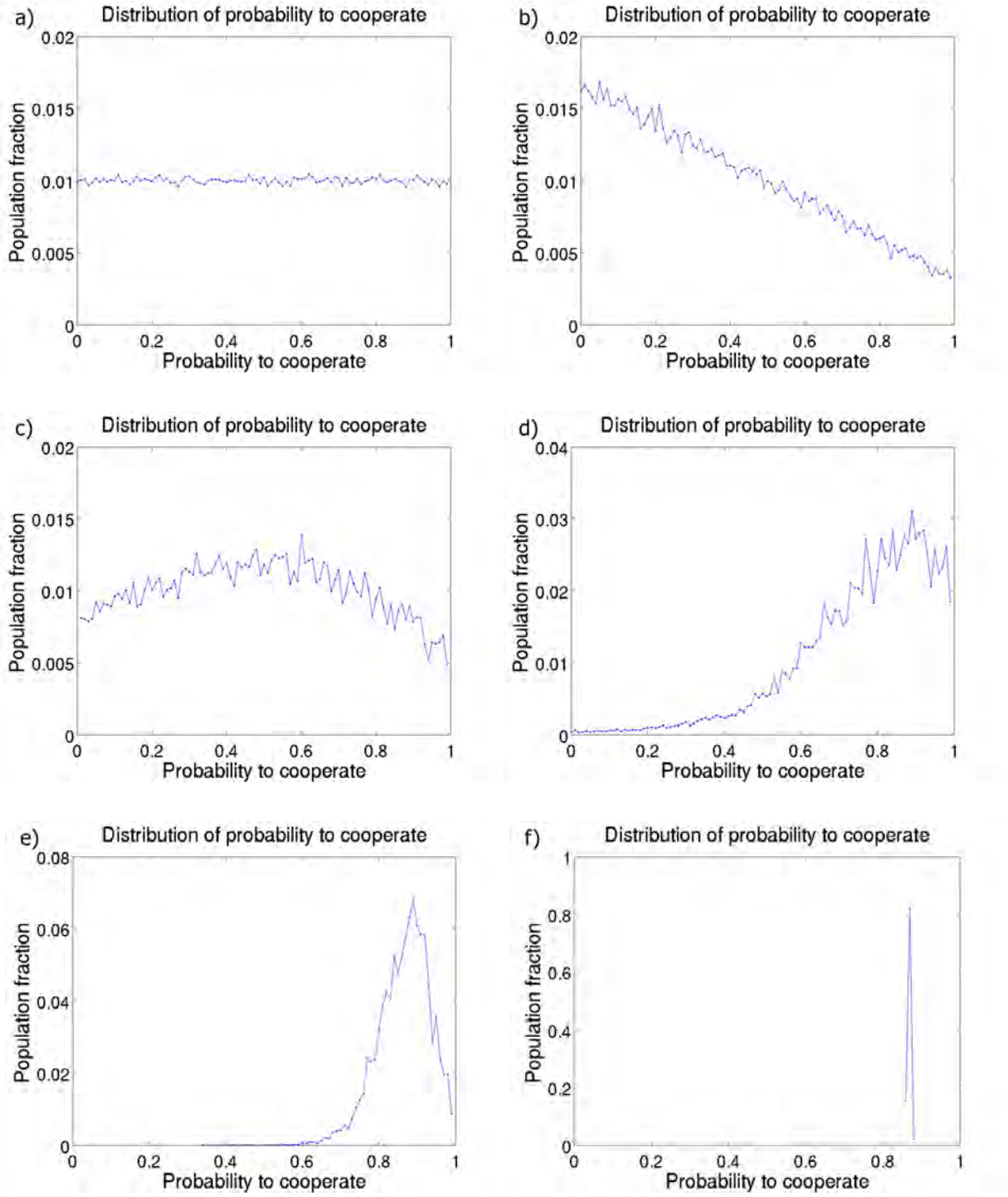

Figure 5.15: Distribution of the probability to cooperate at different time steps in evolving prisoner's dilemma. Time elapses from a) to f). a) Time at 0. b) Time at 1. c) Time at 3. d) Time at 11. e) Time at 50. f) Time at 28329.

or nearly unconditional cooperators, with high cooperation probability, leaves fewer players to be exploited by those more selfish individuals. What is worse for these selfish individuals, they tend to cluster due to the nearby reproduction. As a result, they are soon superseded by random individuals with cooperator fraction near 50%. This illustrates the key role of stochasticity in phenotype determination: Although unconditional or nearly unconditional cooperators are vulnerable to unconditional or nearly unconditional defectors, random individuals are able to survive (Figure 5.15(b)), which serves as a reservior for cooperative phenotypes. Cooperators, on the contrary to defectors, benefit from clustering with each other. Furthermore as payoff matrix (5.4) shows, the reward for cooperation increases with cooperator fraction. In other words, altruism is advantageous to avoid exploitation by defectors. Such a positive feedback favors coopertors, so the peak of the population moves to higher and higher cooperation probability as shown in Figure 5.15(c) $\sim$ (f), and the cooperator fraction continues to rise, too. When will it stop? It depends on the details of the model for equilibrium such as the update rates shown in Figure 5.11 and 5.12. Therefore, despite the initial boom of defectors, cooperators at last dominate the whole community.

In short, stochastic phenotype determination maintains the coexistence of cooperation and defection, while the evolutionary landscape pumps up cooperator fractions.

5.6 Other Evolving Games

Besides the evolving prisoner's dilemma, we have also designed an evolving snowdrift game

$$\begin{array}{c} \\ C \\ D \end{array} \begin{array}{c} \begin{array}{cc} C & \quad D \end{array} \\ \begin{pmatrix} c & \eta + f(1-c\eta)d \\ (1-\eta)c+\eta d & fd \end{pmatrix} \end{array}, \tag{5.6}$$

and another game with frequent transitions between prisoner's dilemma and snowdrift game

$$\begin{array}{c} \\ C \\ D \end{array} \begin{array}{c} \begin{array}{cc} C & \quad D \end{array} \\ \begin{pmatrix} fc & \eta \\ (1-\eta)c+d & fd \end{pmatrix} \end{array}, \quad c \tag{5.7}$$

with the same set of parameters (5.5). In both games, not only coexistence but also the same level of cooperator fraction as in the evolving prisoner's dilemma, is achieved.

Therefore, in an evolving stochastic game, the payoff matrix alone is far from enough to determine the fate of the whole community. Stochasticity embedded in the phenotype determination process encourages

cooperation. Since the stochastic phenotype mechanism mimics the universal stochasticity in gene expression, such as transcription and translation, our models demonstrate that the cooperator fraction alone is not enough to reveal the competition type, whether it is prisoner's dilemma or snowdrift game, among individuals. In other word, stochastic phenotype masks the type of rules in nature.

5.7 Comparison with Previous Models

Last, we would like to compare our model to previous ones. The same in classic game theory, but different from iterated games, our players have no memory either of their opponents' or their own's previous phenotypes (or strategies). However, their payoff is affected by the community as a whole through the cooperator fraction f in the evolving matrix. This attributes to the dynamic landscape. Although not correlated in time, each player's phenotype is determined by the same genotype through its life span. The stochastic phenotype differentiates our plays from classic plays. This attributes to the stochastic phenotype determination process. Hence our players are somewhere between classic players and iterated ones.

Furthermore, by incorporating cooperator fraction f in the payoff matrix, we provide a mean field level background to every individual, similar to inserting the magnetization in the effective field in the Ising model. In this way, the cooperative or defective phenotypes of individuals affect the population. In other words, cooperation benefits the whole community as the elements in the payoff matrixes (5.4), (5.6), and (5.7) increase with higher cooperator fraction. The positive feedback pumps up the cooperator fraction.

5.8 Conclusion

In this chapter, we propose a novel stochastic mechanism encouraging cooperation in evolutionary game theory. We have successfully achieved high cooperation fractions in the community even when the governing rule falls in the regime of prisoner's dilemma, let alone other rules. Such dominance of cooperation, irrespective of the detailed type of rules, is consistent with the wide observation of cooperation in nature. Our mechanism significantly stresses stochasticity in the map from genotype to phenotype, and evolutionary landscape, with which different rules such as prisoner's dilemma and snowdrift game yield comparable cooperator fractions. Therefore, cooperator fraction, as a collective and emergent quantity, is not necessarily determined by the detailed type of competition, but rather may subject to stochastic phenotype and evolutionary landscape, which are able to mask the underlying type of competition. Such a landscape provides altruisms an alternative way to escape exploitation by defectors.

Chapter 6

Evolutionary Robust Strategies for Delivery of Antibiotics

6.1 Introduction

6.1.1 Challenge, Innovation and Impact

For more than half a century, treatments against bacterial infections have focused primarily on delivering classes of molecule that are broadly toxic to the bacteria in the human body. However, this approach is not sustainable because microbial communities can share antibiotic resistance genes through a variety of mechanisms of horizontal gene transfer [58]. Recently it was discovered that horizontal gene transfer rates between pathogenic and commensal *Enterobacteriaceae* may be boosted by up to several orders of magnitude in gut inflammation [202]. Frequent horizontal gene transfer leads to unexpectedly rapid emergence of antibiotic resistance and even multidrug resistance (MDR) [203, 204]. For example, methicillin-resistant *Staphylococcus aureus* (MRSA), which is resistant to a wide range of drugs such as aminoglycosides, macrolides, tetracycline, chloramphenicol, and lincosamides besides the commonly known methicillin [205], was estimated in 2005 [206] with an incidence rate of 31.8 per 100,000 and mortality rate of 6.3 per 100,000, i.e., about 95,000 cases and 19,000 deaths every year in the United States. Vancomycin is empirically most frequently used to treat MRSA infections [206], but its minimum inhibiting concentration (MIC) has significantly increased for clinical isolates over the years [207]. Vancomycin-resistant *S. aureus* (VRSA) [208] ascends as a new clinical challenge [204]. What is worse, emergence of MDR and extensively-drug-resistant (XDR), which is resistant to at least 3 out of 6 classes of drugs, *Mycobacterium tuberculosis* (MDR-TB and XDR-TB) is rising worldwide [120]. Totally drug-resistant (TDR) tuberculosis was reported and documented in Italy in 2007 [209], Iran in 2009 [210, 211] and India in 2011 [212, 213]. The return of dark ages before the discovery of antibiotics is looming on the horizon.

The innovations presented here are smart strategies, based upon a quantitative understanding of the evolutionary response of bacterial communities. If successful they could provide a new paradigm and transform our approach to treating diseases with an evolutionary or collective component, a class that includes not

just bacterial infections but also cancer and HIV.

6.1.2 Rationale

Our proposed strategies are radically different from current practice [204]. First, conventional strategies using broad-spectrum antibiotics do not differentiate between the pathogens and the beneficial microbiota that are normally resident in our bodies. This population vastly outnumbers the invasive pathogens, at least at the beginning of an infection, and can help suppress the infection by competing with the pathogens for limited resources of nutrients, thereby dominating the carrying capacity of the host ecosystem (e.g. the gastrointestinal tract). Furthermore, under exposure to antibiotics, this beneficial population becomes enriched in antibiotic resistance genes, which can be readily transmitted to the pathogens. The widely-recognized conclusion is that the next generation antibiotics should be selective, either narrow-spectrum which target pathogens and Gram-positive beneficial bacteria, or ultra-narrow-spectrum, which target pathogens only.

However, this is not sufficient to avoid the eventual emergence of antibiotic resistance, although it will delay the onset according to our preliminary calculations. Instead, we propose to minimize the possible influence of antibiotic resistance genes by applying a negligible selective pressure to the pathogens. Our idea begins with the observation that, in many cases, pathogens use quorum sensing to coordinate their attack when they are sufficiently numerous [214]. Our working hypothesis is that we can interfere with quorum sensing channels, but instead of trying to suppress these channels as other works have proposed [215, 216, 217, 218], we will attempt to amplify these signals. Our rationale is that we can thereby induce the premature expression of virulence factors! Although counter-intuitive, this will have the effect of imposing a substantial metabolic load on the pathogens, slowing their growth and further limiting their ability to occupy a biochemical niche in the host. Our preliminary calculations suggest that all these effects prevent the proliferation of pathogens, and when combined with the subsequent and timely application of a single dose of ultra-narrow-spectrum antibiotics can completely suppress the pathogen population before antibiotic resistance genes have spread and before the virulence has reached clinically problematic levels.

6.1.3 Approach

Our plan to attack the challenge of emerging antibiotic resistance has two independent strategies: 1) Narrowing down the spectrum of antibiotics in order to target pathogens precisely and 2) quorum sensing spoofing so as to incur the huge cost on pathogens in virulence factor pre-expression. We design theoretical models to investigate the effectiveness of both strategies and then combine them into an advanced therapy as an evolutionary robust strategy for the delivery of antibiotics. To our knowledge, this sort of two-step treat-

ment cycle has never been proposed in this context, and it differs from all existing approaches in that it will not promote the transmission of antibiotic resistance, and will leave largely intact the hosts beneficial microbiota. It addresses the problem of horizontal gene transfer and the transmission of antibiotic resistance genes, and as such would represent a major advance if successful.

Our approach presents a significant innovation, a novel treatment, and an ambitious attack on the antibiotic resistance problem, significantly departing from current biomedical research undertaken elsewhere. We focus on collective properties such as the response of bacterial communities to antibiotics by their transmission of antibiotic resistance genes, which is a systems or population level phenomenon. The outcome of collective properties is always hard to predict a priori, because of multistability: there are typically a number of possible outcomes, and which one actually occurs is determined by the phase diagram of the system, in other words, the interplay between the different forces active in the system.

In more detail, these forces include the ecological competition between the pathogens and the indigenous bacteria, the dependence of expression of virulence factor on the concentration of quorum sensing molecules, the rate of interspecies horizontal gene transfer and so on. As a result, one must calculate the dynamical behavior of these complex systems and identify, even semi-quantitatively, regions of parameter space where the outcomes are biomedically desirable. In this regard, our approach differs from existing approaches wherein candidate pathways are targeted and the level of systems biology that needs to be quantitatively understood is relatively low: a molecule will either have the desired effect or it won't — but there is no "tuning parameter" other than dose which can be varied in the treatment.

In order to explore the parameter space relevant to each of our components, it is essential to perform individual-level population dynamics simulations of the interactions between the pathogens, the beneficial microbiota, the quorum sensing molecules, and the antibiotic resistance genes, taking into account their possible horizontal transfer. Preliminary results from such simulations shaped the innovative approach we pursue in this chapter and we discuss these simulations below in more detail to motivate our strategy for overcoming the key obstacles presented by the emergence of antibiotic resistance. Their outcome is, however, simple to state: we were unable to find a single-step drug treatment that could eliminate pathogens and not give rise to the emergence of antibiotic resistance at large in the population. A more positive way of stating our conclusion is that the narrow- and ultra-narrow-spectrum antibiotics do delay the onset of the emergence of population-wide antibiotic resistance compared with broad-spectrum antibiotics, but the difference is not qualitative. In a second round of computer simulations, we found that a two-step drug treatment schedule, involving modulating the concentration of quorum sensing molecules, was able to both prevent the emergence of antibiotic resistance at the population level and eliminate the pathogens, at least

as far as is possible given the potential presence of persisters. This innovative strategy, which forms the bulk of our effort, is described below.

6.2 Narrowing Down the Spectrum of Antibiotics

6.2.1 Mechanisms of Conventional Broad-spectrum Antibiotics and Corresponding Resistance

In order to fight against the emergence of antibiotic resistance, we first need to familiarize ourselves with the current status of the battle between pathogens and human race. In other words, we must have a general understanding of how the conventional antibiotics work and how the corresponding antibiotic resistance rises.

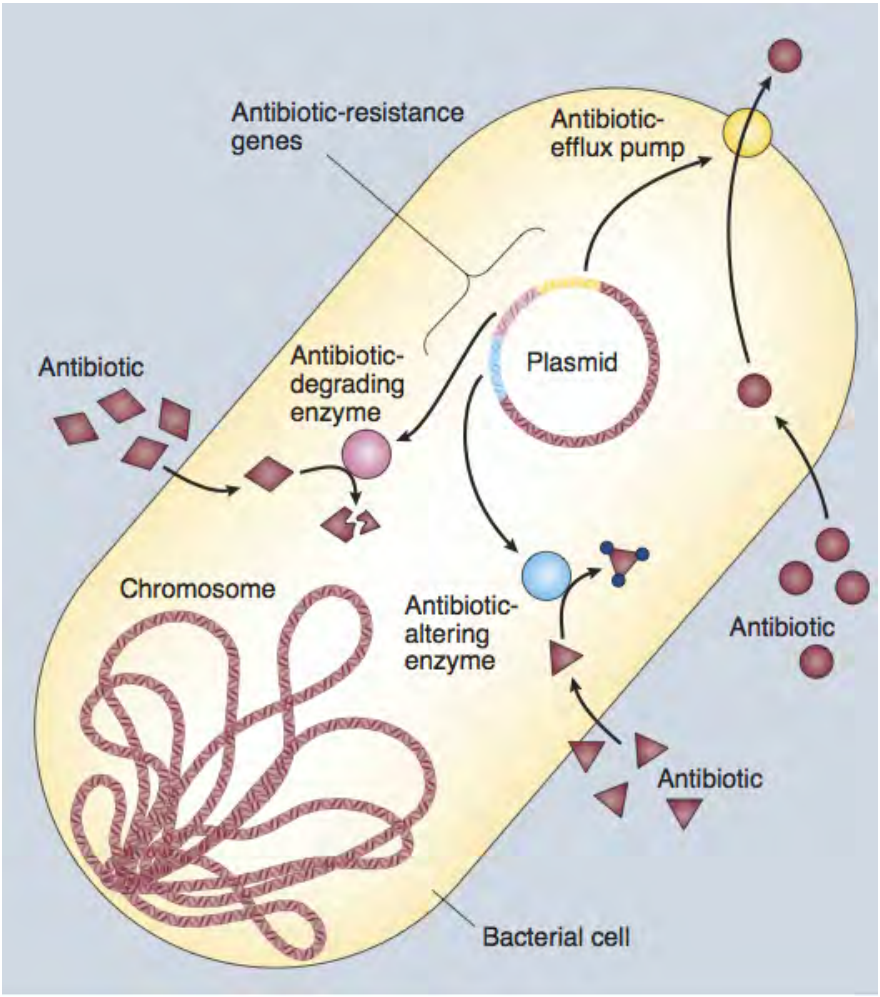

Figure 6.1: Different mechanisms of antibiotic resistance. After Ref. [19].

Although the detailed mechanisms of conventional broad-spectrum antibiotics vary from class to class, they kill bacteria by inhibition of essential bacterial functions. For example, penicillins inhibit cell wall synthesis; tetracyclines inhibit protein synthesis; fluoroquinolones inhibit DNA synthesis; and rifampin inhibits RNA synthesis [19]. By targeting essential bacterial functions, conventional antibiotics are able to effectively reduce bacteria population counts. Ironically, the use of antibiotics to disrupt normal bacterial metabolism and reproduction imposes a severe selection pressure that causes rapid emergence of resistance genes in the population. Antibiotic resistance genes code corresponding enzymes (Figure 6.1) functioning at different levels [19, 4]. They may target at the antibiotic itself by destruction or inactivation. They may target the transportation process by continual pumping out drugs. They may also target at the intracellular level by target protection, target alternation, or bypassing an attacked metabolic step with a new drug-resistant enzyme [19, 5]. For every class of antibiotics that targets an essential physiological function, a resistance mechanism is now known (Table 6.1). Multidrug resistance is engendered either by the accumulation of multiple resistance genes, typically occurring on resistance plasmids, or the acquisition and increased expression of genes coding some very powerful multidrug efflux pumps [205].

Antibiotic class	Example(s)	Target	Mode(s) of resistance
β-Lactams	Penicillins (ampicillin), cephalosporins (cephamycin), penems (meropenem), monobactams (aztreonam)	Peptidoglycan biosynthesis	Hydrolysis, efflux, altered target
Aminoglycosides	Gentamicin, streptomycin, spectinomycin	Translation	Phosphorylation, acetylation, nucleotidylation, efflux, altered target
Glycopeptides	Vancomycin, teicoplanin	Peptidoglycan biosynthesis	Reprogramming peptidoglycan biosynthesis
Tetracyclines	Minocycline, tigecycline	Translation	Monooxygenation, efflux, altered target
Macrolides	Erythromycin, azithromicin	Translation	Hydrolysis, glycosylation, phosphorylation, efflux, altered target
Lincosamides	Clindamycin	Translation	Nucleotidylation, efflux, altered target
Streptogramins	Synercid	Translation	C-O lyase (type B streptogramins), acetylation (type A streptogramins), efflux, altered target
Oxazolidinones	Linezolid	Translation	Efflux, altered target
Phenicols	Chloramphenicol	Translation	Acetylation, efflux, altered target
Quinolones	Ciprofloxacin	DNA replication	Acetylation, efflux, altered target
Pyrimidines	Trimethoprim	C_1 metabolism	Efflux, altered target
Sulfonamides	Sulfamethoxazole	C_1 metabolism	Efflux, altered target
Rifamycins	Rifampin	Transcription	ADP-ribosylation, efflux, altered target
Lipopeptides	Daptomycin	Cell membrane	Altered target
Cationic peptides	Colistin	Cell membrane	Altered target, efflux

Table 6.1: Modes of resistance of commonly used antibiotics. After Ref. [4].

6.2.2 Restricting the Spectrum of Antibiotics

A single bacterium acquires antibiotic resistance genes through two pathways: mutation and horizontal gene transfer. Generally speaking, mutation is a rare event, which depends on mutation rate and population size. Horizontal gene transfer spreads antibiotic resistance genes intra- and inter-species and even across domains [115]. A significant source of resistance genes for pathogens is the beneficial microbial population of the host,

by virtue of its overwhelming population size and the relative ease of inter-species horizontal gene transfer. Thus the rate of acquisition of resistance genes by the pathogen is dependent on the proportion of resistance genes in the beneficial microbiota. When a broad-spectrum antibiotic is used, the impact on the beneficial microbiota will be to select for a resistant sub-population, thus increasing the rate of transfer of resistance genes from the beneficial microbiota to the pathogens. Concomitantly, any method to reduce the proportion of resistance genes in the beneficial microbiota will significantly reduce the rate of transfer of such genes to the pathogens. The best way to achieve this is to remove the selection pressure on the beneficial microbiota, by the use of next-generation antibiotics with specific target species. A side benefit of this strategy is that the pathogens must compete against a beneficial microbial population, whilst simultaneously being under strong selection pressure from the antibiotic.

Bailing out beneficial microbiota from the application of conventional antibiotics will bring profound impact on human health, probably more than what is established and justified currently. For example, it is recognized [219, 220] that intestinal bacteria, such as *Bacillus subtilis* and *Escherichia coli*, synthesize vitamin K, which is essential for human health. Besides their role as nutrition especially vitamin providers and invasion protectors against pathogens, certain correlations between compositional shifts in beneficial microbiota and long-term physiological changes have been suggested [184], such as association between eradicating *Helicobacter pylori* and increased risks of asthma and allergies [221]. Saving and reviving beneficial microbiota may conduce not only to antibiotic resistance but also other public health problems such as obesity [184].

Hence, the ideal scenario is to kill the specific pathogenic strains, but with no side effect on the beneficial microbiota. The latter can be either Gram-positive or Gram-negative strains, with the Gram-negatives possessing an extra cell membrane that often blocks the influx of small molecules. Narrow-spectrum antibiotics do not distinguish between pathogens and non-pathogens but are typically selective for either the Gram-positive or Gram-negative bacteria. Here we use the term "ultra-narrow-spectrum antibiotics" to refer to classes of antibiotic that affect only the pathogens, as being developed by our collaborator Douglas A. Mitchell. We show and compare the victims for different spectrum of antibiotics in Figure 6.2.

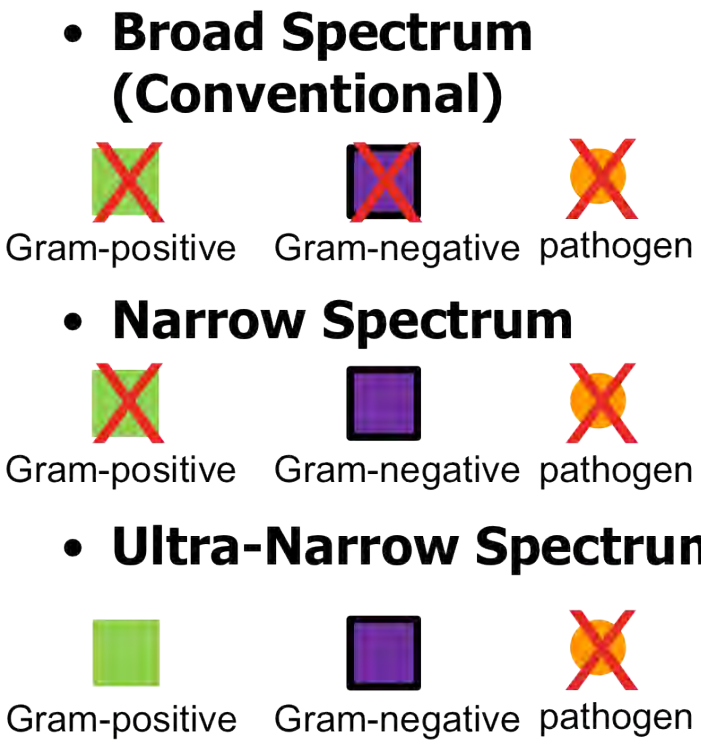

Figure 6.2: Illustration of antibiotics targeting different spectrums. Red crosses indicate victims.

6.3 Population Dynamics for Broad-, Narrow-, and Ultra-Narrow Spectrum Antibiotics

6.3.1 Goal

In order to quantify the effectiveness of restricting the range of antibiotics, we performed preliminary calculations using an individual-level model of the population. In this calculation, the behavior and dynamics of every organism is simulated, including birth-death processes, horizontal gene transfer, mutation and resource allocation within the community. Each bacterium, Gram-positive, Gram-negative or pathogenic, may acquire the resistance gene by mutation or intra- or inter-species horizontal gene transfer.

We have studied both spatial homogeneity and heterogeneity, yielding qualitatively same results. With the same initial conditions and biological measurable parameter settings, we would like to compare how effective it is in applying different antibiotics, and how rapid it is for the corresponding antibiotic resistance to emerge, spread and dominate.

6.3.2 Cost for Antibiotic Resistance

Usually there is a metabolic load associated with carrying antibiotic resistance genes [222, 5]. Such a metabolic cost is strain- and gene-specific (Table 6.2), and subject to epistasis and environmental conditions, with caveats that it might be cost-free in some rare cases [5] or shared among the whole bacterial community [223].

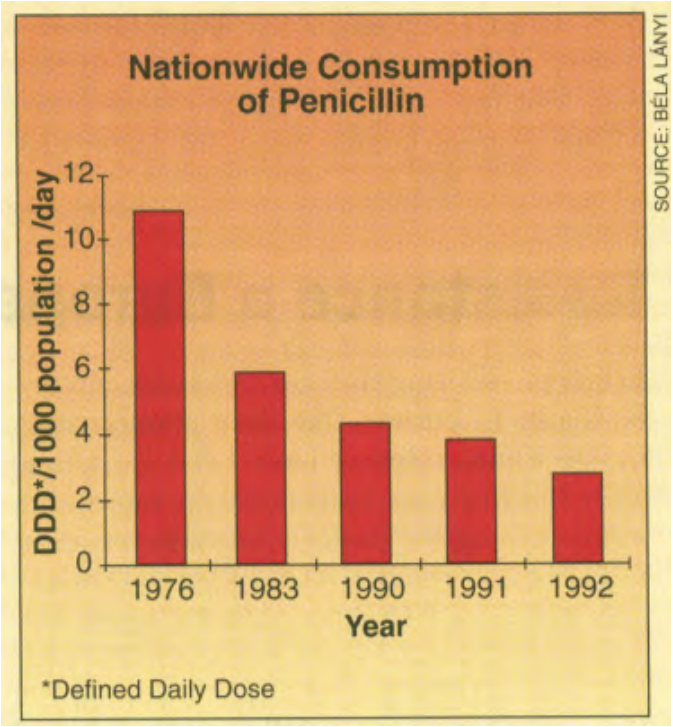

Figure 6.3: Hungary's penicillin consumption fell in over a decade. After Ref. [20].

The expensive biological cost for most antibiotic resistance strains inspires a ray of hope to revert pathogens to drug sensitivity with reduced volume of antibiotic use. For example, penicillin-resistant pneumococcus infections in Hungary [20] fell from 50% to 34% in over a decade's reduced nationwide consumption (Figure 6.3). Finland [21] decreed policies to regulate macrolide antibiotics consumption (Figure 6.4) and documented erythromycin resistance from throat-swab and pus samples dropping from 16.5 % to 8.6 % in 5 years (Figure 6.5).

Surveillance and regulation of antibiotic usage seems to be effective [224], but entails a long period [225] to see a decline in resistance and requires further confirmation [226]. Taiwan, for instance, with restricted antibiotic usage reported decreased resistance to penicillin, but not to erythromycin *Streptococcus pneumoniae* from 1998 to 2003. More depressingly, UK reported [22] persistent sulphonamide resistance in *Escherichia coli*, which was 39.7% in 1991 and 46.0% in 1999, despite drastic reduction in prescription of

Bacteria	Resistance	Cost*	Assay system
Salmonella enterica subsp. *enterica* serovar Typhimurium	Streptomycin	Variable	Mice and *in vitro*
	Rifampicin	Variable	Mice and *in vitro*
	Nalidixic acid	Yes	Mice and *in vitro*
	Ciprofloxacin	Yes	Chickens and *in vitro*
	Fusidic acid	Variable	Mice and *in vitro*
	Mupirocin	Yes	Mice, nematodes and *in vitro*
	Actinonin	Yes	Mice, nematodes and *in vitro*
Escherichia coli	Streptomycin	Variable	*In vitro*
	Norfloxacin	Variable	Mice and *in vitro*
	Rifampicin	Variable	*In vitro*
	Fosfomycin	Yes	Urine and *in vitro*
Campylobacter jejuni	Ciprofloxacin	Variable	Chickens
Mycobacterium tuberculosis	Isoniazid	Yes	Mice
	Rifampicin	Yes	Macrophages and *in vitro*
Mycobacterium bovis	Isoniazid	Yes	Mice
Mycobacterium smegmatis	Streptomycin	Variable	*In vitro*
Staphylococcus aureus	Fusidic acid	Variable	Rats and *in vitro*
	Rifampicin	Variable	Biofilms and *in vitro*
	Mupiricin	No	Mice and *in vitro*
	Methicillin	Yes	*In vitro*
	Vancomycin	Variable	*In vitro*
Staphylococcus epidermidis	Fusidic acid	Yes	Humans
	Ciprofloxacin	No	Humans
Streptococcus pneumoniae	Gemifloxacin	Yes	Mice and *in vitro*
Helicobacter pylori	Clarithromycin	Yes	Mice and *in vitro*
Chlamydia psittaci	Spectinomycin	Yes	*In vitro*
Pseudomonas aeruginosa	Fluoroquinolone	Variable	*In vitro*
Pseudomonas fluorescens	Rifampicin	Yes	Soil
Listeria monocytogenes	Class IIa bacteriocin	Yes	*In vitro*
Neisseria meningitidis	Sulfonamide	Yes	*In vitro*

Table 6.2: Metabolic cost for antibiotic resistance is strain- and gene-specific. "Yes" indicates elongation in generation time from several percent up to 400%. "Variable" indicates some mutations suffer a cost while some do not. After Ref. [5].

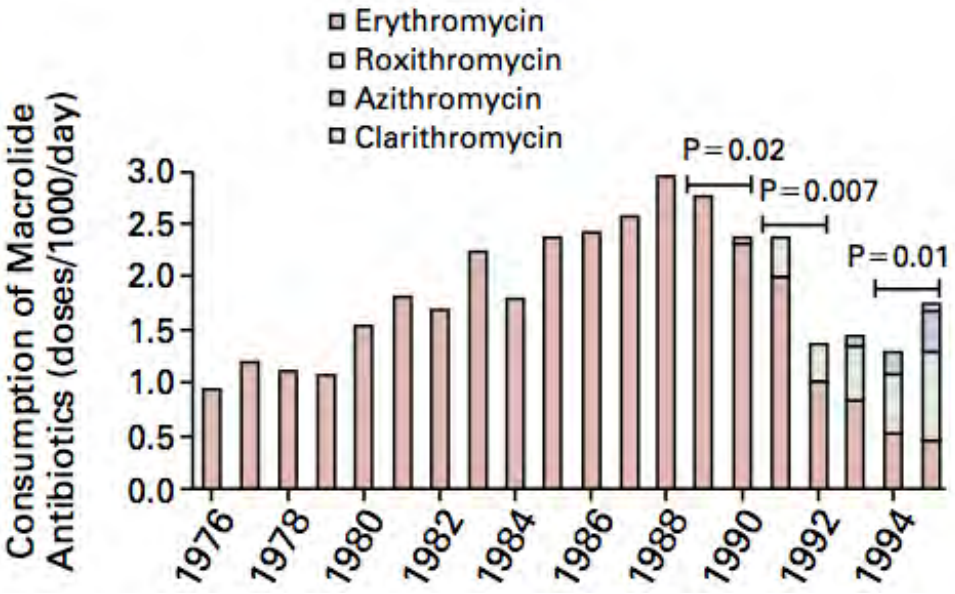

Figure 6.4: Finland's macrolide antibiotics consumption by outpatients from 1976 through 1995. Total consumption decreased from 2.40 daily doses per 1000 inhabitants per day in 1991 to 1.38 in 1992 and remained low afterwards. After Ref. [21].

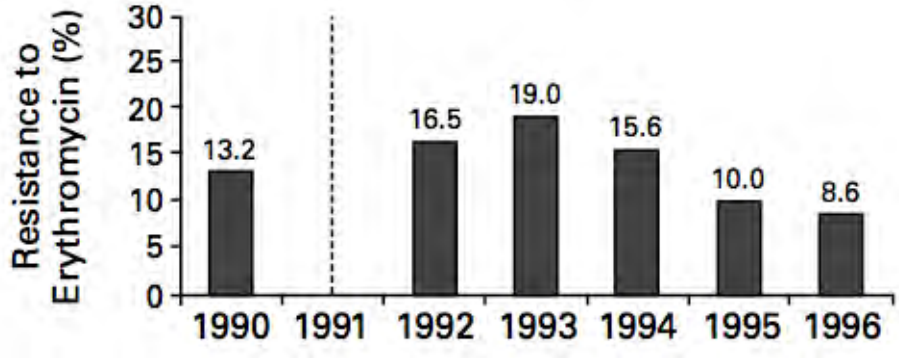

Figure 6.5: Finland's erythromycin resistance from throat-swab and pus samples from 1990 through 1996. The dashed line indicates unavailability of data in 1991. Erythromycin resistance among group A streptococcal isolates dropped from 16.5 % in 1992 to 8.6 % in 1996. After Ref. [21].

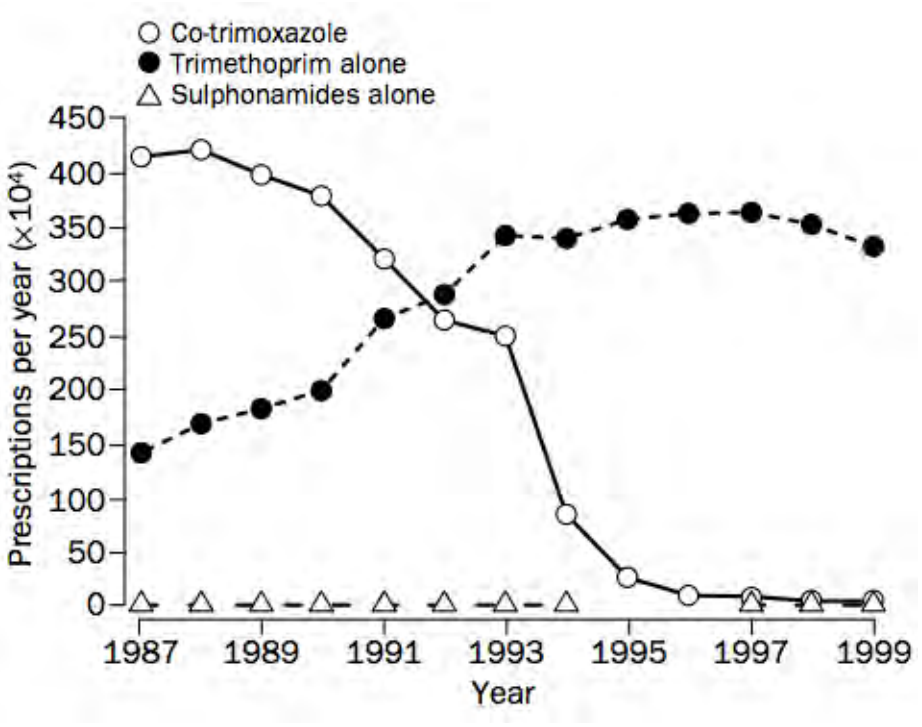

Figure 6.6: Switch of UK's prescriptions from co-trimoxazole, which is a combination of sulphamethoxazole and trimethoprim, to trimethoprim alone in the 1990s. Sulphonamide usage slumped from 320,000 prescriptions per year in 1991 to 7,000 in 1999. After Ref. [22].

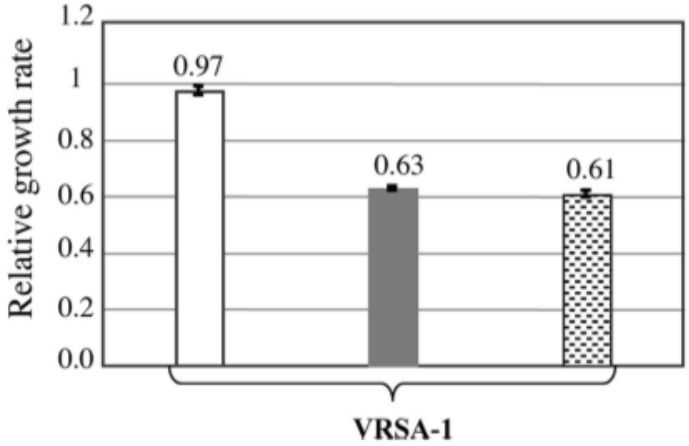

Figure 6.7: Comparison of growth rates of VRSA-1 relative to susceptible MRSA strain HIP11713 between non-induced (white) and induced (shaded and dotted) cultures. Fitness cost is nearly 40% for resistance but dramatically drops to 3% without induction. White: brain heart infusion (BHI) broth without vancomycin. Shaded: pregrown without vancomycin and subcultured with 1/50 the minimum inhibitory concentration (MIC) of vancomycin. Dotted: pregrown and subcultured with 1/50 the MIC of vancomycin. After Ref. [23].

Bacteria	Resistance mutation	Resistance to	Compensatory mutation	Resistance in compensated mutant	Selection system
Salmonella enterica subsp. *enterica* serovar Typhimurium	*rpsL*	Streptomycin	Intragenic	Maintained	Mice
	rpsL	Streptomycin	Extragenic (*rpsD* or *rpsE*)	Maintained	Laboratory medium
	gyrA	Nalidixic acid	Intragenic	Maintained	Mice
	rpoB	Rifampicin	Intragenic	Maintained	Mice
	fusA	Fusidic acid	True reversion	Lost	Mice
	fusA	Fusidic acid	Intragenic	Often maintained	Laboratory medium
	fmt and *folD*	Actinonin	Intragenic	Maintained	Laboratory medium
	fmt	Actinonin	Extragenic (*metZ* and *metW* amplification)	Maintained	Laboratory medium
Escherichia coli	*gyrA* and *marR*	Fluoroquinolones	Extragenic (*parC*)	Increased	Constructed* or laboratory medium
	gyrA, *parC* and *marR*	Fluoroquinolones	*gyrA*-2	Increased	Constructed*
	rpsL	Streptomycin	Extragenic (*rpsD* or *rpsE*)	Maintained	Laboratory medium
	rpoB	Rifampicin	Intragenic	Maintained	Laboratory medium
Staphylococcus aureus	*fus*	Fusidic acid	Intragenic	Maintained or lost	Laboratory medium
	rrl	Linezolid	Gene conversion	Lost	Laboratory medium
Streptocccus pneumoniae	*gyrA*, *parC* and *parE*	Fluoroquinolones	Intragenic	Maintained or increased	Constructed*
Mycobacterium tuberculosis	*katG*	Isoniazid	Extragenic (*ahpC*)	Maintained	Humans
Neisseria meningitidis	*sul2*	Sulfonamide	Intragenic	Maintained	Humans

Table 6.3: Compensatory evolution ameliorates fitness cost of antibiotic resistance. Second site mutations stabilizing resistance are more common compared with true reversion. After Ref. [5].

nearly 80% over the 9-year period (Figure 6.6).

Epidemiological statistics are precious but it is hard to rely on them to establish sound correlations. Genetic investigations leading by D.I. Andersson et al. [222, 227, 226, 228, 229, 5] expects true reversion to drug sensitivity to be slow if not impossible for two reasons. First, compensatory evolution ameliorating fitness cost together with cost-free resistance is able to fix antibiotic resistance. Table 6.3 shows that second site mutations stabilizing resistance are more common compared with true reversion. More specifically, Ref. [230] demonstrated that among 81 independent lineages of an *rpsl* gene mutation conferring streptomycin resistance in *Salmonella typhimurium*, only 4 reverted while 77 lineages acquired compensatory mutations and retained streptomycin resistance. Higher mutation rates and population bottlenecks together fix compensatory mutations instead of reversion [231]. Second, co-selection between resistance mechanisms and other selected markers prevents potential reversion. Such a genetic linkage explained the persistent sulphonamide resistance in UK in the 1990s as mentioned above [22].

Besides, the expensive metabolic cost is under regulation. M.L. Foucault et al. [23] demonstrated that the fitness cost of the VanA-type glycopeptide resistance carried by clinical methicillin-resistant *Staphylococcus aureus* (MRSA) isolates is 20% to 38% but shrinks to 0.4% to 3% without induction (Figure 6.7). The huge reduction of metabolic cost in the absence of induction turns the vision of reduced resistance or reversion to drug sensitive genotype with discreet and regulated antibiotic consumption more miserable.

We will circumvent all these complications in the metabolic cost and simply model it as a slightly lower birth rate.

6.3.3 Methods

The real interactions in the micro-organismal world are complicated considering the huge population, myriad species, and various mechanisms. The microbial population in the human gut, for example, on the order of 10^{14}, outnumbers eukaryotic cells by an order of magnitude [232], covering over 1000 bacterial species with at least 160 species for each individual [62], and engaging in dynamic interactions with profound implications [233, 234]. As a minimal model, we regard all Gram-positive as a super strain, all Gram-negatives as another one, and pathogens as the third. We consider intraspecies competition within Gram-positives and Gram-negatives separately although competition between them exists in nature because, generally speaking, these two coexist with each other and Gram-negatives have a larger population size than that of Gram-positives. That is to say we allow a higher carrying capacity for Gram-negatives than for Gram-positives. We do not impose a similar carrying capacity on pathogens so that they may burst and induce diseases. The beneficial microbiota suppress the population of pathogens competing for limited resources and space such as the

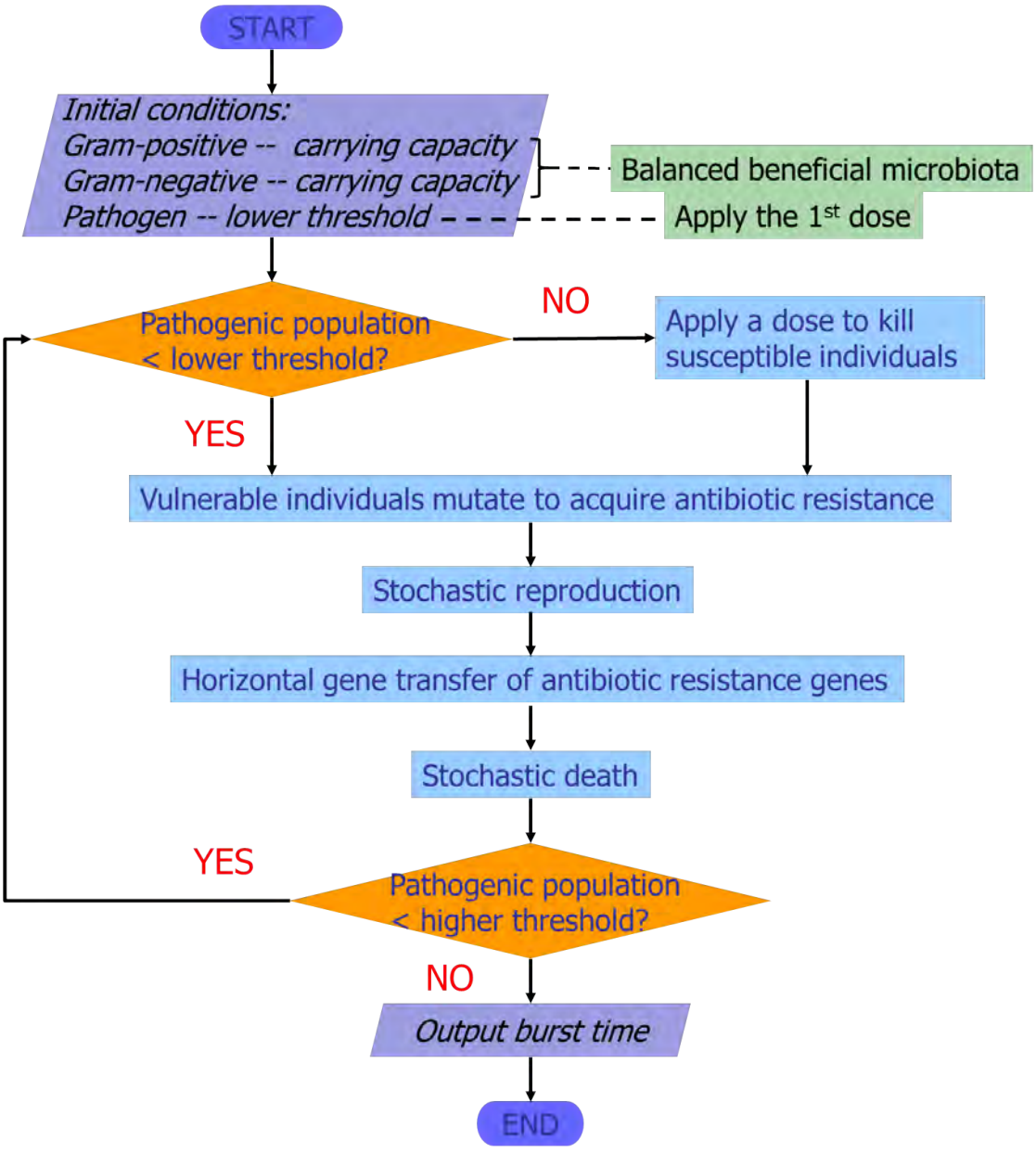

Figure 6.8: Flow chart of simulation steps to compare different spectrum of antibiotics.

membrane.

For the purpose of making a caricature of the behavior of pathogens, there are two predetermined population thresholds that govern the entire system behavior. The lower threshold marks the onset of the hosts symptoms, at which point, a dose of antibiotics is taken, which kills a certain percent of pathogens determined by the killing rate. Whether Gram-positives and Gram-negatives suffer at the same time depends on the kind of antibiotics applied. Timely doses keep pathogens under good control unless antibiotic resistance develops. The higher threshold indicates runaway proliferation of antibiotic resistant pathogens, or in other words, the death of the host due to antibiotic resistance. Our goal is to investigate and thus compare the emergence of antibiotic resistance for the new and conventional antibiotics when the higher threshold is reached. There is a cost to carry the antibiotic resistance genes, which is modeled with a lower birth rate. Each bacterium, either Gram-positive, Gram-negative or pathogenic, may acquire the resistance gene via mutation or intra- or inter-species horizontal gene transfer. Generally inter-species horizontal gene transfer rate is an order of magnitude larger than that of intra-species, while the latter is again an order of magnitude larger than that of mutation.

Figure 6.8 sketches a flow chart of simulation procedures. Initially both Gram-positives and Gram-negatives approach their carrying capacity, respectively, indicating balanced beneficial microbiota. The population of pathogens is at the lower threshold to induce the first dose. When the clock starts to tick, the following events occur. First a new dose is applied if the pathogenic population exceeds the lower threshold. The survivors, if vulnerable, may mutate to gain antibiotic resistance. These resistance genes will transfer horizontally both intra- and inter-species among vulnerable individuals. Every individual in the community may reproduce and die according to their respective birth and death rate. The growth of the beneficial microbiota is limited by their carrying capacity, and the birth of pathogens is suppressed by the beneficial microbiota subject to their density. Offspring of an antibiotic resistant parent maintain resistant. Then the clock ticks again and the sequence of events restarts.

Real simulation code is provided in Appendix C.

6.3.4 Results and Discussions

First we would like to present simulation results in well-mixed populations. Figure 6.9 $\sim$ Figure 6.11 show the time evolution of the populations for Gram-positives, Gram-negatives, and pathogens, respectively, for new and conventional antibiotics with the same initial conditions. The birth rate for the beneficial microbiota without antibiotic resistance is 20% and drops to 10% for bearing the resistance genes, and the death rate is 15%. The corresponding rates for pathogens are 60%, 50% and 0, respectively. The beneficial microbiota

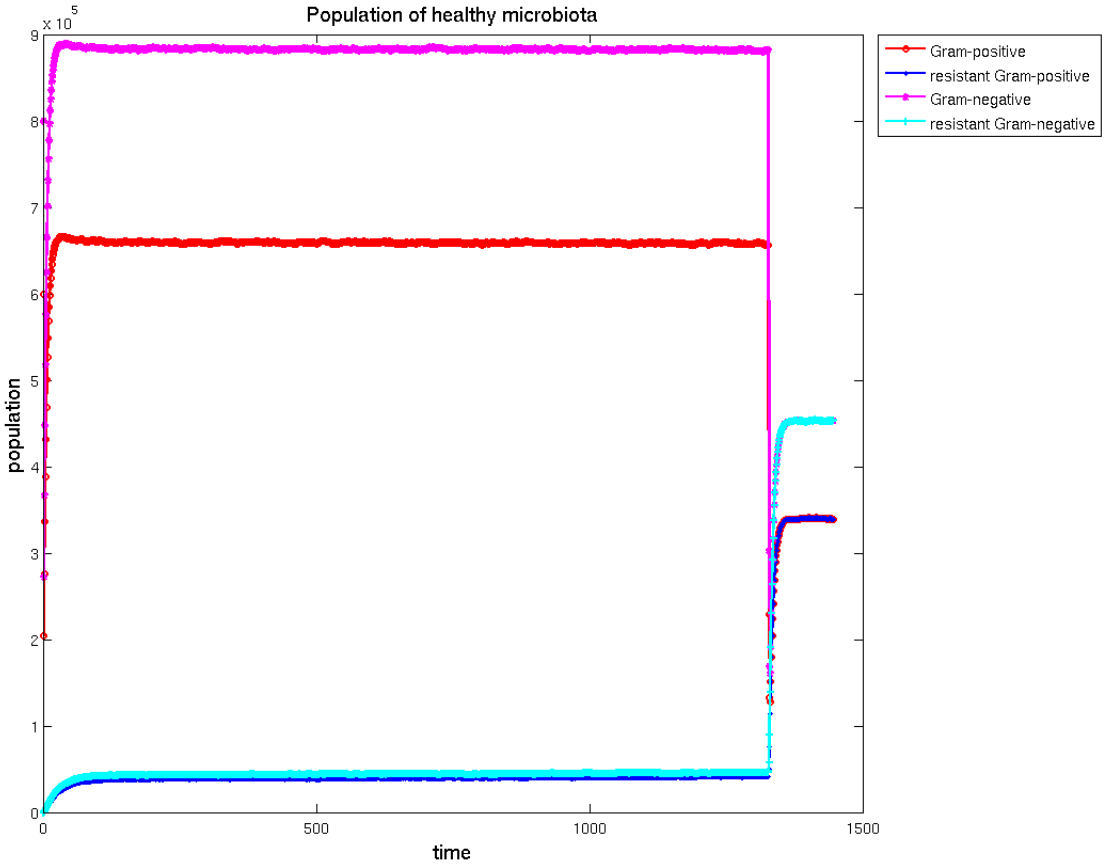

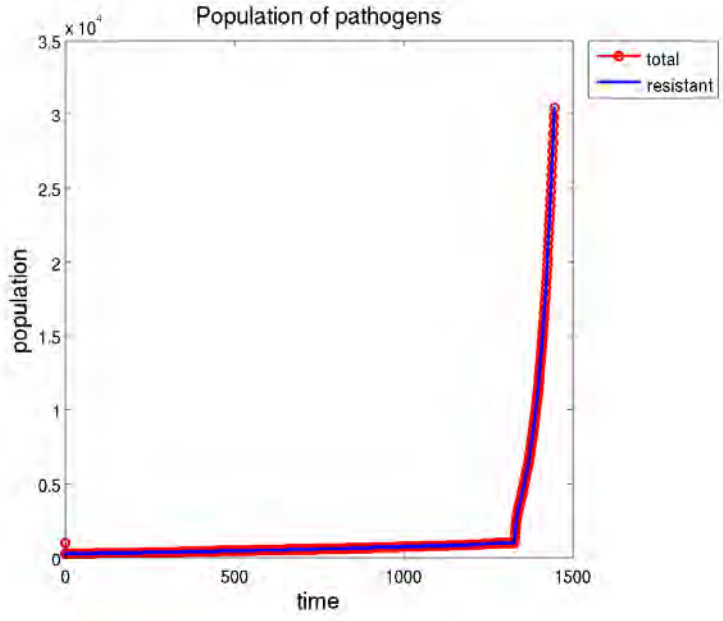

Figure 6.9: Time evolution for the total and resistant population of Gram-positives, Gram-negatives and pathogens, respectively, using broad spectrum antibiotics.

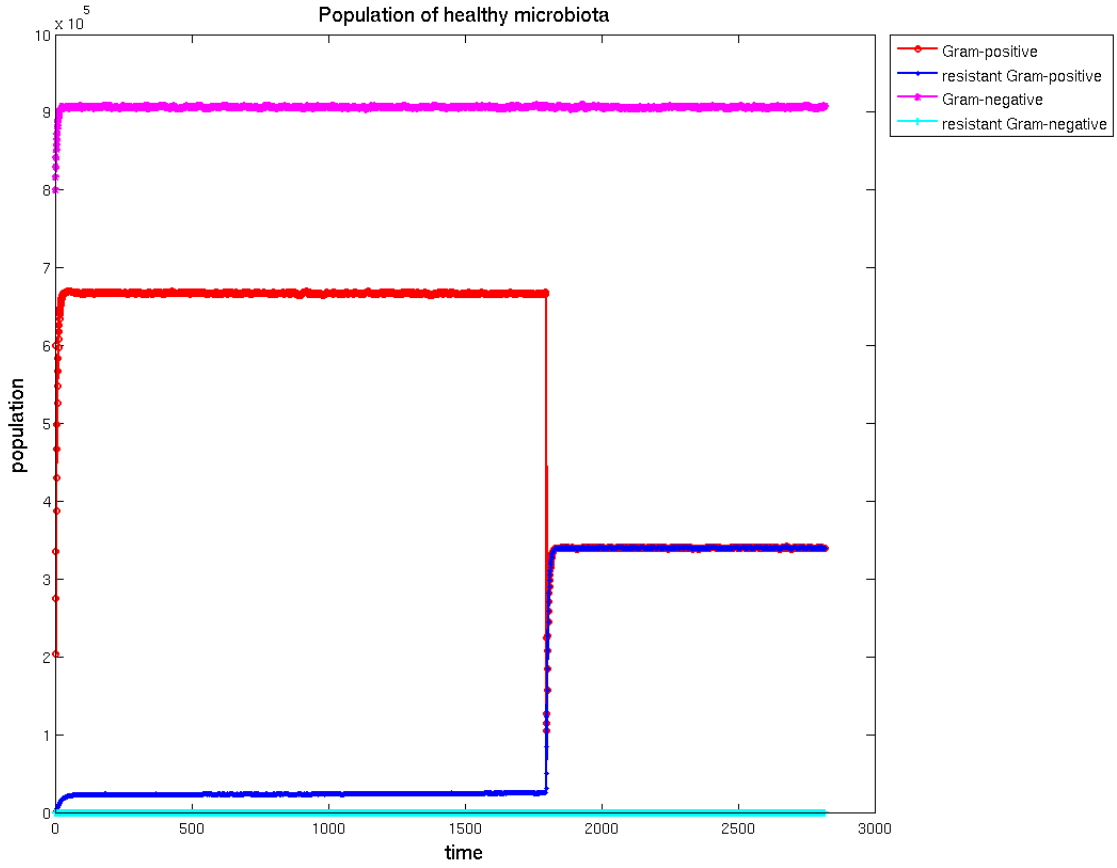

Figure 6.10: Time evolution for the total and resistant population of Gram-positives, Gram-negatives and pathogens, respectively, using narrow spectrum antibiotics.

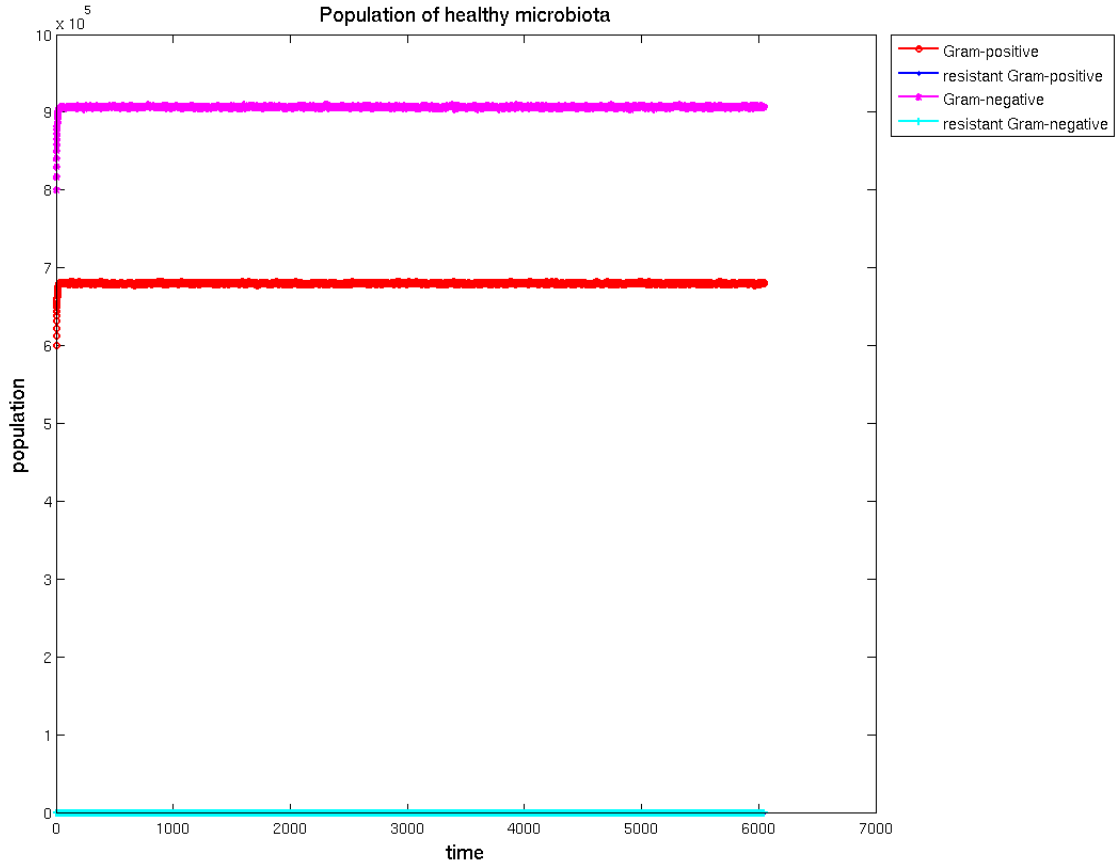

Figure 6.11: Time evolution for the total and resistant population of Gram-positives, Gram-negatives and pathogens, respectively, using ultra-narrow spectrum antibiotics.

suppress 80% local birth of pathogens. Antibiotics kill 80% vulnerable species. The mutation rate to acquire antibiotic resistance is 0.2%. Horizontal gene transfer rates for intra- and inter-species are 2% and 20%, respectively. The lower threshold for the dose is 1000 while the higher for burst is 30000. All the simulations start at time step 0. We can see that in Figure 6.9 for broad spectrum antibiotics, the first does is applied at the time step 1, which kills the majority of Gram-positives, Gram-negatives, and pathogens. Later all the three species recover their population with increased antibiotic resistance. At time step 1329, the second dose is applied. Since almost all the pathogens are antibiotic resistant at this time, the only effect is to eradicate the beneficial microbiota, which releases the suppression pressure for pathogens and led to the eventual burst. In Figure 6.10, the population of Gram-negative fluctuates around its carrying capacity, not affected by narrow spectrum antibiotics. The burst time almost doubles that in Figure 6.9. Figure 6.11 is the simulation for ultra-narrow spectrum antibiotics, where pathogens are always suppressed by the beneficial microbiota. It takes a much longer time of about 4.5 times as that in the broad spectrum case for pathogens to retrieve their population size and develop antibiotic resistance. By comparison, Figure 6.9 $\sim$ Figure 6.11 illustrate the importance of the beneficial microbiota.

We run 3000 simulations of the population dynamics under three different treatments: broad-spectrum, narrow-spectrum and ultra-narrow-spectrum but everything else is held constant in the simulations. We observe a clear trend in the probability distribution of times (vertical axis in Figure 6.12) at which there is runaway proliferation of resistant pathogens, compared across three classes of antibiotics. Figure 6.12 shows the statistics for the runaway time for broad-, narrow- and ultra-narrow spectrum antibiotics, and the mean runaway times (in system time steps) are 1374, 2783 and 5917, respectively. Significantly, the time for runaway proliferation of resistant pathogens is increased by about half an order of magnitude through the use of ultra-narrow-spectrum antibiotics, compared with current practice.

Including spatial inhomogeneity, Figure 6.13 presents statistics for the runaway time for broad-, narrow- and ultra-narrow spectrum antibiotics, and the mean runaway times (in system time steps) are 132, 459 and 1259, respectively. Here we run 500 simulations for each case with the same parameter settings as the non-spatial version. Each individual diffuses randomly with average diffusion length 4 during each time step on a 257×257 lattice with periodic boundary conditions. In the spatial version here the time for runaway proliferation of resistant pathogens is increased by nearly an order of magnitude through the use of ultra-narrow-spectrum antibiotics in comparison with the broad-spectrum antibiotics. Comparing Figure 6.12 and Figure 6.13, we can see that spatial and non-spatial models yield qualitatively the same result.

This preliminary result suggests that we can meaningfully expand the window during which the next-generation antibiotics will be effective through the use of targeted strategies. However, even these strategies

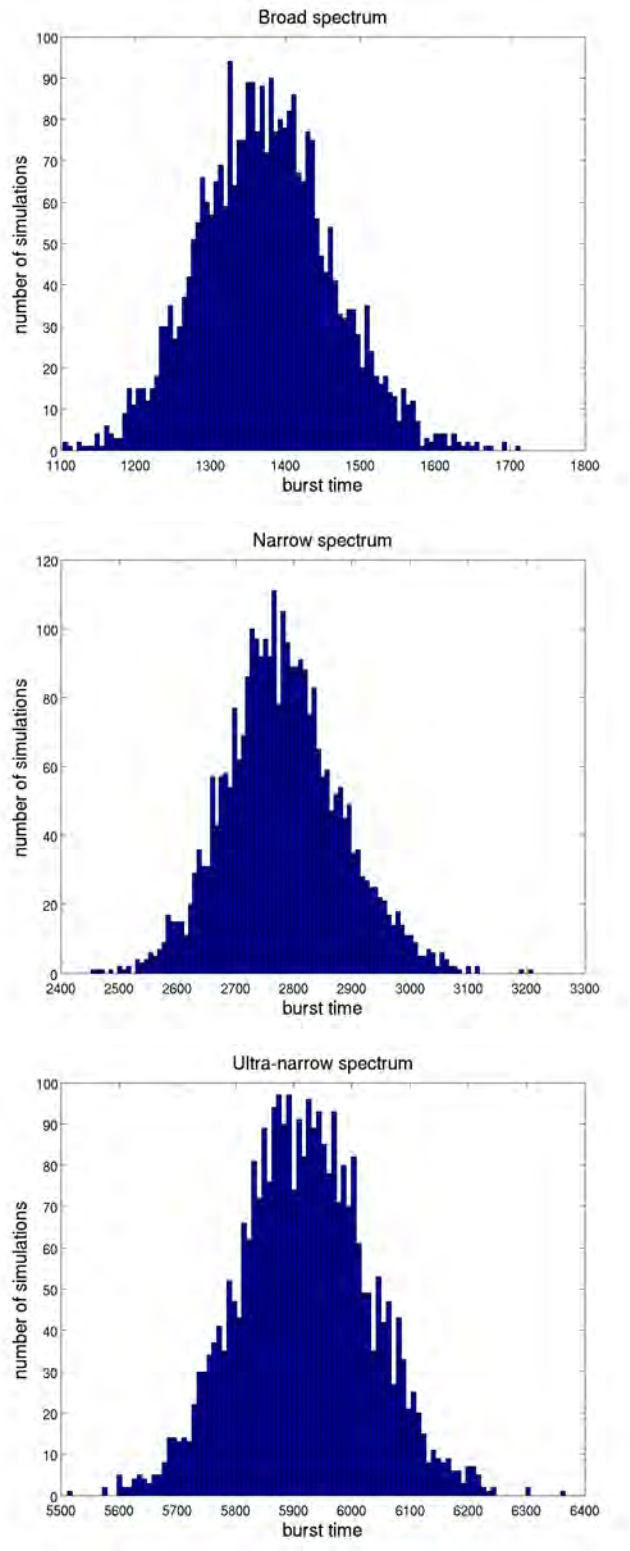

Figure 6.12: In the spatial homogeneous model, frequency VS onset time for runaway proliferation of resistant pathogens for different types of antibiotics. The mean onset times for broad, narrow and ultra-narrow spectrum antibiotics are 1374, 2783 and 5917, respectively, showing half an order of magnitude improvement.

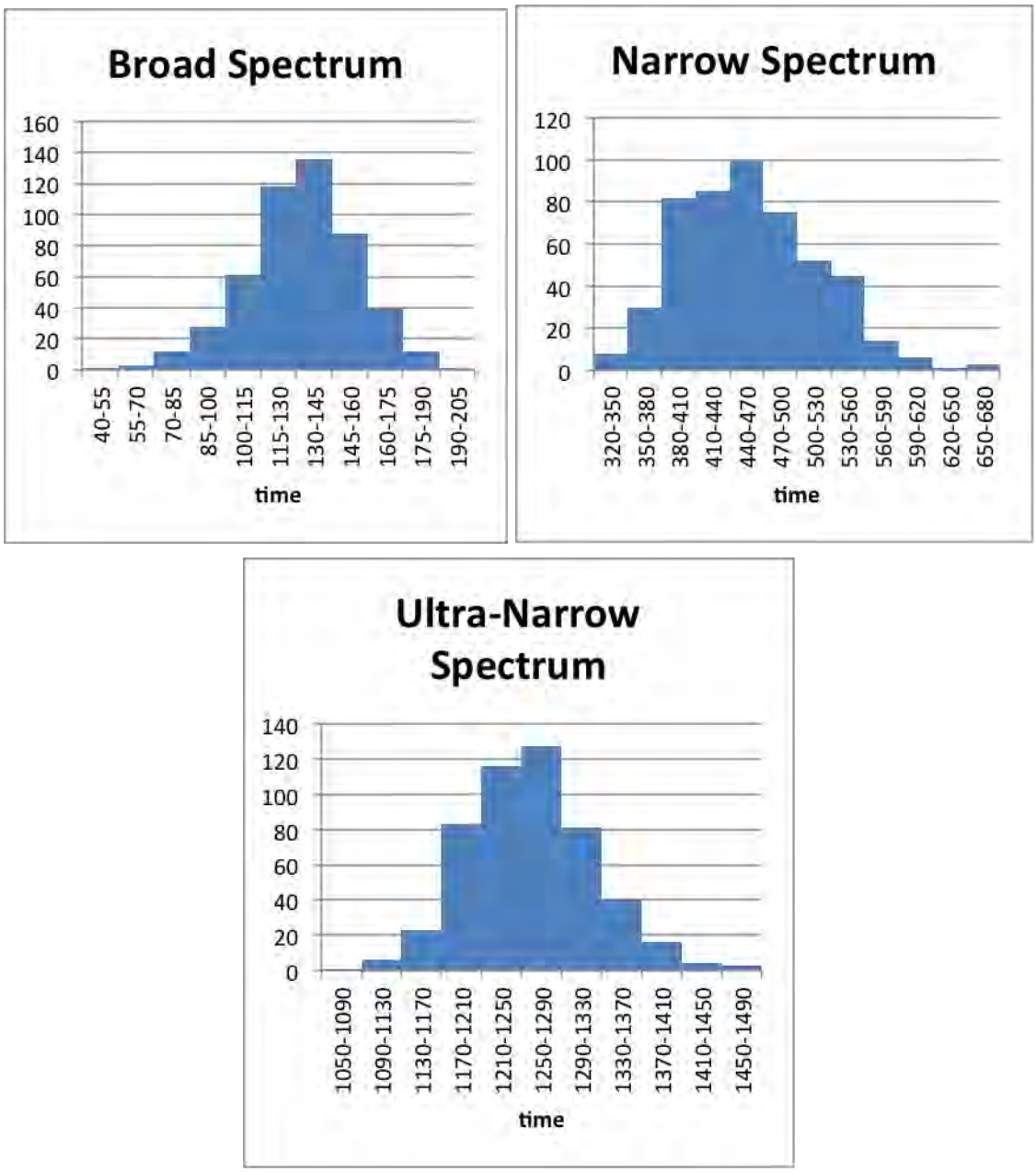

Figure 6.13: In the spatial inhomogeneous model, frequency VS onset time for runaway proliferation of resistant pathogens for different types of antibiotics. The mean onset times for broad, narrow and ultra-narrow spectrum antibiotics are 132, 459 and 1259, respectively, showing nearly an order of magnitude improvement.

eventually result in the emergence of antibiotic resistance. In order to break the paradigm of antimicrobials inevitably leading to emergence of resistance, we need to use a strategy that goes beyond the simple direct conflicts that bacteria use between themselves for antagonistic interactions. What is more, as Lee et al. [223] pointed out, bacteria may share antibiotic resistant products, which exempts the cost to carry the resistance genes for every bacterium. The cooperative behavior among bacteria exacerbates human's condition in the arms race. It calls for ideal antibiotics with no resistance.

6.4 Quorum Sensing Spoofing

6.4.1 Reducing Selection Pressure by Community Effect

In the above plan for the new antibiotics, we successfully extend the time scale for the emergence of antibiotic resistance. However, we see that the conventional method of disturbing essential bacterial functions, although efficient in bacterial elimination, also imposes such an intensive selection pressure that resulted in rapid resistance. Aiming at the design of next generation of antibiotics with presumably no resistance, we need to reconcile the conflict between effective decimation and small selection pressure.

Generally speaking, disease is caused not by a single pathogenic bacterium or a small group, but by the bacterial community as a whole. It is very expensive for a small population of pathogens to express toxins, as this may trigger a response by beneficial microbiota and the immune system. Thus, in order to coordinate the expression of virulence, bacteria ubiquitously employ a cell-to-cell communication mechanism called quorum sensing (whose details differ between Gram-positive and Gram-negative bacteria), in which a signaling molecule known as an autoinducer is produced by the bacteria, and whose concentration is effectively monitored by the bacteria [235]. When the population is small, autoinducers released by cells quickly diffuse away and dilute. Thus the cells will receive little feedback from the environment. When the population is large, enough signaling molecules, either imported into the cells or received by receptors at the cell membrane, will initiate the transcription of target genes for mid/late stage virulence factors (often toxins). Sufficient expression of virulence factors causes disease. This suggests that in order to keep the total expression of virulence factors under control, one does not necessarily need to invoke high selection pressure on the bacterial community, thus potentially avoiding antibiotic resistance. One promising approach is to block the reception of cognate autoinducers [215, 216, 217, 218] but mutation against blockage has recently been reported in experiments [236]. Thus, we propose an even more innovative approach, which we call Quorum Sensing Spoofing (QSS). Our seemingly counter-intuitive goal is to promote the premature expression of virulence factors.

6.4.2 Quorum Sensing Spoofing (QSS)

Quorum sensing is essential in bacterial communication to monitor population density. By coordinating the expression of virulence factors, bacteria can share the cost of toxin production and can prevail against competitors for their niche, but this is only an effective strategy for them once their population is sufficiently large. If their population is small, the host's defenses are able to defeat the infection. Thus, we propose to force the pre-expression of virulence factors by adding autoinducers when the bacterial population is still small. Bacteria are spoofed by their own quorum sensing mechanism when they detect high enough density of autoinducers. Expressing virulence when the actual population is still small is a huge cost to a cell and exposes it to attack from the surrounding microbiota and the host immune system. In this way bacteria suffer from delayed growth due to the metabolic load of pre-expression of virulence factors.

Let us emphasize three points. First, QSS will work because we spoof bacteria into choosing the wrong strategy by pre-expressing virulence when the population size is still small. This is something that intrinsically they try to avoid and quorum sensing presumably evolved to avoid making this bad choice. Second, QSS is a safe treatment, because the total bacterial population is small enough that the overall level of virulence is small. Third, QSS is not expected to induce resistance because, contrary to the conventional paradigm, it does not add any alien molecules or chemical compounds. What we add are autoinducers already present in the environment. Thus, bacteria will continue to undergo their normal metabolism, but their wrong choice of pre-expression leads them to a dead end.

6.4.3 Methods

Here we would like to show our individual-level simulations of how the QSS strategy would work on a model microbial community. We do not differentiate beneficial microbiota into Gram-positives or Gram-negatives. We consider intra-species competition and the suppression from local beneficial microbiota toward pathogens due to limited resources and space. Pathogens expressing virulence factors grow at a much lower birth rate than usual as a cost for virulence. Each cell will produce and release autoinducers into the environment, which will diffuse around and hydrolyze after some time. Cells sensing enough autoinducers within a certain period will express virulence. We manually set up two thresholds for pathogenic population in the simulation. The lower threshold is the time to take a dose, when extra autoinducers are added for enforced expression of virulence. The higher threshold is the time the disease develops, which is the actual threshold for pathogens to express virulence.

Figure 6.14 sketches a flow chart of simulation procedures for QSS. We run the simulation on a two-dimensional lattice to include spatial inhomogeneity. The initial population of the beneficial microbiota

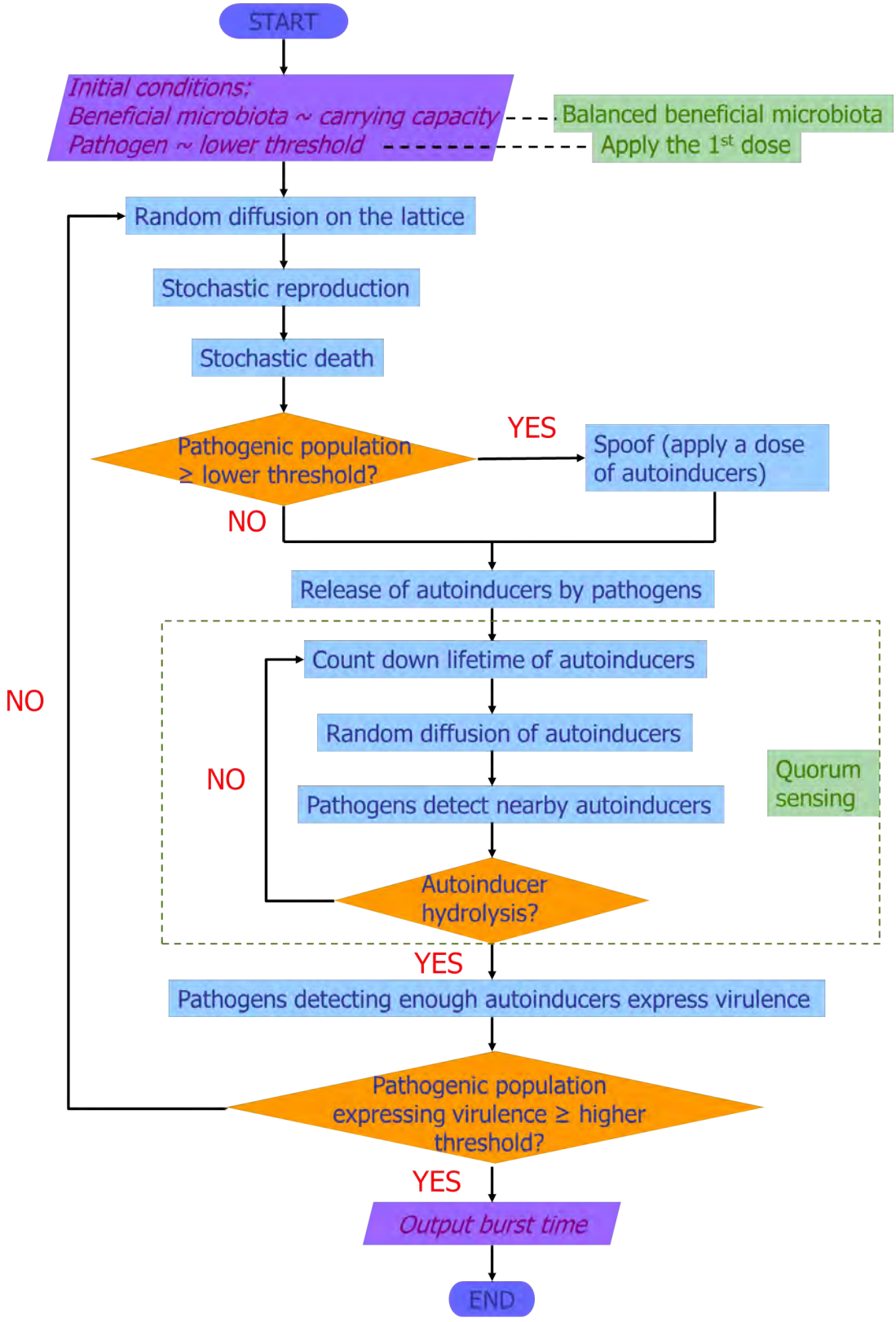

Figure 6.14: Flow chart of simulation steps for QSS.

approaches their carrying capacity and that of the pathogens is a little away from the lower threshold for dose. When the clock ticks, a sequence of events occurs. The community diffuses over the lattice. Each individual may reproduce and die according to their birth and death rates. The birth of the beneficial microbiota is limited by the carrying capacity while that of pathogens is suppressed by the local density of the beneficial microbiota. If the population of pathogens exceeds the lower threshold, a dose is applied for spoofing. All the autoinducers, either manually added or produced by pathogens, diffuse around for a while before hydrolization. Pathogens detecting enough autoinducers express virulence and then grow at a lower birth rate. If the population of pathogens expressing virulence surpasses the higher threshold for disease, the host is killed and the simulation stops. Otherwise, the clock ticks on.

6.4.4 Results and Discussions

We show the simulation results running on a 257×257 lattice for Quorum Sensing Spoofing in Figure 6.15. The birth and death rates for the beneficial microbiota are 20% and 15%, respectively. The birth rate for pathogens not expressing virulence is 50%, which slumps to 5% for expression, and their death rate is 3%. The beneficial microbiota suppress 30% local birth of pathogens. The lower threshold for dose is 1200 and the higher for disease is 4500. As a comparison, in the upper panel, when no treatment is given, pathogens coordinate their expression of virulence at about 19 time steps, thus initiating a disease state in the host. In the lower panel, with QSS treatment, the majority of the pathogen population is forced to express their virulence far below the higher threshold of disease. Then the population steadily falls below the lower threshold and the treatment is stopped. Following the cessation of treatment, the pathogen population revives, thus initiating another cycle of treatment. Note that the pathogen population remains bounded for arbitrary long times. Actually we have run the simulation for much longer time steps where the population of pathogens is always under good control.

Hitherto we have demonstrated Quorum Sensing Spoofing as a safe and effective antibiotic strategy. The highlight is that it will not cause antibiotic resistance because no alien molecules are introduced and we do not disturb bacterial metabolism, such as replication, regulation or gene expression processes. The strategy is robust to details but has two caveats. It should not be used if the pathogen population is already close to the higher threshold where pathogenesis would naturally occur, in which case, QSS will be a fatal disaster. It should not be used when the pathogen population is so small that the drug is diluted and time wastes waiting for the slow drop of pathogenic population in an exponential form as shown in Figure 6.16, where the lower threshold shrinks to 0.

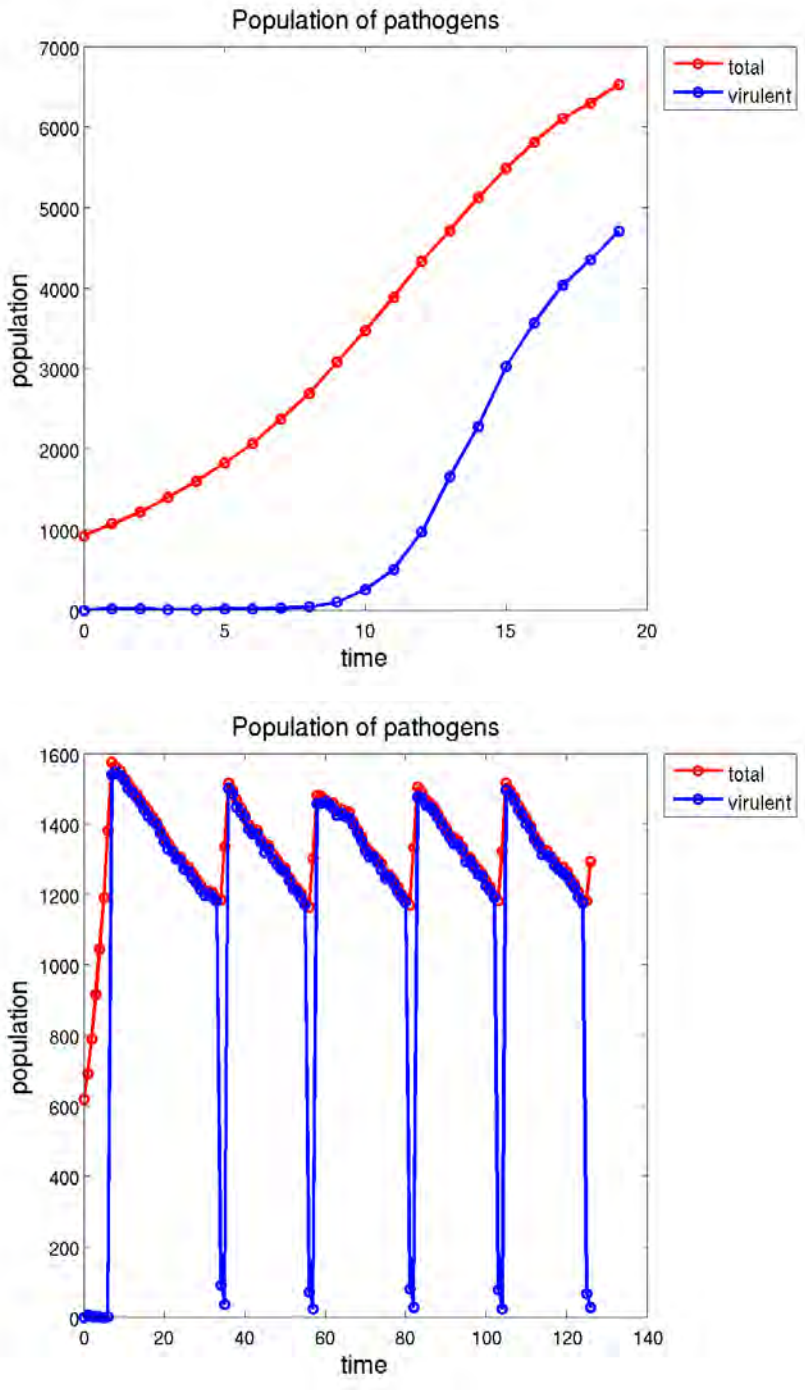

Figure 6.15: Time development of pathogen population (vertical axis). Upper panel: wild. As a control, without QSS disease develops at time step 19. Lower panel: QSS employed. Using QSS, the population of pathogens is always under control. No disease is detected.

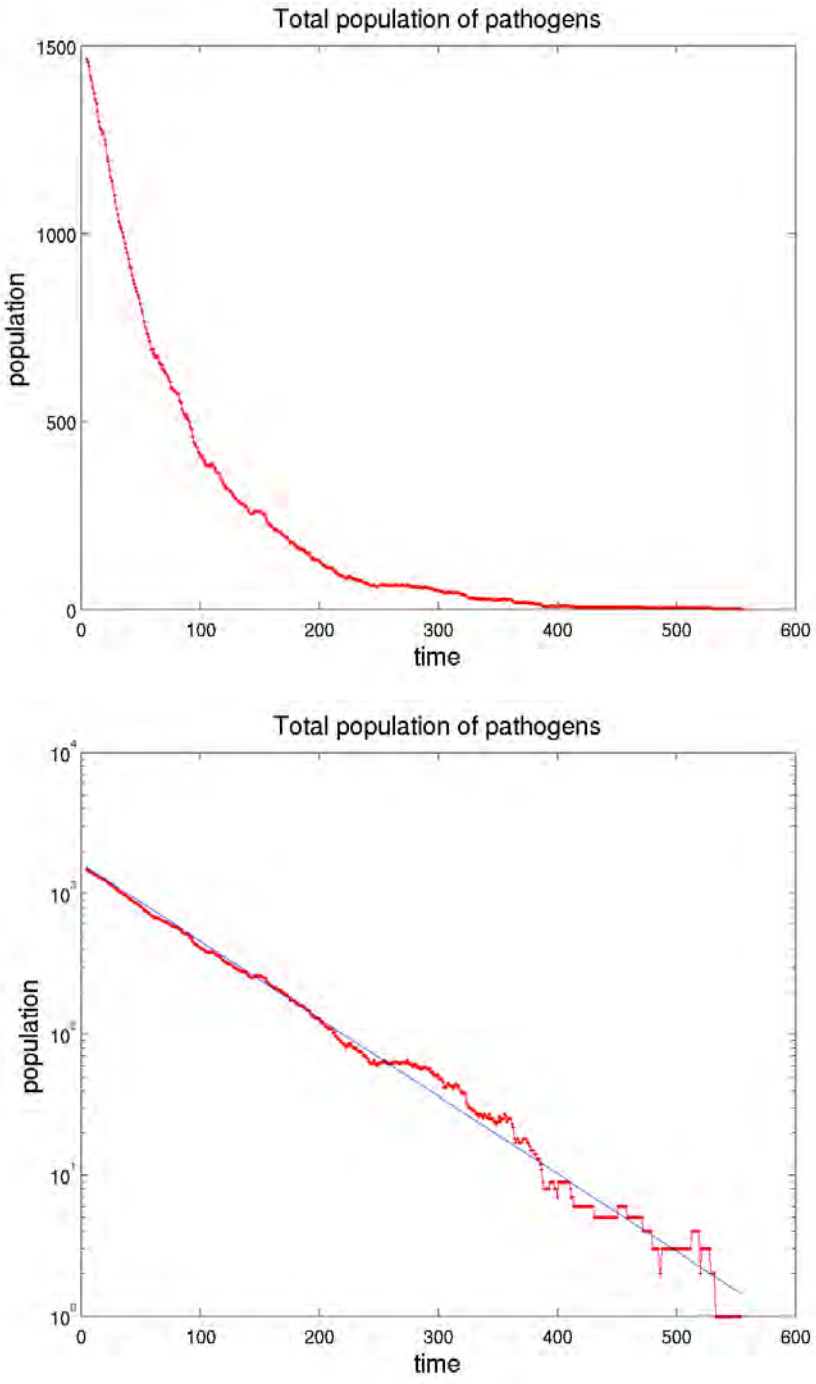

Figure 6.16: Decrease of pathogenic population follows an exponential form.

6.5 Drug Combination

6.5.1 Quorum Sensing Spoofing + Ultra-Narrow Spectrum Antibiotics

QSS is a promising strategy but there are two potential problems. The first is: from a clinical standpoint, when is the best time to take the first dose? When a patient suffers from some symptoms, the population of pathogens might already have reached the higher threshold, when is dangerous to take any extra autoinducers. The second is: how to improve its efficiency when the pathogen population is small? Naturally, if treatment is stopped, the pathogens will begin to regrow their population. Thus, there is a danger that the patient may end up with "QSS addiction".

To solve these two problems, we propose to combine ultra-narrow spectrum antibiotics with Quorum Sensing Spoofing. To see if this can be effective, we performed preliminary simulations of this strategy, as before but now we allow mutation to generate resistance genes against ultra-narrow antibiotics, but of course no resistance against the quorum sensing signaling molecules. We checked (1) the effect of drug combination and (2) emergence of antibiotic resistance against ultra-narrow antibiotics.

6.5.2 Methods

This time we will have five thresholds as shown in Figure 6.17. From the highest to the lowest, the first threshold h_4 is the population of pathogens above which the host is killed due to proliferation. The second threshold h_3 is the population at which there is detection of symptoms of the infection, above which the patient will take a dose of ultra-narrow antibiotics in order to reduce the population of pathogens below threshold h_2. Then the patient will change to QSS till threshold h_1, when QSS loses efficiency. Regime $h_1 \sim h_2$ is safe and efficient for QSS as we discussed earlier. Ideally, we want regime $h_1 \sim h_2$ as large as possible. Below h_1, we switch back to ultra-narrow spectrum antibiotics to eradicate the pathogen efficiently. Threshold h_0 is the lower bound for treatment, below which no medicine will be taken.

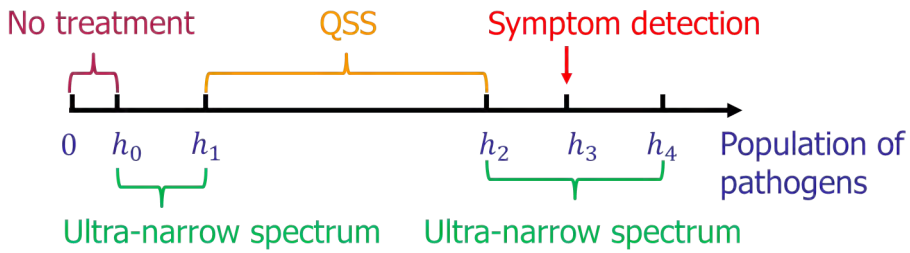

Figure 6.17: Different thresholds important for the combination strategy of QSS + ultra-narrow spectrum antibiotics.

The simulation procedures are roughly the same as the model for Quorum Sensing Spoofing except the selection of antibiotics according to the pathogenic population.

6.5.3 Results and Discussions

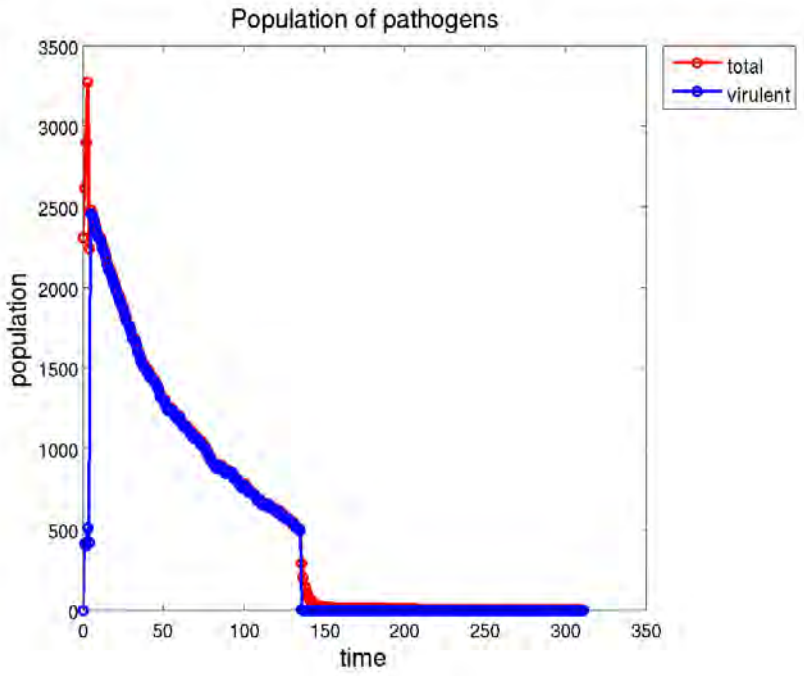

Figure 6.18: A treatment cycle for drug combination for $h_0 = 0$. The red line indicates total population while the blue line indicates pathogens expressing virulence factors.

We show a full treatment cycle in Figure 6.18 with the following set of parameters: $h_0 = 0$, $h_1 = 500$, $h_2 = 2500$, $h_3 = 3000$, $h_4 = 4500$, the killing rate of the ultra-narrow antibiotics is 40% while mutation rate equals 0.02% and intra-species horizontal gene transfer rate 2%. We can see that drug combination works effectively and safely. To investigate the emergence of resistance against ultra-narrow spectrum antibiotics, we tune h_0 to a nonzero (100) value keeping else the same, and show the simulation in Figure 6.19. We can see that not only the total population of pathogens is always small and under good control, but also that of resistant pathogens is always small and negligible even the time steps increase by an order of magnitude. Hence we are led to the hypothesis that motivates our *in vitro* and *in vivo* proposed research: combining Quorum Sensing Spoofing with ultra-narrow antibiotics appears to be effective in suppressing the emergence and spread of resistance genes, and offers a safe and effective treatment strategy.

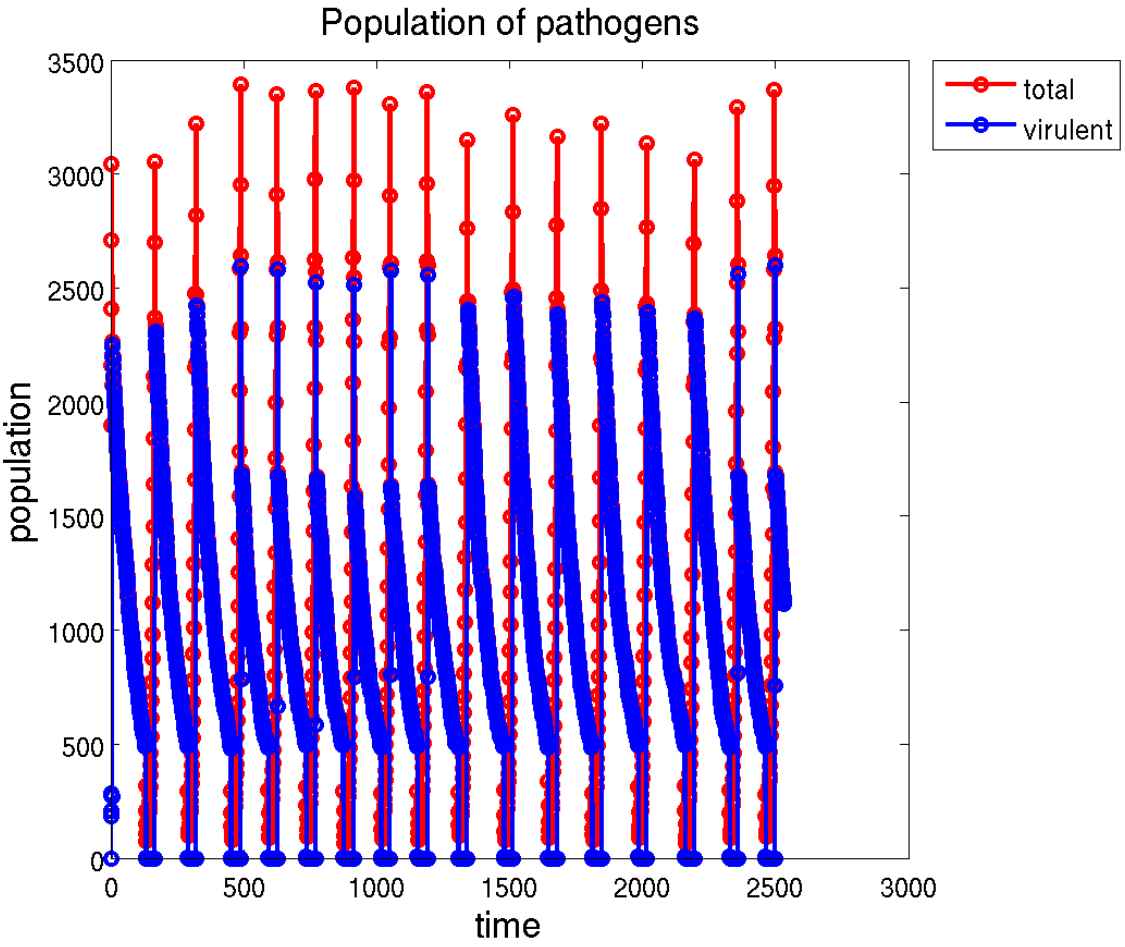

Figure 6.19: A treatment cycle for drug combination for $h_0 = 100$. The red line indicates total population while the blue line indicates pathogens expressing virulence factors.

6.6 Conclusion

In this chapter, we investigate non-conventional antibiotics and their treatment. Recognizing the huge importance and visible and hidden benefits of the beneficial microbiota [184], we narrow down the victims in antibiotic treatment. Compared with conventional antibiotics, where Gram-positives, Gram-negatives and pathogens all suffer, narrow and especially ultra-narrow spectrum antibiotics show long delayed emergence of resistance.

We design a brand new strategy naming Quorum Sensing Spoofing. Adding extra autoinducers, we successfully spoof bacteria to pre-express their virulence and thus suffer from the burden of pre-expression. QSS highlights no antibiotic resistance.

Last we propose a treatment plan combining ultra-narrow spectrum antibiotics and Quorum Sensing Spoofing. The basic idea is to take full advantage of Quorum Sensing Spoof and extend the treatment regime and increase the efficiency by switching to ultra-narrow spectrum antibiotics. We can achieve safety and efficiency in treatment. Furthermore, emergence of resistance against ultra-narrow spectrum antibiotics is highly reduced by alternating drugs.

With the rise in antibiotic resistance and the lack of financial incentive for large pharmaceutical companies to pursue novel antibiotics, humankind risks losing the fight against bacterial pathogens. Despite their apparent success, conventional and proposed antibiotics suffer from a fundamental drawback: all existing antibiotics target essential life processes of bacteria, such as translation or cell wall biosynthesis, and thus represent the ultimate selective pressure for an organism. The distinguishing aspect of our research philosophy is this: future antibiotics should not target essential metabolic pathways but instead directly target key aspects of the pathogenic mechanism. Our research will exhibit no effects on primary metabolism, because in our proposed strategies it is communication systems and collective properties of a community that are hijacked and repurposed. By limiting our treatment to those bacteria that are actively causing disease (i.e. biosynthesizing toxins and actively subverting our immune systems), our approach of quorum sensing spoofing followed by ultra-narrow spectrum antibiotics significantly limits the number of targeted bacteria. Thus, the clinical shelf life of the antimicrobial drug is extended. Moreover, this anti-virulence strategy preserves the symbiotic bacteria that play a vital role in human physiology and compete against pathogens. Experiments *in vitro* and *in vivo* will be performed by my advisor Nigel Goldenfeld's collaborators.

Chapter 7

Conclusions

In this dissertation, I presented my discoveries and innovations in the population dynamics of virus-host systems, social life of micro-organisms, evolutionary game theory, and medicine.

I derived a mean-field theory for the population dynamics of viruses and their hosts. I identified a novel limit cycle robust to fluctuations in the presence of lysogeny, which manifests and recognizes lysogens' role as a genetic reservoir. Such a cycle can be tested in experiments.

In the social life of budding yeast, I proposed a theory of cooperation directly linking game theory and experimental measurable quantities. The methods can be used in the design of future experiments to manipulate collective properties of micro-organism communities.

In evolutionary game theory, I invented a novel mechanism with biological interpretations to explain the ubiquitous cooperation in biology. The dominance of cooperators in the model is independent of the detailed rules.

Perhaps the most practically useful piece of my thesis work is the application of population dynamics to medicine. First, I verified the effectiveness to slow down the rapid emergence of antibiotic resistance with narrow-spectrum and especially ultra-narrow-spectrum antibiotics. Last but not last, I invented a brand new scheme of Quorum Sensing Spoofing, which may guide the next generation of antibiotics. I also designed candidate treatment cycles combining Quorum Sensing Spoofing with ultra-narrow spectrum antibiotics. The schemes will be tested in laboratory.

7.1 Thoughts and Reflections

It is recognized that biology provides physics with the second law of thermodynamics while physics provides biology with microscopy. In exchange for a law with an instrument, is physics too mean?

Walking through the same forest, physicists may tend to appreciate the similarities between different trees while biologists probably would like to study the trees one by one, or even leaf by leaf.

Physics, generally speaking, tackles universal phenomena such as phase transitions. It is the strength

of physicists to find simple and unifying explanations for complicated phenomena. In biology, there also exist universal phenomena such as coexistence and cooperation as I mentioned in this dissertation. Hence methods and approaches in physics might contribute to these universal problems in biology, too.

Biological interactions are usually so complicated that it requires large effort to measure and quantify the system. Focusing on detailed and specific systems for a long time, sometimes people tend to lose and forget the big picture. Besides due to experimental restrictions some experimental data are hard to obtain such as data on evolutionary and ecological timescales. Once in a while it helps to sit back and see the big picture such as evolution and ecology. It is the job of physics to remind and ask biology the real important questions, e.g., the origin of life.

Different disciplines are divided so that time and effort can be focused on the specific branch of problem. However as long as a problem is solved, it does not matter what branch of knowledge is used. Sometimes jumping across branches may offer panorama of the whole forest. The differences and similarities between different branches may become clearer so that one can ask the right and important questions.

Besides, interdisciplinary research may help to bring new ideas. For example, my idea of Quorum Sensing Spoofing is intrinsically simple. As Nigel commented, it should have been proposed years ago, but was not. Coming to the field of medicine as an outlier, I am not restricted to the routine methods in search of new antibiotics. What is more, I am equipped with analytical tools and simulation skills that help to solve the problem. More importantly, trained as a physicist, the way of thinking, reasoning and tackling problems will all help to broaden the horizon, which might be the key in interdisciplinary research.

Furthermore, important questions across disciplines may share some kind of similarity such as cooperation in game theory and in biology. Another example I would like emphasize is irreversibility. Irreversibility breaks the symmetry of time, which is essentially important in physics. The question in biology is irreversibility in evolution. Current research on antibiotic resistance suggests that in most cases acquisition of antibiotic resistance genes is irreversible, which means that strains tend to have second site mutations to mediate the cost for antibiotic resistance instead of reverting to antibiotic sensitivity in the absent of antibiotics. What is the criterion for reversibility and irreversibility in biology? Once found, we human may have more confidence against not only antibiotics but also cancers.

I hope one day we can say that biology rewards physics with the second law of thermodynamics while physics rewards biology with the origin of life.

Appendix A

Transition Matrices for the Lysis-only Model

Here we provide the transition matrices, which are the probabilities for the change in the population in each time step in the lysis-only model.

$$\begin{aligned} T\left(m+1,n|m,n\right) &= b\mu\left(1-\nu\right)\left(1-\omega\right)\frac{2m\left(K-m\right)}{K\left(K-1\right)} \\ &= \widetilde{b}m\left(1-\frac{m}{K}\right), \end{aligned} \tag{A.1}$$

$$\begin{aligned} \widetilde{b} &= \frac{2b\mu\left(1-\nu\right)\left(1-\omega\right)}{K-1} \\ &\approx \frac{2b\mu\left(1-\nu\right)\left(1-\omega\right)}{K}. \end{aligned} \tag{A.2}$$

$$\begin{aligned} T\left(m-1,n|m,n\right) &= c\mu\left(1-\nu\right)\omega\frac{m}{K} + d\mu\left(1-\nu\right)\left(1-\omega\right)\frac{m\left(m-1\right)}{K\left(K-1\right)} \\ &= \widetilde{c}m + \widetilde{d}m\left(\frac{m}{K}-\frac{1}{K}\right) \\ &\approx \widetilde{c}m + \widetilde{d}\frac{m^2}{K}, \end{aligned} \tag{A.3}$$

$$\widetilde{c} = \frac{c\mu\left(1-\nu\right)\omega}{K}, \tag{A.4}$$

$$\begin{aligned} \widetilde{d} &= \frac{d\mu\left(1-\nu\right)\left(1-\omega\right)}{K-1} \\ &\approx \frac{d\mu\left(1-\nu\right)\left(1-\omega\right)}{K}. \end{aligned} \tag{A.5}$$

$$\begin{aligned} T\left(m-1,n+\alpha-1|m,n\right) &= e\mu\nu\left(1-\omega\right)\frac{2m\left(K-m\right)}{K\left(K-1\right)}\frac{n}{W} \\ &= \widetilde{e}mn\left(1-\frac{m}{K}\right), \end{aligned} \tag{A.6}$$

$$\begin{aligned}\widetilde{e} &= \frac{2e\mu\nu\,(1-\omega)}{(K-1)\,W} \\ &\approx \frac{2e\mu\nu\,(1-\omega)}{KW}.\end{aligned} \tag{A.7}$$

$$\begin{aligned}T\,(m-1,n+\beta-1|m,n) &= f\mu\,\nu(1-\omega)\,\frac{m\,(m-1)}{K\,(K-1)}\frac{n}{W} \\ &= \widetilde{f}\frac{m^2 n}{K},\end{aligned} \tag{A.8}$$

$$\begin{aligned}\widetilde{f} &= \frac{f\mu\,\nu(1-\omega)}{(K-1)\,W} \\ &\approx \frac{f\mu\,\nu(1-\omega)}{KW}.\end{aligned} \tag{A.9}$$

$$\begin{aligned}T\,(m,n-1|m,n) &= g\,(1-\mu)\,\nu\frac{n}{W} \\ &= \widetilde{g}n,\end{aligned} \tag{A.10}$$

$$\widetilde{g} = \frac{(1-\mu)\,\nu}{W}. \tag{A.11}$$

All the other transition matrixes are zero. Noting that all the events in Table 2.2 are Markov processes, we know that the time evolution for the probability with m hosts and n phages at time t will be

$$\begin{aligned}\frac{d}{dt}P\,(m,n,t) &= T\,(m,n|m-1,n)\,P\,(m-1,n,t) \\ &+ T\,(m,n|m+1,n)\,P\,(m+1,n,t) \\ &+ T\,(m,n|m+1,n+\alpha-1)\,P\,(m+1,n+\alpha-1,t) \\ &+ T\,(m,n|m+1,n+\beta-1)\,P\,(m+1,n+\beta-1,t) \\ &+ T\,(m,n|m,n+1)\,P\,(m,n+1,t) \\ &- [T\,(m+1,n|m,n) + T\,(m-1,n|m,n) \\ &+ T\,(m-1,n+\alpha-1|m,n) + T\,(m-1,n+\beta-1|m,n) \\ &+ T\,(m,n-1|m,n)]P\,(m-1,n,t)\,.\end{aligned} \tag{A.12}$$

Applying summations according to Eq. (2.3), we will get

$$\begin{aligned}\frac{d\langle m\rangle}{dt} &= \langle T(m+1,n|m,n)\rangle - \langle T(m-1,n|m,n)\rangle \\ &\quad - \langle T(m-1,n+\alpha-1|m,n)\rangle \\ &\quad - \langle T(m-1,n+\beta-1|m,n)\rangle \\ &\approx \left(\widetilde{b}+\widetilde{d}\right)\langle m\rangle\left(1-\frac{\langle m\rangle}{K}\right) - \left(\widetilde{c}+\widetilde{d}\right)\langle m\rangle \\ &\quad - \widetilde{e}\langle m\rangle\langle n\rangle\left[1-\left(1-\frac{\widetilde{f}}{\widetilde{e}}\right)\frac{\langle m\rangle}{K}\right], \end{aligned} \tag{A.13a}$$

$$\begin{aligned}\frac{d\langle n\rangle}{dt} &= (\alpha-1)\langle T(m-1,n+\alpha-1|m,n)\rangle \\ &\quad + (\beta-1)\langle T(m-1,n+\beta-1|m,n)\rangle \\ &\quad - \langle T(m,n-1|m,n)\rangle \\ &= (\alpha-1)\ \widetilde{e}\langle m\rangle\langle n\rangle\left[1-\left(1-\frac{(\beta-1)\widetilde{f}}{(\alpha-1)\widetilde{e}}\right)\frac{\langle m\rangle}{K}\right] \\ &\quad - \widetilde{g}\langle n\rangle. \end{aligned} \tag{A.13b}$$

Let

$$r = \widetilde{b}+\widetilde{d}, \tag{A.14a}$$

$$\phi = \widetilde{e}, \tag{A.14b}$$

$$\gamma = \alpha-1, \tag{A.14c}$$

$$d_m = \widetilde{c}+\widetilde{d}, \tag{A.14d}$$

$$d_n = \widetilde{g}, \tag{A.14e}$$

$$a_m = 1-\frac{\widetilde{f}}{\widetilde{e}}, \tag{A.14f}$$

$$a_n = 1-\frac{(\beta-1)\widetilde{f}}{(\alpha-1)\widetilde{e}}, \tag{A.14g}$$

which is Eq. (2.6), we can arrive at Eq. (2.5).

Appendix B

Transition Matrices for the Lysogeny-lysis Model

In this appendix, we provide details for the derivations of the lysogeny-lysis model.

According to Table 3.1 and Table 3.2, we can obtain the following non-zero transition matrixes:

$$\begin{aligned} T\left(m+1,s,n|m,s,n\right) &= b\mu\left(1-\nu\right)\left(1-\omega\right)\frac{2m\left(K-m-s\right)}{K\left(K-1\right)} \\ &= \widetilde{b}m\left(1-\frac{m+s}{K}\right), \end{aligned} \tag{B.1}$$

$$\begin{aligned} \widetilde{b} &= \frac{2b\mu\left(1-\nu\right)\left(1-\omega\right)}{K-1} \\ &\approx \frac{2b\mu\left(1-\nu\right)\left(1-\omega\right)}{K}. \end{aligned} \tag{B.2}$$

$$\begin{aligned} T\left(m,s+1,n|m,s,n\right) &= b\mu\left(1-\nu\right)\left(1-\omega\right)\frac{2s\left(K-m-s\right)}{K\left(K-1\right)} \\ &= \widetilde{b}s\left(1-\frac{m+s}{K}\right). \end{aligned} \tag{B.3}$$

$$\begin{aligned} T\left(m-1,s,n|m,s,n\right) &= c\mu\left(1-\nu\right)\omega\frac{m}{K} \\ &\quad + d\mu\left(1-\nu\right)\left(1-\omega\right)\frac{m\left(m-1\right)}{K\left(K-1\right)} \\ &\quad + \frac{1}{2}d\mu\left(1-\nu\right)\left(1-\omega\right)\frac{2ms}{K\left(K-1\right)} \\ &= \widetilde{c}m+\widetilde{d}m\frac{m+s}{K}, \end{aligned} \tag{B.4}$$

$$\widetilde{c} = \frac{c\mu\left(1-\nu\right)\omega}{K}, \tag{B.5}$$

$$\widetilde{d} = \frac{d\mu\left(1-\nu\right)\left(1-\omega\right)}{K-1}$$

$$\approx \frac{d\mu\,(1-\nu)\,(1-\omega)}{K}. \tag{B.6}$$

$$\begin{aligned} T\,(m, s-1, n|m, s, n) &= c\mu\,(1-\nu)\,\omega\frac{s}{K} \\ &+ d\mu\,(1-\nu)\,(1-\omega)\,\frac{s\,(s-1)}{K\,(K-1)} \\ &+ \frac{1}{2}d\mu\,(1-\nu)\,(1-\omega)\,\frac{2ms}{K\,(K-1)} \\ &= \widetilde{c}s + \widetilde{d}s\frac{m+s}{K}. \end{aligned} \tag{B.7}$$

$$\begin{aligned} T\,(m-1, s, n+\alpha+1|m, s, n) &= e\mu\nu\,(1-\omega)\,\frac{2m\,(K-m-s)}{K\,(K-1)}\frac{n}{W} \\ &= \widetilde{e}mn\left(1-\frac{m+s}{K}\right), \end{aligned} \tag{B.8}$$

$$\begin{aligned} \widetilde{e} &= \frac{2e\mu\nu\,(1-\omega)}{(K-1)\,W} \\ &\approx \frac{2e\mu\nu\,(1-\omega)}{KW}. \end{aligned} \tag{B.9}$$

$$\begin{aligned} T\,(m-1, s, n+\beta+1|m, s, n) &= f\mu\,\nu(1-\omega)\,\frac{m\,(m-1)}{K\,(K-1)}\frac{n}{W} \\ &+ f\mu\,\nu(1-\omega)\,\frac{2ms}{K\,(K-1)}\frac{n}{W} \\ &= \widetilde{f}mn\frac{m+2s}{K}, \end{aligned} \tag{B.10}$$

$$\begin{aligned} \widetilde{f} &= \frac{f\mu\,\nu(1-\omega)}{(K-1)\,W} \\ &\approx \frac{f\mu\,\nu(1-\omega)}{KW}. \end{aligned} \tag{B.11}$$

$$\begin{aligned} T\,(m-1, s+1, n-1|m, s, n) &= h\mu\nu\,(1-\omega)\,\frac{2m\,(K-m-s)}{K\,(K-1)}\frac{n}{W} \\ &+ k\mu\nu\,(1-\omega)\,\frac{m\,(m-1)}{K\,(K-1)}\frac{n}{W} \\ &+ k\mu\nu\,(1-\omega)\,\frac{2ms}{K\,(K-1)}\frac{n}{W} \\ &= \widetilde{h}mn\left(1-\frac{m+s}{K}\right) + \widetilde{k}mn\frac{m+2s}{K}, \end{aligned} \tag{B.12}$$

$$\begin{aligned}\widetilde{h} &= \frac{2h\mu\nu\left(1-\omega\right)}{\left(K-1\right)W} \\ &\approx \frac{2h\mu\nu\left(1-\omega\right)}{KW},\end{aligned} \tag{B.13}$$

$$\begin{aligned}\widetilde{k} &= \frac{k\mu\nu\left(1-\omega\right)}{\left(K-1\right)W} \\ &\approx \frac{k\mu\nu\left(1-\omega\right)}{KW}.\end{aligned} \tag{B.14}$$

$$\begin{aligned}T\left(m,s-1,n+\alpha|m,s,n\right) &= p\mu\left(1-\nu\right)\left(1-\omega\right)\frac{2s\left(K-m-s\right)}{K\left(K-1\right)} \\ &= \widetilde{p}s\left(1-\frac{m+s}{K}\right),\end{aligned} \tag{B.15}$$

$$\begin{aligned}\widetilde{p} &= \frac{2p\mu\left(1-\nu\right)\left(1-\omega\right)}{K-1} \\ &\approx \frac{2p\mu\left(1-\nu\right)\left(1-\omega\right)}{K}.\end{aligned} \tag{B.16}$$

$$\begin{aligned}T\left(m,s-1,n+\beta|m,s,n\right) &= q\mu\left(1-\nu\right)\left(1-\omega\right)\frac{s\left(s-1\right)}{K\left(K-1\right)} \\ &\quad + q\mu\left(1-\nu\right)\left(1-\omega\right)\frac{2ms}{K\left(K-1\right)} \\ &= \widetilde{q}s\frac{2m+s}{K},\end{aligned} \tag{B.17}$$

$$\begin{aligned}\widetilde{q} &= \frac{q\mu\left(1-\nu\right)\left(1-\omega\right)}{K-1} \\ &\approx \frac{q\mu\left(1-\nu\right)\left(1-\omega\right)}{K}.\end{aligned} \tag{B.18}$$

$$\begin{aligned}T\left(m,s,n-1|m,s,n\right) &= g\left(1-\mu\right)\nu\frac{n}{W} \\ &= \widetilde{g}n,\end{aligned} \tag{B.19}$$

$$\widetilde{g} = \frac{\left(1-\mu\right)\nu}{W}. \tag{B.20}$$

Ignoring fluctuations and correlations, we derive the populations dynamics at the mean field level. The

time evolution for population size is

$$\begin{aligned}
\frac{d\langle m\rangle}{dt} &= \langle T(m+1,s,n|m,s,n)\rangle - \langle T(m-1,s,n|m,s,n)\rangle - \langle T(m-1,s,n+\alpha-1|m,s,n)\rangle \\
&\quad - \langle T(m-1,s,n+\beta-1|m,s,n)\rangle - \langle T(m-1,s+1,n-1|m,s,n)\rangle \\
&= \left(\widetilde{b}+\widetilde{d}\right)\langle m\rangle\left(1-\frac{\langle m\rangle+\langle s\rangle}{K}\right) - \left(\widetilde{c}+\widetilde{d}\right)\langle m\rangle \\
&\quad - \left(\widetilde{e}+\widetilde{h}\right)\langle m\rangle\langle n\rangle\left\{1-\frac{1}{K}\left[\left(1-\frac{\widetilde{f}+\widetilde{k}}{\widetilde{e}+\widetilde{h}}\right)\langle m\rangle + \left(1-2\cdot\frac{\widetilde{f}+\widetilde{k}}{\widetilde{e}+\widetilde{h}}\right)\langle s\rangle\right]\right\}, \qquad \text{(B.21a)} \\
\frac{d\langle s\rangle}{dt} &= \langle T(m,s+1,n|m,s,n)\rangle - \langle T(m,s-1,n|m,s,n)\rangle + \langle T(m-1,s+1,n-1|m,s,n)\rangle \\
&\quad - \langle T(m,s-1,n+\alpha|m,s,n)\rangle - \langle T(m,s-1,n+\beta|m,s,n)\rangle \\
&= \left(\widetilde{b}+\widetilde{d}\right)\langle s\rangle\left(1-\frac{\langle m\rangle+\langle s\rangle}{K}\right) - \left(\widetilde{c}+\widetilde{d}\right)\langle s\rangle \\
&\quad - \widetilde{h}\langle m\rangle\langle n\rangle\left\{1-\frac{1}{K}\left[\left(1-\frac{\widetilde{k}}{\widetilde{h}}\right)\langle m\rangle + \left(1-2\cdot\frac{\widetilde{k}}{\widetilde{h}}\right)\langle s\rangle\right]\right\} \\
&\quad - \widetilde{p}\langle s\rangle\left\{1-\frac{1}{K}\left[\left(1-2\cdot\frac{\widetilde{q}}{\widetilde{p}}\right)\langle m\rangle + \left(1-\frac{\widetilde{q}}{\widetilde{p}}\right)\langle s\rangle\right]\right\}, \qquad \text{(B.21b)} \\
\frac{d\langle n\rangle}{dt} &= (\alpha-1)\langle T(m-1,s,n+\alpha-1|m,s,n)\rangle + (\beta-1)\langle T(m-1,s,n+\beta-1|m,s,n)\rangle \\
&\quad - \langle T(m-1,s+1,n-1|m,s,n)\rangle + \alpha\langle T(m,s-1,n+\alpha|m,s,n)\rangle + \beta\langle T(m,s-1,n+\beta|m,s,n)\rangle \\
&\quad - \langle T(m,s,n-1|m,s,n)\rangle \\
&= \left[(\alpha-1)\widetilde{e}-\widetilde{h}\right]\langle m\rangle\langle n\rangle\left\{1-\frac{1}{K}\left[\left(1-\frac{(\beta-1)\widetilde{f}-\widetilde{k}}{(\alpha-1)\widetilde{e}-\widetilde{h}}\right)\langle m\rangle + \left(1-2\cdot\frac{(\beta-1)\widetilde{f}-\widetilde{k}}{(\alpha-1)\widetilde{e}-\widetilde{h}}\right)\langle s\rangle\right]\right\} \\
&\quad + \alpha\widetilde{p}\langle s\rangle\left\{1-\frac{1}{K}\left[\left(1-2\cdot\frac{\beta\widetilde{q}}{\alpha\widetilde{p}}\right)\langle m\rangle + \left(1-\frac{\beta\widetilde{q}}{\alpha\widetilde{p}}\right)\langle s\rangle\right]\right\} - \widetilde{g}\langle n\rangle. \qquad \text{(B.21c)}
\end{aligned}$$

Let

$$r = \widetilde{b}+\widetilde{d}, \qquad \text{(B.22a)}$$

$$d_1 = \widetilde{c}+\widetilde{d}, \qquad \text{(B.22b)}$$

$$d_2 = \widetilde{p}, \qquad \text{(B.22c)}$$

$$d_3 = \widetilde{g}, \qquad \text{(B.22d)}$$

$$\phi_1 = \widetilde{e}+\widetilde{h}, \qquad \text{(B.22e)}$$

$$\phi_2 = \widetilde{h}, \qquad \text{(B.22f)}$$

$$a_1 = \frac{\widetilde{f}+\widetilde{k}}{\widetilde{e}+\widetilde{h}}, \qquad \text{(B.22g)}$$

$$a_{21} = \frac{\widetilde{k}}{\widetilde{h}}, \tag{B.22h}$$

$$a_{22} = \frac{\widetilde{q}}{\widetilde{p}}, \tag{B.22i}$$

$$a_{31} = \frac{(\beta - 1)\,\widetilde{f} - \widetilde{k}}{(\alpha - 1)\,\widetilde{e} - \widetilde{h}}, \tag{B.22j}$$

$$a_{32} = \frac{\beta \widetilde{q}}{\alpha \widetilde{p}}, \tag{B.22k}$$

which is Eq. (3.4), and omit angle-brackets for simplicity, Eq. (B.21) can be written as Eq. (3.3).

Appendix C

Simulation Code of Population Dynamics for Broad-, Narrow-, and Ultra-Narrow Spectrum Antibiotics

Here I provide working code written in C++ for the simulation described in Section 6.3.3.

```
//: Anti11.cpp
// output time evolution of population of Gram-positives,
// Gram-negatives, pathegons, and their resistant correspondence

#include <iostream>
#include <fstream>
#include <ctime>
#include <cstdlib>
#include <cmath>
#include "require.h"
using namespace std;

// setup global constants
const bool killGP = 0;          // kill Gram-positives
const bool killGN = 0;          // kill Gram-negatives
const double mBL = 0.1;         // microbe-birth-low
const double mBH = 0.2;         // microbe-birth-high
const double mD = 0.15;         // microbe-death
const double mS = 0.8;          // microbe-suppression
const double pBL = 0.5;         // pathogen-birth-low
const double pBH = 0.6;         // pathogen-birth-high
const double pD = 0;            // pathogen-death
const double dK = 0.8;          // drug-kill
```

```
const double mutation = 0.002;  // mutation-rate
const double HGTintra = 0.02;   // HGT-intraspecies
const double HGTinter = 0.2;    // HGT-interspecies
const long tDose = 1000;                    // threshold-dose
const long tBurst = 30000;              // threshold-burst
const long kUT = 4e5;                   // unit carrying-capacity
const long kGP = 6e5;                   // carrying-capacity of Gram-positives
const long kGN = 8e5;                   // carrying-capacity of Gram-negatives

long hours;                                             // time step
long popGP, popGN, popP, popRGP, popRGN, popRP;



void setup(){
        hours = 0;
        popGP = kGP;
        popGN = kGN;
        popP = tDose;
        popRGP = 0;
        popRGN = 0;
        popRP = 0;
}

long gen(long n, double rate){
        long r = 0;
        for (long i = 0; i < n; ++i)
                if ((double)rand() / (double)RAND_MAX < rate) ++r;
        return r;
}

void kill(){
        if (popP >= tDose){
```

```
                popP -= gen(popP - popRP, dK);

                if (killGP) popGP -= gen(popGP - popRGP, dK);
                if (killGN) popGN -= gen(popGN - popRGN, dK);
        }
}

void mutate(){
        popRP += gen(popP - popRP, mutation);

        if (killGP) popRGP += gen(popGP - popRGP, mutation);
        if (killGN) popRGN += gen(popGN - popRGN, mutation);
}

void reproduce_help(long& n1, long& n2, double rate1, double rate2){
        long x = gen(n1 - n2, rate1);
        long y = gen(n2, rate2);
        n2 += y;
        n1 += x + y;
}

void reproduce(){
        double sr = pow((double)1 - mS, (double)(popGP + popGN) / (double)kUT);
        double c1 = (double)kGP / (double)popGP;
        double c2 = (double)kGN / (double)popGN;
        reproduce_help(popP, popRP, sr * pBH, sr * pBL);
        reproduce_help(popGP, popRGP, c1 * mBH, c1 * mBL);
        reproduce_help(popGN, popRGN, c2 * mBH, c2 * mBL);
}

void hgt(){
        long iP = 0, iGP = 0, iGN = 0;
```

```
        iP = gen(popRP, HGTintra);

        if (killGP){
                iGP = gen(popRGP, HGTintra);
                iP += gen(popRGP, HGTinter);
                iGP += gen(popRP, HGTinter);
        }
        if (killGN){
                iGN = gen(popRGN, HGTintra);
                iP += gen(popRGN, HGTinter);
                iGN += gen(popRP, HGTinter);
        }
        if (killGP && killGN){
                iGP += gen(popRGN, HGTintra);
                iGN += gen(popRGP, HGTintra);
        }
//      cout << iP << " " << iGP << " " << iGN << endl;

        popRP += min(iP, popP - popRP);
        if (killGP) popRGP += min(iGP, popGP - popRGP);
        if (killGN) popRGN += min(iGN, popGN - popRGN);
}

void survive_help(long& n1, long& n2, double rate){
        long x = gen(n1 - n2, rate);
        long y = gen(n2, rate);
        n2 -= y;
        n1 -= x + y;
}

void survive(){
        survive_help(popP, popRP, pD);
```

```
        survive_help(popGP, popRGP, mD);
        survive_help(popGN, popRGN, mD);
}


int main(int argc, char* argv[]){
        const char* fid = argc > 1 ? argv[1] : "01";
        string fname("Anti11_.dat");
        fname.insert(7, fid);
        ofstream out(fname.c_str());
        assure(out, fname.c_str());
        out << "killGP " << killGP << endl;
        out << "killGN " << killGN << endl;
        out << "mBL " << mBL << endl;
        out << "mBH " << mBH << endl;
        out << "mD " << mD << endl;
        out << "mS " << mS << endl;
        out << "pBL " << pBL << endl;
        out << "pBH " << pBH << endl;
        out << "pD " << pD << endl;
        out << "dK " << dK << endl;
        out << "mutation " << mutation << endl;
        out << "HGTintra " << HGTintra << endl;
        out << "HGTinter " << HGTinter << endl;
        out << "tDose " << tDose << endl;
        out << "tBurst " << tBurst << endl;
        out << "kUT " << kUT << endl;
        out << "kGP " << kGP << endl;
        out << "kGN " << kGN << endl;

        srand(time(0));
        setup();
```

```
        out << "\nhours\tpopGP\tpopRGP\tpopGN\tpopRGN\tpopP\tpopRP\n";
        out << "START\n";
        out << hours << "\t" << popGP << "\t" << popRGP << "\t"
            << popGN << "\t" << popRGN << "\t" << popP << "\t"
            << popRP << endl;
        while (popP < tBurst){
                hours++;
                kill();
                mutate();
                reproduce();
                hgt();
                survive();
                out << hours << "\t" << popGP << "\t" << popRGP << "\t"
                        << popGN << "\t" << popRGN << "\t" << popP << "\t"
                        << popRP << endl;
        }
        //      out << "END\n";
        out.close();
}///:~
```

References

[1] J.B. Birks. *Rutherford at Manchester*. Heywood, 1962.

[2] M. De Paepe and F. Taddei. Viruses' life history: towards a mechanistic basis of a trade-off between survival and reproduction among phages. *PLoS Biol*, 4(7):e193, 2006.

[3] M.A. Duffy and L. Sivars-Becker. Rapid evolution and ecological host–parasite dynamics. *Ecology Letters*, 10(1):44–53, 2007.

[4] J. Davies and D. Davies. Origins and evolution of antibiotic resistance. *Microbiology and Molecular Biology Reviews*, 74(3):417–433, 2010.

[5] D.I. Andersson and D. Hughes. Antibiotic resistance and its cost: is it possible to reverse resistance? *Nature Reviews Microbiology*, 8(4):260–271, 2010.

[6] Tree of Life. `http://tolweb.org/tree/learn/concepts/whatisphylogeny.html`.

[7] W.F. Doolittle. Phylogenetic classification and the universal tree. *Science*, 284(5423):2124–2128, 1999.

[8] M. Ptashne. *A Genetic Switch: Phage Lambda Revisited*. CSHL Press, 2004.

[9] A.E. Clatworthy, E. Pierson, and D.T. Hung. Targeting virulence: a new paradigm for antimicrobial therapy. *Nature chemical biology*, 3(9):541–548, 2007.

[10] H.W. Ackermann. Phage classification and characterization. *Methods Mol Biol*, 501:127–140, 2009.

[11] J.S. Weitz and J. Dushoff. Alternative stable states in host–phage dynamics. *Theoretical Ecology*, 1(1):13–19, 2008.

[12] M. Chaplin. Enzymes and Enzyme Technology. `http://www.lsbu.ac.uk/biology/enzyme/practical1.html`.

[13] J. Gore, H. Youk, and A. Van Oudenaarden. Snowdrift game dynamics and facultative cheating in yeast. *Nature*, 459(7244):253–256, 2009.

[14] M.A. Brockhurst, A.D. Morgan, A. Fenton, and A. Buckling. Experimental coevolution with bacteria and phage: The Pseudomonas fluorescens—Φ2 model system. *Infection, Genetics and Evolution*, 7(4):547–552, 2007.

[15] R.J. Woods, J.E. Barrick, T.F. Cooper, U. Shrestha, M.R. Kauth, and R.E. Lenski. Second-order selection for evolvability in a large escherichia coli population. *Science*, 331(6023):1433–1436, 2011.

[16] P.J. Choi, L. Cai, K. Frieda, and X.S. Xie. A stochastic single-molecule event triggers phenotype switching of a bacterial cell. *Science*, 322(5900):442–446, 2008.

[17] J. Gore, H. Youk, and A. Van Oudenaarden. Snowdrift game dynamics and facultative cheating in yeast. *Nature*, 459(7244):253–256, 2009.

[18] E. Lieberman, C. Hauert, and M.A. Nowak. Evolutionary dynamics on graphs. *Nature*, 433(7023):312–316, 2005.

[19] S.B. Levy and B. Marshall. Antibacterial resistance worldwide: causes, challenges and responses. *Nature medicine*, 10:S122–S129, 2004.

[20] R. Nowak. Hungary sees an improvement in penicillin resistance. *Science (New York, NY)*, 264(5157):364, 1994.

[21] H. Seppälä, T. Klaukka, J. Vuopio-Varkila, A. Muotiala, H. Helenius, K. Lager, P. Huovinen, et al. The effect of changes in the consumption of macrolide antibiotics on erythromycin resistance in group a streptococci in finland. *New England Journal of Medicine*, 337(7):441–446, 1997.

[22] V.I. Enne, D.M. Livermore, P. Stephens, and L. Hall. Persistence of sulphonamide resistance in escherichia coli in the uk despite national prescribing restriction. *The lancet*, 357(9265):1325–1328, 2001.

[23] M.L. Foucault, P. Courvalin, and C. Grillot-Courvalin. Fitness cost of vana-type vancomycin resistance in methicillin-resistant staphylococcus aureus. *Antimicrobial agents and chemotherapy*, 53(6):2354–2359, 2009.

[24] J.C. Venter, M.D. Adams, E.W. Myers, P.W. Li, R.J. Mural, G.G. Sutton, H.O. Smith, M. Yandell, C.A. Evans, R.A. Holt, et al. The sequence of the human genome. *Science*, 291(5507):1304–1351, 2001.

[25] International Human Genome Sequencing Consortium. Finishing the euchromatic sequence of the human genome. *Nature*, 431:931–945, 2004.

[26] C.K. Stover, X.Q. Pham, A.L. Erwin, S.D. Mizoguchi, P. Warrener, M.J. Hickey, F.S.L. Brinkman, W.O. Hufnagle, D.J. Kowalik, M. Lagrou, et al. Complete genome sequence of Pseudomonas aerugínosa PA 01, an opportunistic pathogen. *Nature(London)*, 406(6799):959–964, 2000.

[27] A. Goffeau, B.G. Barrell, H. Bussey, R.W. Davis, B. Dujon, H. Feldmann, F. Galibert, J.D. Hoheisel, C. Jacq, M. Johnston, et al. Life with 6000 genes. *Science*, 274(5287):546–546, 1996.

[28] H.W. Mewes, K. Albermann, M. Bähr, D. Frishman, A. Gleissner, J. Hani, K. Heumann, K. Kleine, A. Maierl, S.G. Oliver, et al. Overview of the yeast genome. *Nature*, 387(6632 Suppl):7–8, 1997.

[29] The C. elegans Sequencing Consortium. Genome sequence of the nematode C. elegans: a platform for investigating biology. *Science*, 282:2012–2018, 1998.

[30] S.A. Goff, D. Ricke, T.H. Lan, G. Presting, R. Wang, M. Dunn, J. Glazebrook, A. Sessions, P. Oeller, H. Varma, et al. A draft sequence of the rice genome (Oryza sativa L. ssp. japonica). *Science*, 296(5565):92–100, 2002.

[31] J. Yu, S. Hu, J. Wang, G.K.S. Wong, S. Li, B. Liu, Y. Deng, L. Dai, Y. Zhou, X. Zhang, et al. A draft sequence of the rice genome (Oryza sativa L. ssp. indica). *Science*, 296(5565):79–92, 2002.

[32] C. Sequencing et al. Initial sequence of the chimpanzee genome and comparison with the human genome. *Nature*, 437(7055):69, 2005.

[33] R. Maranger and D.F. Bird. Viral abundance in aquatic systems: a comparison between marine and fresh waters. *Marine ecology progress series. Oldendorf*, 121(1):217–226, 1995.

[34] S. Chibani-Chennoufi, A. Bruttin, M.L. Dillmann, and H. Brussöw. Phage-Host Interaction: an Ecological Perspective. *Journal of Bacteriology*, 186(12):3677–3686, 2004.

[35] C.M. Santelli, B.N. Orcutt, E. Banning, W. Bach, C.L. Moyer, M.L. Sogin, H. Staudigel, and K.J. Edwards. Abundance and diversity of microbial life in ocean crust. *Nature*, 453(7195):653, 2008.

[36] A.C. Ortmann and C.A. Suttle. High abundances of viruses in a deep-sea hydrothermal vent system indicates viral mediated microbial mortality. *Deep-Sea Research Part I*, 52(8):1515–1527, 2005.

[37] P.G. Falkowski, T. Fenchel, and E.F. Delong. The microbial engines that drive earth's biogeochemical cycles. *Science*, 320(5879):1034–1039, 2008.

[38] M. Syvanen. Horizontal gene transfer: evidence and possible consequences. *Annual Review of Genetics*, 28(1):237–261, 1994.

[39] H. Ochman, J.G. Lawrence, E.A. Groisman, et al. Lateral gene transfer and the nature of bacterial innovation. *Nature*, 405(6784):299–304, 2000.

[40] S.W. Wilhelm and C.A. Suttle. Viruses and Nutrient Cycles in the Sea. *Bioscience*, 49:781–788, 1999.

[41] C.A. Suttle. Viruses in the sea. *Nature*, 437(7057):356–361, 2005.

[42] M.G. Weinbauer and F. Rassoulzadegan. Are viruses driving microbial diversification and diversity? *Environmental Microbiology*, 6(1):1–11, 2004.

[43] S. Sharma, Z. Szele, R. Schilling, J.C. Munch, and M. Schloter. Influence of Freeze-Thaw Stress on the Structure and Function of Microbial Communities and Denitrifying Populations in Soil. *Applied and Environmental Microbiology*, 72(3):2148–2154, 2006.

[44] R.K. Monson, D.L. Lipson, S.P. Burns, A.A. Turnipseed, A.C. Delany, M.W. Williams, and S.K. Schmidt. Winter forest soil respiration controlled by climate and microbial community composition. *Nature*, 439(7077):711–714, 2006.

[45] J. Schimel, T.C. Balser, and M. Wallenstein. Microbial stress-response physiology and its implications for ecosystem function. *Ecology*, 88(6):1386–1394, 2007.

[46] C.A. Suttle. Marine viruses—major players in the global ecosystem. *Nature Reviews Microbiology*, 5(10):801–812, 2007.

[47] R. Danovaro, A. Dell, C. Corinaldesi, M. Magagnini, R. Noble, C. Tamburini, and M. Weinbauer. Major viral impact on the functioning of benthic deep-sea ecosystems. *Nature*, 454(7208):1084–1087, 2008.

[48] R.D. Bardgett, C. Freeman, and N.J. Ostle. Microbial contributions to climate change through carbon cycle feedbacks. *ISME Journal*, 2(8):805–814, 2008.

[49] F. Rohwer and R.V. Thurber. Viruses manipulate the marine environment. *Nature*, 459:207–212, 2009.

[50] C.R. Woese. On the evolution of cells. *Proceedings of the National Academy of Sciences*, 99(13):8742–8747, 2002.

[51] N. Goldenfeld and C. Woese. Biology's next revolution. *Nature*, 445:369, 2007.

[52] J.C.D. Hotopp, M.E. Clark, D.C.S.G. Oliveira, J.M. Foster, P. Fischer, M.C.M. Torres, J.D. Giebel, N. Kumar, N. Ishmael, S. Wang, et al. Widespread lateral gene transfer from intracellular bacteria to multicellular eukaryotes. *Science*, 317(5845):1753–1756, 2007.

[53] J.C.D. Hotopp. Horizontal gene transfer between bacteria and animals. *Trends in Genetics*, 27(4):157–163, 2011.

[54] J.K. Pace, C. Gilbert, M.S. Clark, and C. Feschotte. Repeated horizontal transfer of a dna transposon in mammals and other tetrapods. *Proceedings of the National Academy of Sciences*, 105(44):17023–17028, 2008.

[55] B. Palenik, Q. Ren, V. Tai, and IT Paulsen. Coastal Synechococcus metagenome reveals major roles for horizontal gene transfer and plasmids in population diversity. *Environmental Microbiology*, 11(2):349–359, 2009.

[56] N. Goldenfeld and C. Woese. Life is physics: Evolution as a collective phenomenon far from equilibrium. *Annu. Rev. Condens. Matter Phys.*, 2(1):375–399, 2011.

[57] C. Szpirer, E. Top, M. Couturier, and M. Mergeay. Retrotransfer or gene capture: a feature of conjugative plasmids, with ecological and evolutionary significance. *Microbiology*, 145(12):3321–3329, 1999.

[58] C.S. Smillie, M.B. Smith, J. Friedman, O.X. Cordero, L.A. David, and E.J. Alm. Ecology drives a global network of gene exchange connecting the human microbiome. *Nature*, 480(7376):241–244, 2011.

[59] K. Bæk, S. Svenningsen, H. Eisen, K. Sneppen, and S. Brown. Single-cell Analysis of λ Immunity Regulation. *Journal of Molecular Biology*, 334(3):363–372, 2003.

[60] J.H. Paul. Prophages in marine bacteria: dangerous molecular time bombs or the key to survival in the seas? *The ISME Journal*, 2(6):579, 2008.

[61] C. Mora, D.P. Tittensor, S. Adl, A.G.B. Simpson, and B. Worm. How many species are there on earth and in the ocean? *PLoS Biol*, 9(8):e1001127, 2011.

[62] J. Qin, R. Li, J. Raes, M. Arumugam, K.S. Burgdorf, C. Manichanh, T. Nielsen, N. Pons, F. Levenez, T. Yamada, et al. A human gut microbial gene catalogue established by metagenomic sequencing. *Nature*, 464(7285):59–65, 2010.

[63] G.E. Hutchinson. The paradox of the plankton. *The American Naturalist*, 95(882):137–145, 1961.

[64] R. Petersen. The paradox of the plankton: an equilibrium hypothesis. *American naturalist*, 109(965-967):35, 1975.

[65] J. Huisman and F.J. Weissing. Biodiversity of plankton by species oscillations and chaos. *Nature*, 402(6760):407–410, 1999.

[66] S. Avrani, O. Wurtzel, I. Sharon, R. Sorek, and D. Lindell. Genomic island variability facilitates prochlorococcus-virus coexistence. *Nature*, 474(7353):604–608, 2011.

[67] W.D. Hamilton. The genetical evolution of social behaviour. i. *Journal of theoretical biology*, 7(1):1–16, 1964.

[68] W.D. Hamilton. The genetical evolution of social behaviour. i. *Journal of theoretical biology*, 7(1):17–52, 1964.

[69] G.R. Jones and J.M. George. The experience and evolution of trust: Implications for cooperation and teamwork. *Academy of management review*, 23(3):531–546, 1998.

[70] R. Hudson and F. Trillmich. Sibling competition and cooperation in mammals: challenges, developments and prospects. *Behavioral Ecology and Sociobiology*, 62(3):299–307, 2008.

[71] M. Bekoff. Social play behaviour. cooperation, fairness, trust, and the evolution of morality. *Journal of Consciousness Studies*, 8(2):81–90, 2001.

[72] G.S. Wilkinson. Reciprocal altruism in bats and other mammals. *Ethology and Sociobiology*, 9(2-4):85–100, 1988.

[73] R.A. Adams and J.A. Simmons. Directionality of drinking passes by bats at water holes: is there cooperation? *Acta chiropterologica*, 4(2):195–199, 2002.

[74] L.A. Dugatkin. *Cheating monkeys and citizen bees: the nature of cooperation in animals and humans*. Harvard Univ Pr, 2000.

[75] B. Hölldobler and E.O. Wilson. *The ants*. Belknap Press, 1990.

[76] J. Smith. The social evolution of bacterial pathogenesis. *Proceedings of the Royal Society of London. Series B: Biological Sciences*, 268(1462):61–69, 2001.

[77] T. Nogueira, D.J. Rankin, M. Touchon, F. Taddei, S.P. Brown, and E.P.C. Rocha. Horizontal gene transfer of the secretome drives the evolution of bacterial cooperation and virulence. *Current Biology*, 19(20):1683–1691, 2009.

[78] A.M. Poole. Horizontal gene transfer and the earliest stages of the evolution of life. *Research in microbiology*, 160(7):473–480, 2009.

[79] S.E. Mc Ginty, D.J. Rankin, and S.P. Brown. Horizontal gene transfer and the evolution of bacterial cooperation. *Evolution*, 65(1):21–32, 2011.

[80] S.P. Brown and R.A. Johnstone. Cooperation in the dark: signalling and collective action in quorum-sensing bacteria. *Proceedings of the Royal Society of London. Series B: Biological Sciences*, 268(1470):961–965, 2001.

[81] M. Juhas, L. Eberl, and B. Tümmler. Quorum sensing: the power of cooperation in the world of pseudomonas. *Environmental Microbiology*, 7(4):459–471, 2005.

[82] J.J. Kuzdzal-Fick, S.A. Fox, J.E. Strassmann, and D.C. Queller. High relatedness is necessary and sufficient to maintain multicellularity in dictyostelium. *Science*, 334(6062):1548–1551, 2011.

[83] S. Proshkin, A.R. Rahmouni, A. Mironov, and E. Nudler. Cooperation between translating ribosomes and rna polymerase in transcription elongation. *Science*, 328(5977):504–508, 2010.

[84] Y. Liu, A. Chu, I. Chakroun, U. Islam, and A. Blais. Cooperation between myogenic regulatory factors and six family transcription factors is important for myoblast differentiation. *Nucleic acids research*, 38(20):6857–6871, 2010.

[85] R.E. Lenski. Richard Lenski Experimental Evolution. `http://myxo.css.msu.edu/`.

[86] J.E. Barrick, D.S. Yu, S.H. Yoon, H. Jeong, T.K. Oh, D. Schneider, R.E. Lenski, and J.F. Kim. Genome evolution and adaptation in a long-term experiment with escherichia coli. *Nature*, 461(7268):1243–1247, 2009.

[87] A.P. Hendry, J.K. Wenburg, P. Bentzen, E.C. Volk, and T.P. Quinn. Rapid evolution of reproductive isolation in the wild: evidence from introduced salmon. *Science*, 290(5491):516–518, 2000.

[88] J.S. Weitz, H. Hartman, and S.A. Levin. Coevolutionary arms races between bacteria and bacteriophage. *Proceedings of the National Academy of Sciences*, 102(27):9535–9540, 2005.

[89] L.H. Caporale. Foresight in genome evolution. *American scientist*, 91(3):234–241, 2003.

[90] S. Sonea. A bacterial way of life. *Nature*, 331(6153):216, 1988.

[91] M.B. Sullivan, D. Lindell, J.A. Lee, L.R. Thompson, J.P. Bielawski, and S.W. Chisholm. Prevalence and Evolution of Core Photosystem II Genes in Marine Cyanobacterial Viruses and Their Hosts. *PLoS Biol*, 4(8):e234, 2006.

[92] E.S. Anderson. Possible importance of transfer factors in bacterial evolution. *Nature*, 209:637–638, 1966.

[93] N.G. Anderson. Evolutionary significance of virus infection. *Nature*, 227:1346–1347, 1970.

[94] J. Filee, P. Forterre, and J. Laurent. The role played by viruses in the evolution of their hosts: a view based on informational protein phylogenies. *Res. Microbiol*, 154:237–243, 2003.

[95] D. Lindell, J.D. Jaffe, M.L. Coleman, M.E. Futschik, I.M. Axmann, T. Rector, G. Kettler, M.B. Sullivan, R. Steen, W.R. Hess, et al. Genome-wide expression dynamics of a marine virus and host reveal features of co-evolution. *Nature*, 449(7158):83–86, 2007.

[96] C. Pal, M. Macia, A. Oliver, I. Schachar, and A. Buckling. Coevolution with viruses drives the evolution of bacterial mutation rates. *Nature*, 450:1079–1081, 2007.

[97] H. Hadas, M. Einav, I. Fishov, and A. Zaritsky. Bacteriophage T4 development depends on the physiology of its host Escherichia coli. *Microbiology*, 143(1):179–185, 1997.

[98] S.J. Williamson, L.A. Houchin, L. McDaniel, and J.H. Paul. Seasonal Variation in Lysogeny as Depicted by Prophage Induction in Tampa Bay, Florida. *Applied and Environmental Microbiology*, 68(9):4307–4314, 2002.

[99] H. Brussöw, C. Canchaya, and W.D. Hardt. Phages and the Evolution of Bacterial Pathogens: from Genomic Rearrangements to Lysogenic Conversion. *Microbiology and Molecular Biology Reviews*, 68(3):560–602, 2004.

[100] S.J. Williamson and J.H. Paul. Nutrient stimulation of lytic phage production in bacterial populations of the Gulf of Mexico. *Aquatic Microbial Ecology*, 36(1):9–17, 2004.

[101] H. Brussöw. Phage therapy: the Escherichia coli experience. *Microbiology*, 151(7):2133–2140, 2005.

[102] M. Rosvall, I.B. Dodd, S. Krishna, and K. Sneppen. Network models of phage-bacteria coevolution. *Physical Review E*, 74(6):066105, 2006.

[103] S.J. Williamson, S.C. Cary, K.E. Williamson, R.R. Helton, S.R. Bench, D. Winget, and K.E. Wommack. Lysogenic virus — host interactions predominate at deep-sea diffuse-flow hydrothermal vents. *The ISME Journal*, 2(11):1112–1121, 2008.

[104] J.S. Weitz. Evolutionary Ecology of Bacterial Viruses. *Microbe*, 3(4):171, 2008.

[105] A.R. Wallace. On the law which has regulated the introduction of new species. *Annals and Magazine of Natural History*, 16(2):184–196, 1855.

[106] K.M. Ibrahim, R.A. Nichols, and G.M. Hewitt. Spatial patterns of genetic variation generated by different forms of dispersal during range expansion. *Heredity*, 77(3):282–291, 1996.

[107] O. Hallatschek and D.R. Nelson. Gene surfing in expanding populations. *Theoretical Population Biology*, 73(1):158–170, 2008.

[108] O. Hallatschek and K.S. Korolev. Fisher waves in the strong noise limit. *Physical Review Letters*, 103(10):108103, 2009.

[109] K. S. Korolev, Mikkel Avlund, Oskar Hallatschek, and David R. Nelson. Genetic demixing and evolutionary forces in the one-dimensional stepping stone model. *Reviews of Modern Physics (in press)*, 2009.

[110] A.J. McKane and T.J. Newman. Stochastic models in population biology and their deterministic analogs. *Physical Review E*, 70(4):041902, 2004.

[111] T. Butler and N. Goldenfeld. Robust ecological pattern formation induced by demographic noise. *Physical Review E*, 80(3):030902(R), 2009.

[112] A. Babic, A.B. Lindner, M. Vulic, E.J. Stewart, and M. Radman. Direct visualization of horizontal gene transfer. *Science*, 319(5869):1533, 2008.

[113] T. Yoshida, S.P. Ellner, L.E. Jones, B.J.M. Bohannan, R.E. Lenski, and N.G. Hairston Jr. Cryptic population dynamics: rapid evolution masks trophic interactions. *PLoS Biol*, 5(9):e235, 2007.

[114] N.L. Held and R.J. Whitaker. Viral biogeography revealed by signatures in Sulfolobus islandicus genomes. *Environmental Microbiology*, 11(2):457–466, 2009.

[115] A.A. Salyers and C.F. Amabile-Cuevas. Why are antibiotic resistance genes so resistant to elimination? *Antimicrobial Agents and Chemotherapy*, 41(11):2321–2325, 1997.

[116] T.M. Barbosa and S.B. Levy. The impact of antibiotic use on resistance development and persistence. *Drug Resistance Updates*, 3(5):303–311, 2000.

[117] C.T. Bergstrom, M. Lo, and M. Lipsitch. Ecological theory suggests that antimicrobial cycling will not reduce antimicrobial resistance in hospitals. *Proceedings of the National Academy of Sciences*, 101(36):13285–13290, 2004.

[118] S.B. Levy. Factors impacting on the problem of antibiotic resistance. *Journal of Antimicrobial Chemotherapy*, 49(1):25–30, 2002.

[119] G.A. Bolan, P.F. Sparling, and J.N. Wasserheit. The emerging threat of untreatable gonococcal infection. *New England Journal of Medicine*, 366(6):485–487, 2012.

[120] N.S. Shah, A. Wright, G.H. Bai, L. Barrera, F. Boulahbal, N. Martín-Casabona, F. Drobniewski, C. Gilpin, M. Havelková, R. Lepe, et al. Worldwide emergence of extensively drug-resistant tuberculosis. *Emerging Infectious Diseases*, 13(3):380–387, 2007.

[121] R. Laxminarayan and G.M. Brown. Economics of antibiotic resistance: a theory of optimal use. *Journal of Environmental Economics and Management*, 42(2):183–206, 2001.

[122] Z. Wang and N. Goldenfeld. Fixed points and limit cycles in the population dynamics of lysogenic viruses and their hosts. *Physical Review E*, 82(1):011918, 2010.

[123] Z. Wang and N. Goldenfeld. Theory of cooperation in a micro-organismal snowdrift game. *Physical Review E*, 84(2):020902, 2011.

[124] D.E. Bradley. Ultrastructure of bacteriophage and bacteriocins. *Bacteriological Reviews*, 31(4):230–314, 1967.

[125] C. Fauquet. *Virus taxonomy: classification and nomenclature of viruses: eighth report of the International Committee on the Taxonomy of Viruses*. Academic Press, 2005.

[126] R.E. Lenski and R.M. May. The evolution of virulence in parasites and pathogens: reconciliation between two competing hypotheses. *Journal of Theoretical Biology*, 169(3):253–265, 1994.

[127] A.L. Koch. Evolution of temperate pathogens: the bacteriophage/bacteria paradigm. *Virology Journal*, 4(1):121, 2007.

[128] D. Refardt and P.B. Rainey. Tuning a genetic switch: experimental evolution and natural variation of prophage induction. *Evolution*, 2010. Evolution (in press).

[129] B.R. Levin, F.M. Stewart, and L. Chao. Resource-Limited Growth, Competition, and Predation: A Model and Experimental Studies with Bacteria and Bacteriophage. *The American Naturalist*, 111(977):3, 1977.

[130] I.N. Wang, D.E. Dykhuizen, and L.B. Slobodkin. The evolution of phage lysis timing. *Evolutionary Ecology*, 10(5):545–558, 1996.

[131] B.J.M. Bohannan and R.E. Lenski. Effect of resource enrichment on a chemostat community of bacteria and bacteriophage. *Ecology*, 78(8):2303–2315, 1997.

[132] E. Beretta and Y. Kuang. Modeling and analysis of a marine bacteriophage infection with latency period. *Nonlinear Analysis: Real World Applications*, 2(1):35–74, 2001.

[133] J. Fort and V. Méndez. Time-Delayed Spread of Viruses in Growing Plaques. *Physical Review Letters*, 89(17):178101, 2002.

[134] M. Middelboe. Bacterial Growth Rate and Marine Virus-Host Dynamics. *Microbial Ecology*, 40(2):114–124, 2000.

[135] C.P.D. Brussaard. Viral Control of Phytoplankton Populations-a Review 1. *Journal of Eurkaryotic Microbiology*, 51(2):125–138, 2004.

[136] S. Sillankorva, R. Oliveira, M.J. Vieira, I. Sutherland, and J. Azeredo. Pseudomonas fluorescens infection by bacteriophage ΦS1: the influence of temperature, host growth phase and media. *FEMS Microbiology Letters*, 241(1):13–20, 2004.

[137] J.M. Smith. *Models in ecology*. Cambridge University Press, 1978.

[138] T. Butler and D. Reynolds. Predator-prey quasicycles from a path-integral formalism. *Physical Review E*, 79(3):032901, 2009.

[139] Y. Chen, I. Golding, S. Sawai, L. Guo, and E.C. Cox. Population fitness and the regulation of Escherichia coli genes by bacterial viruses. *PLoS Biology*, 3(7):1276, 2005.

[140] N. Chia, I. Golding, and N. Goldenfeld. λ-prophage induction modeled as a cooperative failure mode of lytic repression. *Physical Review E*, 80(3):030901(R), 2009.

[141] R.M. May. Limit cycles in predator-prey communities. *Science (New York, NY)*, 177(4052):900–902, 1972.

[142] A.N. Kolmogorov. Sulla teoria di Volterra della lotta per l'esistenza. *Giornelle dell'Istituto Italiano degli Attuari*, 7:74–80, 1936.

[143] D.T. Gillespie. A general method for numerically simulating the stochastic time evolution of coupled chemical reactions. *J. Comput. Phys*, 22(4):403–434, 1976.

[144] D.T. Gillespie. Exact stochastic simulation of coupled chemical reactions. *J. Phys. Chem*, 81(25):2340–2361, 1977.

[145] A.G. Marr. Growth rate of Escherichia coli. *Microbiology and Molecular Biology Reviews*, 55(2):316–333, 1991.

[146] M. Middelboe, A. Hagström, N. Blackburn, B. Sinn, U. Fischer, NH Borch, J. Pinhassi, K. Simu, and MG Lorenz. Effects of bacteriophages on the population dynamics of four strains of pelagic marine bacteria. *Microbial Ecology*, 42(3):395–406, 2001.

[147] E. Aurell, S. Brown, J. Johanson, and K. Sneppen. Stability puzzles in phage λ. *Physical Review E*, 65(5):41, 2002.

[148] P. Kourilsky. Lysogenization by bacteriophage lambda and the regulation of lambda repressor synthesis. *Virology*, 45(3):853, 1971.

[149] S.C. Jiang and J.H. Paul. Significance of lysogeny in the marine environment: studies with isolates and a model of lysogenic phage production. *Microbial ecology*, 35(3):235–243, 1998.

[150] A.M. Kropinski and R.A. Warren. Isolation and properties of a Pseudomonas acidovorans bacteriophage. *Journal of General Virology*, 6(1):85–93, 1970.

[151] C.D. Jepson and J.B. March. Bacteriophage lambda is a highly stable DNA vaccine delivery vehicle. *Vaccine*, 22(19):2413–2419, 2004.

[152] J.M. Smith. *Evolution and the Theory of Games*. Cambridge Univ Press, 1982.

[153] C. Hauert and G. Szabó. Game theory and physics. *Am. J. Phys.*, 73(5):405–414, 2005.

[154] R. Axelrod, D.E. Axelrod, and K.J. Pienta. Evolution of cooperation among tumor cells. *Proc. Natl. Acad. Sci. USA*, 103(36):13474–13479, 2006.

[155] M.A. Nowak. Five rules for the evolution of cooperation. *Science*, 314(5805):1560–1563, 2006.

[156] J.I. Prosser, B.J.M. Bohannan, T.P. Curtis, R.J. Ellis, M.K. Firestone, R.P. Freckleton, J.L. Green, L.E. Green, K. Killham, J.J. Lennon, et al. The role of ecological theory in microbial ecology. *Nature Reviews Microbiology*, 5(5):384–392, 2007.

[157] T. Antal, H. Ohtsuki, J. Wakeley, P.D. Taylor, and M.A. Nowak. Evolution of cooperation by phenotypic similarity. *Proc. Natl. Acad. Sci. USA*, 106(21):8597–8600, 2009.

[158] A. Traulsen, D. Semmann, R.D. Sommerfeld, H.J. Krambeck, and M. Milinski. Human strategy updating in evolutionary games. *Proceedings of the National Academy of Sciences*, 107(7):2962–2966, 2010.

[159] M.A. Nowak and K. Sigmund. Phage-lift for game theory. *Nature*, 398(6726):367–368, 1999.

[160] P.E. Turner and L. Chao. Prisoner's dilemma in an RNA virus. *Nature*, 398(6726):441–443, 1999.

[161] P.E. Turner and L. Chao. Escape from prisoners dilemma in RNA phage φ6. *American Naturalist*, 161:497–505, 2003.

[162] J.M. Gancedo. Yeast carbon catabolite repression. *Micro. and Mol. Biol. Rev.*, 62(2):334–361, 1998.

[163] N. Goldenfeld. *Lectures on phase transitions and the renormalization group*. Addison-Wesley, Reading, MA, 1992.

[164] J.M. Smith and G.R. Price. The logic of animal conflict. *Nature*, 246(5427):15–18, 1973.

[165] M.A. Nowak and K. Sigmund. Evolutionary dynamics of biological games. *Science*, 303(5659):793–799, 2004.

[166] R.L. Trivers. The evolution of reciprocal altruism. *The Quarterly Review of Biology*, 46(1):35–57, 1971.

[167] R. Axelrod and W.D. Hamilton. The evolution of cooperation. *Science*, 211(4489):1390–1396, 1981.

[168] R. Axelrod. *The Evolution of Cooperation*. Basic Books, 1984.

[169] R. Boyd and J.P. Lorberbaum. No pure strategy is evolutionarily stable in the repeated prisoner's dilemma game. *Nature*, 327:58–59, 1987.

[170] M.A. Nowak and K. Sigmund. Tit for tat in heterogeneous populations. *Nature*, 355(6357):250–253, 1992.

[171] M. Nowak and K. Sigmund. A strategy of win-stay, lose-shift that outperforms tit-for-tat in the prisoner's dilemma game. *Nature*, 364(6432):56–58, 1993.

[172] M.A. Nowak and R.M. May. Evolutionary games and spatial chaos. *Nature*, 359(6398):826–829, 1992.

[173] M.A. Nowak and K. Sigmund. Games on grids. In Law R. Dieckmann U. and Metz J.A.J., editors, *The Geometry of Ecological Interactions: Simplifying Spatial Complexity, Cambridge Studies in Adaptive Dynamics*, pages 135–150. Citeseer, 2000.

[174] C. Hauert and M. Doebeli. Spatial structure often inhibits the evolution of cooperation in the snowdrift game. *Nature*, 428(6983):643–646, 2004.

[175] T. Killingback, M. Doebeli, and N. Knowlton. Variable investment, the continuous prisoner's dilemma, and the origin of cooperation. *Proceedings of the Royal Society of London. Series B: Biological Sciences*, 266(1430):1723–1728, 1999.

[176] T. Killingback and M. Doebeli. 'raise the stakes' evolves into a defector. *Nature*, 400(6744):518, 1999.

[177] A. Szolnoki and G. Szabo. Cooperation enhanced by inhomogeneous activity of teaching for evolutionary prisoner's dilemma games. *EPL (Europhysics Letters)*, 77(3):30004, 2007.

[178] A. Szolnoki, M. Perc, and G. Szabó. Diversity of reproduction rate supports cooperation in the prisoner's dilemma game on complex networks. *The European Physical Journal B-Condensed Matter and Complex Systems*, 61(4):505–509, 2008.

[179] J.M. Pacheco, A. Traulsen, and M.A. Nowak. Coevolution of strategy and structure in complex networks with dynamical linking. *Physical review letters*, 97(25):258103, 2006.

[180] J.M. Pacheco, A. Traulsen, H. Ohtsuki, and M.A. Nowak. Repeated games and direct reciprocity under active linking. *Journal of theoretical biology*, 250(4):723–731, 2008.

[181] F.C. Santos and J.M. Pacheco. Scale-free networks provide a unifying framework for the emergence of cooperation. *Physical Review Letters*, 95(9):98104, 2005.

[182] A. Melbinger, J. Cremer, and E. Frey. Evolutionary game theory in growing populations. *Physical review letters*, 105(17):178101, 2010.

[183] A. Buckling and P.B. Rainey. Antagonistic coevolution between a bacterium and a bacteriophage. *Proceedings of the Royal Society of London. Series B: Biological Sciences*, 269(1494):931–936, 2002.

[184] M. Blaser. Antibiotic overuse: Stop the killing of beneficial bacteria. *Nature*, 476(7361):393–394, 2011.

[185] N. Tokuriki and D.S. Tawfik. Protein dynamism and evolvability. *Science*, 324(5924):203–207, 2009.

[186] D.J. Earl and M.W. Deem. Evolvability is a selectable trait. *Proceedings of the National Academy of Sciences of the United States of America*, 101(32):11531–11536, 2004.

[187] C. Hauert. Effects of space in 2× 2 games. *Int. J. Bifurcat. Chaos*, 12:1531–1548, 2002.

[188] G.P. Wagner and L. Altenberg. Perspective: Complex adaptations and the evolution of evolvability. *Evolution*, 50(3):967–976, 1996.

[189] J. Yu, J. Xiao, X. Ren, K. Lao, and X.S. Xie. Probing gene expression in live cells, one protein molecule at a time. *Science*, 311(5767):1600–1603, 2006.

[190] J.M.G. Vilar, C.C. Guet, and S. Leibler. Modeling network dynamics. *The Journal of cell biology*, 161(3):471–476, 2003.

[191] J.T. Mettetal, D. Muzzey, J.M. Pedraza, E.M. Ozbudak, and A. van Oudenaarden. Predicting stochastic gene expression dynamics in single cells. *Proceedings of the National Academy of Sciences of the United States of America*, 103(19):7304–7309, 2006.

[192] P.A.P. Moran. Random processes in genetics. In *Mathematical Proceedings of the Cambridge Philosophical Society*, volume 54, pages 60–71. Cambridge Univ Press, 1958.

[193] P.A.P. Moran. *The statistical processes of evolutionary theory.* Clarendon Press; Oxford University Press., 1962.

[194] C.P. Roca, J.A. Cuesta, and A. Sánchez. Evolutionary game theory: Temporal and spatial effects beyond replicator dynamics. *Physics of life reviews*, 6(4):208–249, 2009.

[195] N.G. Hairston Jr, W. Lampert, C.E. Cáceres, C.L. Holtmeier, L.J. Weider, U. Gaedke, J.M. Fischer, J.A. Fox, and D.M. Post. Rapid evolution revealed by dormant eggs. *Nature*, 401(6752):446, 1999.

[196] R.B. Huey, G.W. Gilchrist, M.L. Carlson, D. Berrigan, et al. Rapid evolution of a geographic cline in size in an introduced fly. *Science*, 287(5451):308–309, 2000.

[197] S.J. Franks, S. Sim, and A.E. Weis. Rapid evolution of flowering time by an annual plant in response to a climate fluctuation. *Proceedings of the National Academy of Sciences*, 104(4):1278–1282, 2007.

[198] K. Sasaki, S.F. Fox, and D. Duvall. Rapid evolution in the wild: Changes in body size, life-history traits, and behavior in hunted populations of the japanese mamushi snake. *Conservation Biology*, 23(1):93–102, 2009.

[199] M.A. Brockhurst, A.D. Morgan, P.B. Rainey, and A. Buckling. Population mixing accelerates coevolution. *Ecology Letters*, 6(11):975–979, 2003.

[200] M. Doebeli, C. Hauert, and T. Killingback. The evolutionary origin of cooperators and defectors. *Science*, 306(5697):859–862, 2004.

[201] M. Doebeli and C. Hauert. Models of cooperation based on the prisoner's dilemma and the snowdrift game. *Ecology Letters*, 8(7):748–766, 2005.

[202] B. Stecher, R. Denzler, L. Maier, F. Bernet, M.J. Sanders, D.J. Pickard, M. Barthel, A.M. Westendorf, K.A. Krogfelt, A.W. Walker, et al. Gut inflammation can boost horizontal gene transfer between pathogenic and commensal enterobacteriaceae. *Proceedings of the National Academy of Sciences*, 109(4):1269–1274, 2012.

[203] A. Salyers and N.B. Shoemaker. Reservoirs of antibiotic resistance genes. *Animal biotechnology*, 17(2):137–146, 2006.

[204] M.A. Fischbach and C.T. Walsh. Antibiotics for emerging pathogens. *Science*, 325(5944):1089–1093, 2009.

[205] H. Nikaido. Multidrug resistance in bacteria. *Annual Review of Biochemistry*, 78:119–146, 2009.

[206] R.M. Klevens, M.A. Morrison, J. Nadle, S. Petit, K. Gershman, S. Ray, L.H. Harrison, R. Lynfield, G. Dumyati, J.M. Townes, et al. Invasive methicillin-resistant staphylococcus aureus infections in the united states. *JAMA: the journal of the American Medical Association*, 298(15):1763–1771, 2007.

[207] G. Wang, J.F. Hindler, K.W. Ward, and D.A. Bruckner. Increased vancomycin mics for staphylococcus aureus clinical isolates from a university hospital during a 5-year period. *Journal of clinical microbiology*, 44(11):3883–3886, 2006.

[208] L.M. Weigel, D.B. Clewell, S.R. Gill, N.C. Clark, L.K. McDougal, S.E. Flannagan, J.F. Kolonay, J. Shetty, G.E. Killgore, and F.C. Tenover. Genetic analysis of a high-level vancomycin-resistant isolate of staphylococcus aureus. *Science*, 302(5650):1569–1571, 2003.

[209] G.B. Migliori, G. De Iaco, G. Besozzi, R. Centis, and D.M. Cirillo. First tuberculosis cases in italy resistant to all tested drugs. *Euro surveill*, 12(5):E070517, 2007.

[210] A.A. Velayati, M.R. Masjedi, P. Farnia, P. Tabarsi, J. Ghanavi, A.H. ZiaZarifi, and S.E. Hoffner. Emergence of new forms of totally drug-resistant tuberculosis bacilli: super extensively drug-resistant tuberculosis or totally drug-resistant strains in iran. *Chest*, 136(2):420–425, 2009.

[211] A.A. Velayati, P. Farnia, M.R. Masjedi, T.A. Ibrahim, P. Tabarsi, R.Z. Haroun, H.O. Kuan, J. Ghanavi, and M. Varahram. Totally drug-resistant tuberculosis strains: evidence of adaptation at the cellular level. *European Respiratory Journal*, 34(5):1202–1203, 2009.

[212] Z.F. Udwadia, R.A. Amale, K.K. Ajbani, and C. Rodrigues. Totally drug-resistant tuberculosis in india. *Clinical Infectious Diseases*, 2011. First published December 21, 2011, doi:10.1093/cid/cir889.

[213] S. Loewenberg. India reports cases of totally drug-resistant tuberculosis. *The Lancet*, 379(9812):205, 2012.

[214] L.C.M. Antunes, R.B.R. Ferreira, M. Buckner, and B.B. Finlay. Quorum sensing in bacterial virulence. *Microbiology*, 156(8):2271–2282, 2010.

[215] M. Hentzer, H. Wu, J.B. Andersen, K. Riedel, T.B. Rasmussen, N. Bagge, N. Kumar, M.A. Schembri, Z. Song, P. Kristoffersen, et al. Attenuation of pseudomonas aeruginosa virulence by quorum sensing inhibitors. *The EMBO journal*, 22(15):3803–3815, 2003.

[216] M.E. Mattmann and H.E. Blackwell. Small molecules that modulate quorum sensing and control virulence in pseudomonas aeruginosa. *Journal of organic chemistry*, 75(20):6737–6746, 2010.

[217] G. Chen, L.R. Swem, D.L. Swem, D.L. Stauff, C.T. O'Loughlin, P.D. Jeffrey, B.L. Bassler, and F.M. Hughson. A strategy for antagonizing quorum sensing. *Molecular cell*, 42(2):199–209, 2011.

[218] A.G. Palmer, E. Streng, and H.E. Blackwell. Attenuation of virulence in pathogenic bacteria using synthetic quorum-sensing modulators under native conditions on plant hosts. *ACS chemical biology*, 6(12):13481356, 2011.

[219] P.R. Burkholder and I. McVeigh. Synthesis of vitamins by intestinal bacteria. *Proceedings of the National Academy of Sciences of the United States of America*, 28(7):285–289, 1942.

[220] R. Bentley and R. Meganathan. Biosynthesis of vitamin K (menaquinone) in bacteria. *Microbiology and Molecular Biology Reviews*, 46(3):241–280, 1982.

[221] Y. Chen and M.J. Blaser. Inverse associations of helicobacter pylori with asthma and allergy. *Archives of internal medicine*, 167(8):821–827, 2007.

[222] D.I. Andersson and B.R. Levin. The biological cost of antibiotic resistance. *Current Opinion in Microbiology*, 2(5):489–493, 1999.

[223] H.H. Lee, M.N. Molla, C.R. Cantor, and J.J. Collins. Bacterial charity work leads to population-wide resistance. *Nature*, 467(7311):82–85, 2010.

[224] H. Giamarellou and A. Antoniadou. The effect of monitoring of antibiotic use on decreasing antibiotic resistance in the hospital. In D. J. Chadwick and J. Goode, editors, *Ciba Foundation Symposium 207 — Antibiotic Resistance: Origins, Evolution, Selection and Spread*, pages 76–92. John Wiley & Sons, Ltd., Chichester, UK., 2007.

[225] D.J. Austin, K.G. Kristinsson, and R.M. Anderson. The relationship between the volume of antimicrobial consumption in human communities and the frequency of resistance. *Proceedings of the National Academy of Sciences*, 96(3):1152–1156, 1999.

[226] D.I. Andersson. Persistence of antibiotic resistant bacteria. *Current opinion in microbiology*, 6(5):452–456, 2003.

[227] J. Björkman and D.I. Andersson. The cost of antibiotic resistance from a bacterial perspective. *Drug Resistance Updates*, 3(4):237–245, 2000.

[228] D.I. Andersson. The biological cost of mutational antibiotic resistance: any practical conclusions? *Current opinion in microbiology*, 9(5):461–465, 2006.

[229] A.I. Nilsson, A. Zorzet, A. Kanth, S. Dahlström, O.G. Berg, and D.I. Andersson. Reducing the fitness cost of antibiotic resistance by amplification of initiator trna genes. *Proceedings of the National Academy of Sciences*, 103(18):6976–6981, 2006.

[230] S. Maisnier-Patin, O.G. Berg, L. Liljas, and D.I. Andersson. Compensatory adaptation to the deleterious effect of antibiotic resistance in salmonella typhimurium. *Molecular microbiology*, 46(2):355–366, 2002.

[231] B.R. Levin, V. Perrot, and N. Walker. Compensatory mutations, antibiotic resistance and the population genetics of adaptive evolution in bacteria. *Genetics*, 154(3):985–997, 2000.

[232] D.C. Savage. Microbial ecology of the gastrointestinal tract. *Annual Reviews in Microbiology*, 31(1):107–133, 1977.

[233] S. Chibani-Chennoufi, A. Bruttin, M.L. Dillmann, and H. Brüssow. Phage-host interaction: an ecological perspective. *Journal of bacteriology*, 186(12):3677–3686, 2004.

[234] P.J. Turnbaugh, R.E. Ley, M. Hamady, C.M. Fraser-Liggett, R. Knight, and J.I. Gordon. The human microbiome project. *Nature*, 449(7164):804–810, 2007.

[235] T.R. De Kievit and B.H. Iglewski. Bacterial quorum sensing in pathogenic relationships. *Infection and immunity*, 68(9):4839–4849, 2000.

[236] A. Jermy. Antimicrobials: Disruption of quorum sensing meets resistance. *Nature Reviews Microbiology*, 9(11):767–767, 2011.